IL
NUOVO CIMENTO
ORGANO DELLA SOCIETÀ ITALIANA DI FISICA
SOTTO GLI AUSPICI DEL CONSIGLIO NAZIONALE DELLE RICERCHE

VOL. IX, N. 1 *Serie nona* 1 Gennaio 1952

Misure della costante dielettrica di soluzioni saline acquose in alta frequenza.

A. CARRELLI e L. RESCIGNO
Istituto di Fisica dell'Università - Napoli

(ricevuto il 22 Ottobre 1951)

Riassunto. — Sono state fatte misure in alta frequenza ($\omega = 4{,}39 \cdot 10^7$) della costante dielettrica dell'acqua quando in essa siano stati disciolti degli elettroliti. Si è trovato che la costante dielettrica dell'acqua diminuisce e poi aumenta al crescere della concentrazione c, riscontrandosi il minimo in corrispondenza di c dell'ordine di 10^{-3}.

Le misure della costante dielettrica dell'acqua in soluzioni elettrolitiche non hanno ancora raggiunto una conclusione sicura; esse sono state attuate da vari sperimentatori, coi metodi più diversi, e con risultati non molto in accordo fra loro. In questa Nota noi vogliamo riferire di alcune misure attuate, su tale argomento, con un metodo che si presenta semplice, e che quindi permette la raccolta, in modo rapido, di parecchi dati relativi a varie soluzioni. Esso è basato sul fenomeno di risonanza in un circuito in cui c'è una resistenza R ed una capacità C da misurare; la fig. 1 lo riproduce schematicamente. L è la

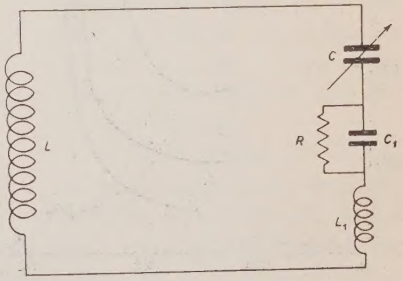

Fig. 1.

bobina che permette un collegamento induttivo con un oscillatore di frequenza $\nu = 7$ MHz non rappresentato in figura; la cella contenente la soluzione elettrolitica è rappresentata schematicamente da una capacità C_1 e da una resistenza R posta in parallelo; in queste misure può parlarsi esplicitamente di capacità della cella, perchè sono stati adoperati due elettrodi estesi e molto vicini (la capacità calcolata approssimativamente dai dati geometrici è di circa 1,6 pF). L'autoinduzione L_1 è accoppiata ad un circuito in cui è un diodo rettificatore che permette di misurare una intensità di corrente proporzionale a quella che circola nel circuito di fig. 1. Facendo ora variare C, si raggiungerà il massimo della corrente del circuito nelle condizioni di risonanza. Evidentemente per ogni soluzione posta nella cella si ha uno speciale valore della capacità C_1 e della resistenza R e quindi una determinata posizione della capacità C ed un determinato valore della corrente, nel massimo di risonanza. Ora, per fare la misura, si pone nella cella C_1 una

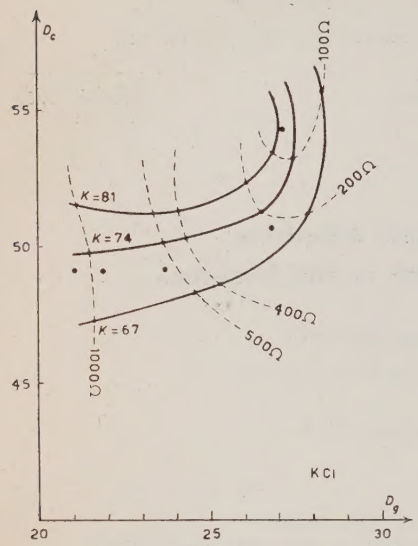

Fig. 2.

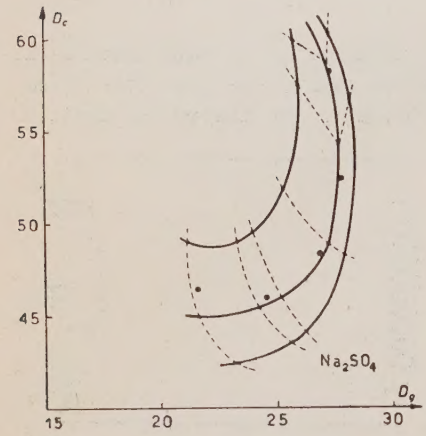

Fig. 3.

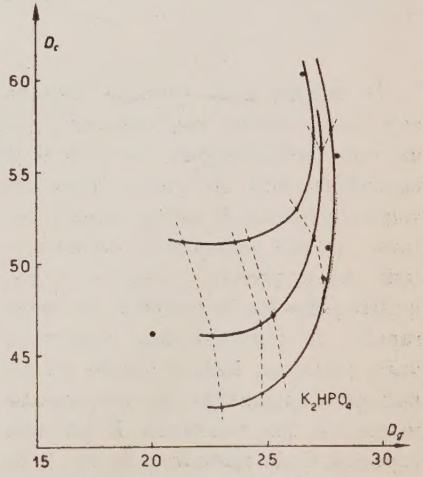

Fig. 4.

serie di soluzioni di acetone in acqua con costante dielettrica K nota e, per ogni soluzione, una serie di resistenze, derivate agli elettrodi, di valore compreso fra 50 e 1 000 ohm, in modo da conoscere per ogni singolo valore della capacità C_1 e della resistenza R la posizione D_c del condensatore C nel massimo della corrente (condizione di risonanza) ed il valore D_g, letto al galvanometro, proporzionale al valore della intensità di corrente, in tali condizioni di risonanza; si ottengono, riportando i valori di D_c e di D_g, due famiglie di curve: le une sono quelle che si ottengono mantenendo costante la resistenza R e facendo variare la capacità C_1; le altre mantenendo invece costante la capacità C_1 e facendo variare la resistenza R (nelle figure sono indicate con curva tratteggiata le isoohmiche, e con curva continua le isofarad). Costruito in tal modo questo reticolato di curve, si può porre nella cella una serie di soluzioni saline di varie concentrazioni, in modo da avere soluzioni a cui competono certi valori di R, e se per la presenza del sale la costanza dielettrica dell'acqua non varia, i punti figurativi delle soluzioni con diversa concentrazione, e cioè con diversa R, si devono trovare su di una linea con andamento compreso fra due successive curve isofarad; in caso diverso, e cioè se c'è variazione di K, la curva deve avere un andamento non parallelo alle isofarad di taratura.

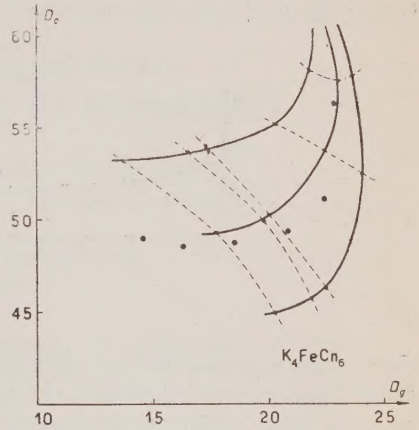

Fig. 5.

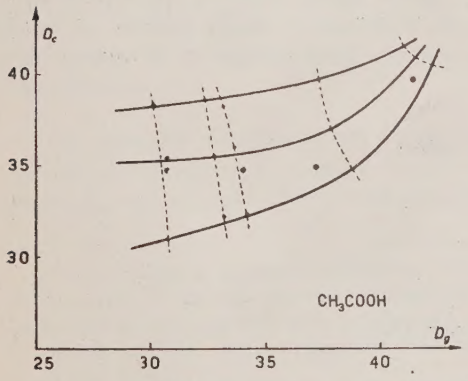

Fig. 6.

Le misure compiute in un primo ciclo sperimentale sono relative alle soluzioni di KCl (1-1), Na_2SO_4 (1-2), KH_2PO_4 (1-3), K_4FeCN_6 (1-4) e di un acido debole, CH_3COOH, le cui concentrazioni, come ordine di grandezza, vanno da 1/100 di mole/litro ad 1/1 000 di mole/litro. Le fig. 2, 3, 4, 5, 6 riportano i risultati ottenuti; da esse risulta che le soluzioni elettrolitiche presen-

tano effettivamente una variazione di costante dielettrica al variare della concentrazione dell'elettrolito. Dalla fig. 2, per esempio, nella quale, una volta per tutte, sono segnati i valori di K e di R nella famiglia delle curve di taratura, e che si riferisce alle soluzioni di KCl, è da notare, più particolarmente,

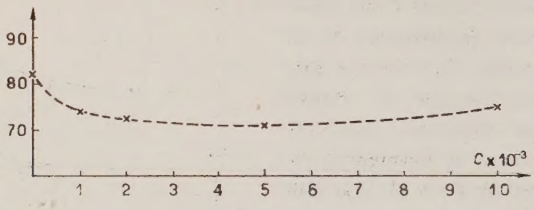

Fig. 7.

che le soluzioni più diluite, e cioè quelle a cui compete una R più grande, danno luogo a punti figurativi che appartengono a curve a cui corrisponde un certo valore di K, mentre i punti rappresentativi di soluzioni più concentrate (e cioè per R più piccolo), vanno a cadere su di una curva a cui corrisponde un valore di K inferiore al precedente, per riappartenere ad una isofarad di valore più vicino al primo per soluzioni di ancora più alta concentrazione. Dai punti figurativi si può, con una certa approssimazione, ricavare l'andamento del valore di K al variare della concentrazione. Tale andamento è riportato in fig. 7 per il K_4FeCN_6. Misure quindi condotte con metodo completamente diverso da quello usato da R. FÜRTH [1] hanno portato ad eguale risultato: una diminuzione e poi un aumento della costante K al crescere di c.

---

[1] R. FÜRTH: *Phis. Zeits.*, 25, 676 (1924).

SUMMARY

Measures have been made at high frequency ($\omega = 4.39 \cdot 10^7$) of the water dielectric constant when some electrolyte has been dissolved in it. It has been found that increasing the concentration c, the dielectric constant of the water diminishes and afterwards increases and the minimum has been ascertained to be when c is in the range of 10^{-3}.

A Phenomenological Theory of Cosmic Radiation in the Atmosphere (*).

P. Caldirola, R. Fieschi e P. Gulmanelli
Department of Physics - University of Milan

(ricevuto il 25 Ottobre 1951)

Summary. — The experimental results on the composition of cosmic radiation at the top of the atmosphere are used to develop a phenomenological theory of all processes which occur in the cosmic radiation while it traverses the atmosphere. We have computed the distribution of the fast nucleonic component (protonic and neutronic), the distribution of the mesonic component and its energy spectrum and positive excess at various altitudes, and the distribution of the electronic component. The latitude effects due to the earth's magnetic field are studied accurately. The theoretical results obtained are discussed, in the light of the most recent experimental data.

Introduction.

The primary component of cosmic radiation, which in traversing the atmosphere gives rise to most of the processes subject to experimental investigation, was thought [1] [2], until recently, to be formed mainly of protons.

(*) This paper is an organic exposition of the results obtained by one of the authors (P. Caldirola) and his coworkers during the last two years. Some of these results have already been published in preliminary papers:
P. Caldirola: *Atti del Congresso Internazionale di Como*, in *Suppl. Nuovo Cimento*, **6**, 511 (1949).
P. Caldirola: *Nuovo Cimento*, **6**, 565 (1949) (referred to as I).
P. Caldirola and A. Loinger: *Nuovo Cimento*, **7**, 161 (1950) (II).
P. Caldirola and G. Zin: *Nuovo Cimento*, **7**, 575 (1950) (III).
P. Caldirola and P. Gulmanelli: *Nuovo Cimento*, **8**, 229 (1951) (IV).
P. Caldirola, R. Fieschi and P. Gulmanelli: *Nuovo Cimento*, **8**, 508 (1951) (V).

[1] T. H. Johnson: *Rev. Mod. Phys.*, **11**, 208 (1939).
[2] M. Schein, W. P. Jesse and E. O. Wollan: *Phys. Rev.*, **59**, 615, 930 (1941).

More recent experiments (3) have proved that protons represent about 70÷75% of the primary radiation, while the remaining part is formed essentially of α-particles and of a smaller number of heavier nuclei.

The main problem in cosmic ray theory is to predict the existence and the behaviour in the atmosphere of the various components which arise from the primary protons and nuclei; and several attempts have already been made in this direction. Here we shall tackle the problem with the simplest hypothesis by studying in detail the following questions: *a*) the variation of the nucleonic component through the atmosphere; *b*) the origin and behaviour of the mesonic component, with emphasis on the existence of a positive excess varying with energy, altitude and latitude; and *c*) the origin and behaviour of the electronic component. We shall also study the latitude effect on the nucleonic and mesonic components, since this effect is connected with the process of generation of mesons.

Two different theories about meson production have been worked out some time ago: the multiple production theory due to WATAGHIN (4), HEISENBERG (5) and OPPENHEIMER LEWIS and WOUTHUISEN (6); and the plural production theory due to HEITLER and JANOSSY (7). Recent experiments have lead (8) physicists to believe that meson production has an intermediate character: in the collision between two nucleons the production is practically single up to a certain energy and then becomes multiple with increasing multiplicity for higher energies. A more satisfactory theory of meson production may then be the one recently developed by FERMI (9).

The scheme that we have adopted since 1949 is essentially phenomenological, though qualitatively based on the meson theory of nuclear forces. Indeed this theory in its « symmetrical » form justifies qualitatively the main

---

(3) P. FREIER, E. L. LONGFREN, E. P. NEY and F. OPPENHEIMER: *Phys. Rev.*, **74**, 1818 (1948); H. L. BRADT and B. PETERS: *Phys. Rev.*, **74**, 1838 (1948).

(4) G. WATAGHIN: *Phys. Rev.*, **74**, 975 (1948).

(5) W. HEISENBERG: *Nature*, **164**, 65 (1949); *Atti del Congr. Int. di Como* in *Suppl. Nuovo Cimento*, **6**, 491 (1949).

(6) H. W. LEWIS, J. R. OPPENHEIMER and S. A. WOUTHUISEN: *Phys. Rev.*, **73**, 127 (1948).

(7) W. HEITLER and L. JANOSSY: *Proc. Phys. Soc.*, A **62**, 374 (1949); A **62**, 669 (1949). The theoretical foundations of the hypothesis assumed here are exposed in the following papers: J. HAMILTON, W. HEITLER and H. W. PENG: *Phys. Rev.*, **64**, 78 (1943); W. HEITLER and P. WALSH: *Rev. Mod. Phys.*, **17**, 252 (1945); L. JANOSSY: *Phys. Rev.*, **64**, 345 (1945). Recently the scheme of HEITLER-JANOSSY has been further developed by MESSEL, particularly concerning low energies: *Communications of the Dublin Institute for Advanced Studies*, Series A. No. 7 (1951).

(8) See papers presented at the Como Conference (Sept. 1949) and relative discussions: *Atti del Congr. Int. di Como* in *Suppl. Nuovo Cimento*, **6**, 310 (1949).

(9) E. FERMI: *Progress in theor. Phys.*, **5**, 570 (1950); *Phys. Rev.*, **81**, 683 (1951).

features of the processes arising from the interaction of nucleons and its frequent failure to yield quantitative results is probably connected [10] with the inapplicability of current quantum methods of calculation to interactions between particles nearer than the elementary length $\lambda_0 = \sim \hbar/\mu_\pi c$ (μ_π = mass of the meson coupled to the nucleons identified with the π-meson). We assume that nuclear interactions are qualitatively of the symmetrical meson type and we derive by semiempirical considerations hypotheses apt to specify quantitatively the laws of interaction. In the collision of two nucleons of sufficiently high energy one or more mesons are created: at the beginning no hypothesis is made on the number of mesons, on their distribution with energy and among the three types π^+, π^-, π^0. Indeed, to derive the distribution law of the nucleonic component in the atmosphere, it is sufficient to specify how the kinetic energy of the incoming nucleon is distributed among the nucleon knocked-on, the scattered one and the mesons created. The comparison of the results with experimental data leads one then to specify the mechanism of creation of mesons and so to adopt hypotheses which allow to describe the process analitically and to calculate the distribution law of mesons in the atmosphere. The distribution of the electronic component is calculated with the theory of electromagnetic showers.

1. – Analysis of the nucleonic component.

1·1. – Interaction between nucleons.

We shall make rather simple assumptions on the energy distribution in the collision of two nucleons with the production of π-mesons in order to obtain expressions amenable to numerical calculation. Our hypotheses are taken from a paper by HÖCKER [11]. The incident nucleon with kinetic energy E gives up in a single collision a fraction $\varepsilon^* E_0$ (ε^* constant) of its energy to the mesons created, while the remaining energy $(1 - \varepsilon^*)E_0 = \varepsilon E_0$ is given to the two nucleons; owing to the high energy of the nucleons involved, we shall assume that the scattered nucleon can assume with equal probability any amount E of energy between 0 and εE_0 so that the nucleon knocked-on will assume the energy $\varepsilon E_0 - E$.

Energetically the creation of mesons in a nucleon-nucleon collision can occur if the energy of the incident nucleon is at least equal to the threshold energy $\mu_\pi c^2$. Obviously, if the energy is very near to the threshold the cross

[10] W. HEISENBERG: *Zeits. f. Phys.*, **101**, 533 (1936).
[11] K. H. HÖCKER: *Zeits. f. Phys.*, **124**, 351 (1948).

section is very small, as the artificial production of mesons proves [12]: the cross section will increase with increasing energy toward the geometric section as one observes in cosmic ray phenomena. For sake of simplicity we shall assume that the cross section σ is « effectively » different from zero only for values of the kinetic energy of the incident nucleon higher than or equal to a critical value E_π; and that for these values of the energy σ is effectively constant. We shall assume also that for energies $\geqslant E_\pi$ the nucleons lose energy only in collision processes with other nucleons: indeed, since $E_\pi = \sim 3$ GeV (GeV $= 10^9$ eV: gigaelectronvolt), the ionization loss for protons is small and the collision of nucleons with nuclei leading to the usual disintegrations has a much smaller cross section.

1·2. – Distribution of fast nucleons in the atmosphere.

We need to consider only the distribution of nucleons with kinetic energy E greater than or equal to the critical value E_π: we shall call these nucleons « fast » [13]. If the cut-off energy of the earth's field $E_\varphi \leqslant E_\pi$, there is no latitude effect on the production of mesons and on the subsequent processes. Here we shall study the global distribution of nucleons subject to the hypothesis $E_\varphi \leqslant E_\pi$: such a distribution can be calculated without further specifications on meson production.

$H(E, l)$ is [14] the total number of nucleons having an energy $\geqslant E$ at a depth l in the atmosphere, measured in units characteristic of the nucleon-nucleon collision [15]; $h(E, l)$ is the corresponding spectral density. So

$$(1) \qquad H(E, l) = \int_E^\infty h(E', l)\, \mathrm{d}E\,; \qquad h(E, l) = -\frac{\partial H(E, l)}{\partial E}\,.$$

---

[12] E. Gardner and C. M. G. Lattes: *Science*, **107**, 270 (1948); J. Burfening, E. Gardner and C. M. G. Lattes: *Phys. Rev.*, **75**, 382 (1949); V. Z. Peterson: *Phys. Rev.*, **79**, 407; **80**, 136 (1950); W. F. Cartwright, C. Richman, M. A. Wilcox, and M. H. Whitehead: *Phys. Rev.*, **78**, 823; **79**, 198 (1950); **81**, 652 (1951).

[13] B. Ferretti: *Nuovo Cimento*, **6**, 379 (1949) has divided the nucleonic component into three classes: *class A*, including nucleons with an energy higher than 600 MeV; *class B*, including nucleons with an energy between 200 and 600 MeV; and *class C* including nucleons with an energy less than about 200 MeV. The fast nucleonic component considered by us is formed by the most energetic fraction of the nucleons belonging to *class A*. This component is the most efficient source of mesons.

[14] The calculations of this section follow those of Höcker.

[15] If we indicate with h the vertical height in centimeters, with σ the nucleon-nucleon cross section in cm^2, with $A = A_0 \exp(-\gamma h)$ ($\gamma = 1/804\,000$) the number of nucleons contained in one cm^3 of atmosphere, we have $\mathrm{d}l = -A(h)\,\mathrm{d}h$: where from $l = (A_0\sigma/\gamma) \exp(-\gamma h)$.

The conservation equation reads:

$$H(E, l+\mathrm{d}l) = H(E, l) + \mathrm{d}H_{>}(E, l) - \mathrm{d}H_{<}(E, l)\,, \tag{2}$$

if $\mathrm{d}H_{>}$ and $\mathrm{d}H_{<}$ are the numbers of nucleons which in the depth $\mathrm{d}l$ have increased their energy above E, or, decreased it below E, respectively. With the assumptions of 1·1 and using the one-dimensional approximation (the scattered particle and the one knocked-on have the same direction as the incident particle) we have:

$$\mathrm{d}H_{<}(E, l) = \int_{E}^{E/\varepsilon} \mathrm{d}E' \cdot h(E', l)\,\mathrm{d}l + \int_{E/\varepsilon}^{\infty} \mathrm{d}E' \cdot h(E', l)\,\mathrm{d}l\,\frac{E}{\varepsilon E'}\,,$$

$$\mathrm{d}H_{>}(E, l) = \int_{E/\varepsilon}^{\infty} \mathrm{d}E' \cdot h(E', l)\,\mathrm{d}l\,\frac{\varepsilon E' - E}{\varepsilon E'}\,.$$

Then equation (2) yields, by partial integration, the following integro-differential equation:

$$-\frac{\partial H(E, l)}{\partial l} = H(E, l) - \frac{2}{\varepsilon}\int_{E/\varepsilon}^{\infty} \mathrm{d}E' \cdot H(E', l)\,\frac{E}{E'^2}\,. \tag{3}$$

The primary component at the top of the atmosphere is formed of protons with an energy spectrum $P(E, 0) = P_0 \cdot E^{-s}$ and of heavy nuclei with a total number of nucleons:

$$H^*(E, 0) = P^*(E, 0) + N^*(E, 0)\,,$$

where P^* and N^* are approximately equal. For the sake of simplicity we shall assume for these nucleons the same energy spectrum as for the primary protons:

$$H^*(E, 0) = H_0^* E^{-s}\,.$$

Since heavier nuclei are less effective than protons to produce mesons by interaction with the nuclei of the air (also because they lose more energy by ionization), we replace the primary nuclear component with an effective component of free nucleons, by putting:

$$H(E, 0) = P(E, 0) + \lambda H^*(E, 0) = (P_0 + \lambda H_0^*)E^{-s} = H_0 E^{-s}\,, \tag{4}$$

where $\lambda < 1$. The solution of (3), with the condition (4), is:

$$H(E, l) = H_0 E^{-s} \exp(-\alpha l) \qquad \left(\alpha = 1 - \frac{2\varepsilon^s}{s+1}\right). \tag{5}$$

This is the distribution law of fast nucleons in the atmosphere. The agree-

ment with experiment is good if s is taken between 1.5 and 2 (we shall choose 1.8 as most authors do) and α is taken to give a mean free path for absorption L between $110 \div 130$ g/cm^2 ([16]). The distribution law of nucleons in the atmosphere can as well be written as:

$$(5') \qquad H(E, x) = H_0 E^{-s} \exp(-x/x_0) \exp(x/x_1) = H_0 E^{-s} \exp(-x/L),$$

and the value of x_0 can be determined from the interaction of nucleons with air nuclei ([17]). Considering also the experimental results ([18]) in materials of atomic weight comparable to that of the air nuclei, one finds that x_0 is between 60 and 80 g/cm^2; the cross section is then slightly smaller than the geometric one (« transparency » of nuclear matter) ([19]).

The exact value of x_0 cannot be found by direct measurements, since in our theory air is schematized as an homogeneous distribution of nucleons. The values mentioned for x_0 and L give, through the identity of equations (5) and (5')

$$\frac{2\varepsilon^s}{s+1} = \frac{x_0}{x_1},$$

a value between 0.5 and 0.9 for ε: a more exact estimate of ε is provided by latitude effects (see n. 6). In our calculations we have assumed $L = 125$ g/cm^2 and $\varepsilon = 3/4$. In the collision between a nucleon of kinetic energy E and a nucleon of the atmosphere, a quarter of E is given to the mesons produced.

2. – Mechanism of meson production.

Let us consider the multiplicity k of meson production in a collision between two nucleons: k will be a function of the energy E of the incident nucleon. The mesonic component of cosmic rays shows a rather definite latitude effect at $\varphi = 45°$: the corresponding cut-off of the proton spectrum equals 3 GeV ([20]).

([16]) G. Bernardini, G. Cortini and A. Manfredini: *Phys. Rev.*, **74**, 1878 (1948); G. Wataghin: *Phys. Rev.*, **71**, 453 (1947); I. Tinlot: *Phys. Rev.*, **73**, 1456 (1948); E. P. George and A. P. Jason: *Nature*, **161**, 248 (1948); R. Maze, A. Fréon, J. Daudin and P. Auger: *Rev. Mod. Phys.*, **21**, 14 (1949).

([17]) G. Wataghin: *Phys. Rev.*, **75**, 693 (1949).

([18]) G. Cocconi: *Phys. Rev.*, **76**, 984 (1949).

([19]) The value assumed for the cross section of nucleon-nucleon interaction determines the value of the thickness of atmospheric matter corresponding to $l = 1$. From the assumed value of L, it follows that $l = 1$ is equivalent to about 72 g/cm^2. Consequently the whole atmospheric depth equals 14.4.

([20]) See L. Janossy: *Cosmic Rays* (Oxford, 1948), page 306.

This suggests that nucleons with an energy of few GeV are already capable of producing mesons: actually most of the mesons must be generated from primary nucleons with energy between 10^9 and a few times 10^{10} eV since the primary spectrum decreases rapidly with energy. In this limited field of energy we may assume for k a constant value: a nucleon of energy E creates in a single collision k mesons π with mean energy (intrinsic + kinetic) $\overline{w}_\pi = \varepsilon^* E/k$ ([21]).

Occhialini, Powell and coworkers ([22]) have shown that the π-mesons transform into μ-mesons with a total mean energy of about 4/5 of that of the generating π-mesons: if one takes E between 1 and 10 GeV, the mean energy of the mesons generated by the primary nucleons will be between $0.2/k$ GeV and $2/k$ GeV. Therefore in this interval of energy k cannot be much greater than 1: otherwise mesons derived from protons of few GeV would be almost absent from the meson spectrum at low altitude in contrast with experimental evidence. Several theoretical and experimental arguments had already been presented to suggest that, for $E \leq 10^9 \div 10^{10}$ eV, k is about unity ([23]): meson production would be predominantly due to plural processes.

We shall assume $k = 1$: this must be considered, however, as an hypothesis to be checked by its consequences on the behaviour of the nucleonic and mesonic components in the atmosphere. Furthermore the assumption will not be valid at high energies. According to the symmetrical theory of meson fields we shall assume that in the nucleon-nucleon collision the following cases can occur.

a) proton-proton collision; two possibilities exist:

$$P - P \quad \begin{cases} P + N + \pi^+ & \text{(probability } \gamma) \\ P + P + \pi^0 & \text{(» } 1 - \gamma) \end{cases}$$

b) neutron-neutron collision; two possibilities exist:

$$N - N \quad \begin{cases} P + N + \pi^- & \text{(probability } \gamma) \\ N + N + \pi^0 & \text{(» } 1 - \gamma) \end{cases}$$

([21]) The experimental results (U. Camerini, P. H. Fowler, W. O. Lock and H. Muirhead: *Phyl. Mag.*, **41**, 413 (1950)) on a power spectrum in the production of mesons do not contradict this assumption. Indeed such a spectrum implies that the mean energy of a meson is proportional to the energy of the incident nucleon.

([22]) C. M. G. Lattes, G. P. S. Occhialini and C. F. Powell: *Nature*, **160**, 413 and 486 (1947). The fraction of energy transferred to the meson is the same, if the meson is in motion or at rest: this can be proved by a Lorentz transformation.

([23]) Various arguments supporting a prevalent production of mesons through plural processes have been presented at the Como Conference (Sept. 1949) by L. Janossy and B. Ferretti.

c) neutron-proton collision; three possibilities exist:

$$\left.\begin{matrix} P+N \\ N+P \end{matrix}\right\} = \begin{cases} P+P+\pi^- & \text{(probability } \nu\text{)} \\ N+N+\pi^+ & \text{(} \quad \text{»} \quad \nu\text{)} \\ P+N+\pi^0 & \text{(} \quad \text{»} \quad 1-2\nu\text{)}. \end{cases}$$

3. – Distribution of fast protons and neutrons in the atmosphere.

3·1. – Solution of the system of integro-differential equations.

The distribution functions $P(E, l)$, $p(E, l)$ for the fast protons and $N(E, l)$, $n(E, l)$ for the fast neutrons are calculated using the scheme of reactions given above and the procedure of HÖCKER (1·2), properly extended.

Let η be the percentage of protons among all nucleons composing the nuclei in the atmosphere, then

$$\frac{\mathrm{d}P_<}{\mathrm{d}l} = \int_E^{E/\varepsilon} p(E', l)\,\mathrm{d}E' + (1-\eta)\nu \int_{E/\varepsilon}^{\infty} p(E', l)\,\mathrm{d}E' + \\ + [\eta + (1-\eta)(1-\nu)] \int_{E/\varepsilon}^{\infty} p(E', l)\,\frac{E}{\varepsilon E'}\,\mathrm{d}E',$$

$$\frac{\mathrm{d}P_>}{\mathrm{d}l} = [(\eta(1-\gamma) + (1-\eta)\nu] \int_{E/\varepsilon}^{\infty} p(E', l)\,\frac{\varepsilon E' - E}{\varepsilon E'}\,\mathrm{d}E' + \\ + [(1-\eta)\gamma + \eta] \int_{E/\varepsilon}^{\infty} n(E', l)\,\frac{\varepsilon E' - E}{\varepsilon E'}\,\mathrm{d}E'.$$

and

$$\frac{\mathrm{d}N_<}{\mathrm{d}l} = \int_E^{E/\varepsilon} n(E', l)\,\mathrm{d}E' + \eta\nu \int_{E/\varepsilon}^{\infty} n(E', l)\,\mathrm{d}E' + \\ + [(1-\eta) + \eta(1-\nu)] \int_{E/\varepsilon}^{\infty} n(E', l)\,\frac{E}{\varepsilon E'}\,\mathrm{d}E',$$

$$\frac{\mathrm{d}N_>}{\mathrm{d}l} = [(1-\eta)(1-\gamma) + \eta\nu] \int_{E/\varepsilon}^{\infty} n(E', l)\,\frac{\varepsilon E' - E}{\varepsilon E'}\,\mathrm{d}E' + \\ + [\eta\gamma + 1 - \eta] \int_{E/\varepsilon}^{\infty} p(E', l)\,\frac{\varepsilon E' - E}{\varepsilon E'}\,\mathrm{d}E'.$$

The conservation equation yields by partial integration the following system of equations:

$$(6)\quad \begin{cases} -\dfrac{\partial P(E,l)}{\partial l} = P(E,l) - [1+\eta(1-\gamma)]\dfrac{E}{\varepsilon}\displaystyle\int_{E/\varepsilon}^{\infty} P(E',l)\,\frac{dE'}{E'^2} - \\ \qquad\qquad - [(1-\eta)\gamma+\eta]\dfrac{E}{\varepsilon}\displaystyle\int_{E/\varepsilon}^{\infty} N(E',l)\,\frac{dE'}{E'^2}\,, \\ -\dfrac{\partial N(E,l)}{\partial l} = N(E,l) - [1+(1-\eta)(1-\gamma)]\dfrac{E}{\varepsilon}\displaystyle\int_{E/\varepsilon}^{\infty} N(E',l)\,\frac{dE'}{E'^2} - \\ \qquad\qquad - [\eta\gamma-(1-\eta)]\dfrac{E}{\varepsilon}\displaystyle\int_{E/\varepsilon}^{\infty} P(E',l)\,\frac{dE'}{E'^2}\,. \end{cases}$$

Obviously by summing these two equations one gets equation (3).

To apply equations (6) to the distribution of the protonic and neutronic components in the atmosphere, we may assume $\eta = 1/2$; then:

$$(6')\quad \begin{cases} -\dfrac{\partial P(E,l)}{\partial l} = P(E,l) - \dfrac{a}{\varepsilon}\displaystyle\int_{E/\varepsilon}^{\infty} P(E',l)\,\frac{E}{E'^2}\,dE' - \dfrac{b}{\varepsilon}\displaystyle\int_{E/\varepsilon}^{\infty} N(E',l)\,\frac{E}{E'^2}\,dE'\,, \\ \qquad\qquad \text{where } a = 1+\frac{1}{2}(1-\gamma) \\ -\dfrac{\partial N(E,l)}{\partial l} = N(E,l) - \dfrac{a}{\varepsilon}\displaystyle\int_{E/\varepsilon}^{\infty} N(E',l)\,\frac{E}{E'^2}\,dE' - \dfrac{b}{\varepsilon}\displaystyle\int_{E/\varepsilon}^{\infty} P(E',l)\,\frac{E}{E'^2}\,dE'\,, \\ \qquad\qquad \text{where } b = \frac{1}{2}(\gamma+1)\,. \end{cases}$$

The solutions of (6'), which satisfy the initial conditions

$$P(E,0) = (P_0 + \lambda H_0^*/2)E^{-s}\,, \qquad N(E,0) = (\lambda H_0^*/2)E^{-s}\,,$$

are:

$$(7)\quad \begin{cases} P(E,l) = \dfrac{E^{-s}}{2}\,[H_0\exp(-\alpha l) + P_0\exp(-\beta l)] \\ N(E,l) = \dfrac{E^{-s}}{2}\,[H_0\exp(-\alpha l) - P_0\exp(-\beta l)] \end{cases} \quad \text{with} \quad \begin{cases} \alpha = 1 - \dfrac{\varepsilon^s(a+b)}{s+1} \\ \beta = 1 - \dfrac{\varepsilon^s(a-b)}{s+1}\,. \end{cases}$$

So the spectral distribution functions are:

$$(8)\quad \begin{cases} p(E, l) = -\dfrac{\partial P(E, l)}{\partial E} = \dfrac{1}{2}\, sE^{-s-1}[H_0 \exp(-\alpha l) + P_0 \exp(-\beta l)] \\ n(E, l) = -\dfrac{\partial N(E, l)}{\partial E} = \dfrac{1}{2}\, sE^{-s-1}[H_0 \exp(-\alpha l) - P_0 \exp(-\beta l)] \\ h(E, l) = -\dfrac{\partial H(E, l)}{\partial E} = H_0 sE^{-s-1} \exp(-\alpha l)\ . \end{cases}$$

There are no direct experiments which allow to determine the probabilities γ and ν. We have assumed $\gamma = 1/2$ and $\nu = 1/3$ thus considering the different possibilities for each type of interaction equally probable for sake of simplicity and owing to the symmetry of nuclear forces [24]; also some later work of QUERCIA, RISPOLI and SCIUTI [25] on the dependence of the positive excess of the mesonic component on altitude and direction upholds the values chosen. These values yield $\alpha = 0.57$ and $\beta = 0.89$.

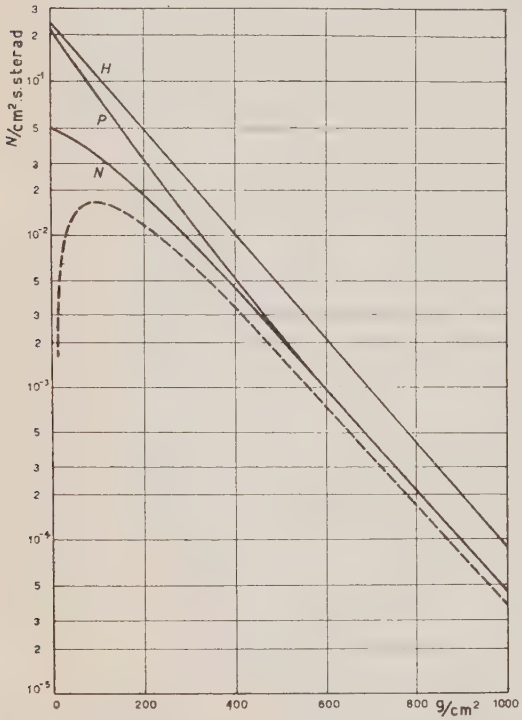

Fig. 1. – Distribution in the atmosphere of fast nucleons ($E > 3$ GeV).

3·2. – Numerical calculations.

Fig. 1 gives the absorption curves of the total nucleonic radiation and of its protonic and neutronic components. The absolute intensities depend on the

[24] This assumption is not verified experimentally for artificial mesons of low energy. However the theoretical arguments which give a greater probability for the production of non-identical particles do not appear to hold for the very fast nucleons considered here.

[25] I. F. QUERCIA, B. RISPOLI and S. SCIUTI: *Nuovo Cimento*, **7**, 715 (1950).

choice of values for H_0 and P_0 discussed in 4·5. The distribution arising from primary protons is represented by the dotted curve. The maximum which occurs there is absent from the curve for all neutrons owing to the large number of them contained in α-particles and heavier nuclei of the primary radiation. The slight maximum that the experimental curve seems to show at about 20 g/cm² is not a difficulty for our theory since we have completely neglected slow neutrons.

4. – Analisis of the mesonic component.

4·1. – Creation of mesons.

The scheme of n. 2 easily yields the espressions for the numbers $\mathrm{d}_l g^+(W_\pi, l)\mathrm{d}W_\pi$, $\mathrm{d}_l g^-(W_\pi, l)\,\mathrm{d}W_\pi$, $\mathrm{d}_l g^0(W_\pi, l)\,\mathrm{d}W_\pi$ of mesons π^+, π^- and π^0 with total energy between W_π, $W_\pi + \mathrm{d}W_\pi$ created between l ad $l + \mathrm{d}l$:

$$\mathrm{d}_l g^+ \mathrm{d}W_\pi = \left\{\left[\frac{\eta}{2} + (1-\eta)/3\right] p(E, l) + \frac{\eta}{3}\cdot n(E, l)\right\} \mathrm{d}E \cdot \mathrm{d}l,$$

$$\mathrm{d}_l g^- \mathrm{d}W_\pi = \left\{\left[\frac{\eta}{3} + (1-\eta)/2\right] n(E, l) + \frac{1-\eta}{3}\,(pE, l)\right\} \mathrm{d}E \cdot \mathrm{d}l\,,$$

$$\mathrm{d}_l g^0 \mathrm{d}W_\pi = \left\{\left[\frac{\eta}{2} + (1-\eta)\,3\right] p(E, l) + \left[\frac{1-\eta}{2} + \eta/3\right] n(E, l)\right\} \mathrm{d}E \cdot \mathrm{d}l\,.$$

Introducing the expressions (8) for $p(E, l)$ and $n(E, l)$ one obtains

$$(9)\quad \begin{cases} \mathrm{d}_l g^+ \mathrm{d}W_\pi = \dfrac{1}{24}\, s \left(\dfrac{W_\pi}{\varepsilon^*}\right)^{-s-1} [7H_0 \exp(-\alpha l) + 3P_0(-\beta l)] \dfrac{\mathrm{d}W_\pi \mathrm{d}l}{\varepsilon^*}\,, \\ \mathrm{d}_l g^- \mathrm{d}W_\pi = \dfrac{1}{24}\, s \left(\dfrac{W_\pi}{\varepsilon^*}\right)^{-s-1} [7H_0 \exp(-\alpha l) - 3P_0(-\beta l)] \dfrac{\mathrm{d}W_\pi \mathrm{d}l}{\varepsilon^*}\,, \\ d_l g^0 \mathrm{d}W_\pi = \dfrac{5}{12}\, s H_0 \left(\dfrac{W_\pi}{\varepsilon^*}\right)^{-s-1} \exp(-\alpha l) \dfrac{\mathrm{d}W_\pi \mathrm{d}l}{\varepsilon^*}\,. \end{cases}$$

We may assume that all the π^+, π^- meson quickly ($\sim 10^{-8}$ s) [26] transform into $\pi^\pm$ mesons according to the scheme

$$\pi^\pm \to \pi^\pm + n^0 \qquad (n^0, \text{ probably a neutrino}),$$

---

[26] The processes of interaction of π-mesons with nuclei is negligible in comparison with that of disintegration in non-condensed matter.

since we do not consider particles with very high energy. The numbers $\mathrm{d}_l g^{\pm}\,\mathrm{d}W_\pi$ give thus the numbers of $\pi^{\pm}$ mesons created in the length $\mathrm{d}l$. By putting $q = 0.8\varepsilon^* \cong 0.2$, we get:

$$(9') \qquad \mathrm{d}_l g^{\pm}(W, l)\,\mathrm{d}W = \frac{1}{24}\, s \left(\frac{W}{q}\right)^{-s-1} [7H_0 \exp(-\alpha l) \pm 3P_0 \exp(-\beta l)]\, \frac{1}{q}\,\mathrm{d}W\,\mathrm{d}l\,.$$

Recent experiments ([27]) on artificial and cosmic rays mesons prove that the neutretto π^0 almost instantaneously (the mean life is smaller than 10^{-14} s) disintegrates into two photons following the scheme

$$\pi^0 \to h\nu_1 + h\nu_2\,,$$

suggested ([28]) by FINKELSTEIN and by VERDE. Therefore we assume that neutrettos do not contribute to the meson component, but only to the electronic one ([29]).

4·2. – Distribution of mesons in the atmoshpere.

$\mu^{\pm}$-mesons can disintegrate (mean life $\tau_0 \cong 2.15 \cdot 10^{-6}$ s) into one electron (+ or —) and into two neutral particles (apparently neutrinos): this would decrease the number of $\mu^{\pm}$ mesons in a lenght $\mathrm{d}l$ by:

$$(10) \qquad \mathrm{d}_l^- g^{\pm}(W, l)\,\mathrm{d}W = g^{\pm}(W, l)\,\frac{\mathrm{d}t}{\tau}\,\mathrm{d}W =$$

$$= \frac{\mu_0 c^2}{\tau_0 W}\, g^{\pm}(W, l)\,\mathrm{d}t\,\mathrm{d}W = \frac{B}{Wl}\, g^{\pm}(W, l)\,\mathrm{d}W\,\mathrm{d}l\,,$$

where

$$B = \frac{1}{\tau_0 c\gamma} \cdot \mu_0 c^2 \cong 1.31 \text{ GeV}\,.$$

Furthermore the ionization losses are given by

$$(11) \qquad \mathrm{d}_l^J g^{\pm}(W, l)\,\mathrm{d}W = \frac{\partial g^{\pm}(W, l)}{\partial W} \left(\frac{\mathrm{d}W}{\mathrm{d}l}\right)_J \mathrm{d}W\,\mathrm{d}l\,,$$

([27]) R. E. MARSHAK: *Phys. Rev.*, **76**, 1736 (1949); A. LOVATI, A. MURA, G. SALVINI and G. TAGLIAFERRI: *Nuovo Cimento*, **7**, 943 (1950); M. F. KAPLON, H. L. BRADT and B. PETERS: *Helv. Phys. Acta*, **23**, 28 (1950); R. BJORKLUND, W. E. CRANDALL, B. J. MOYER and H. F. YORK: *Phys. Rev.*, **77**, 213 (1950); W. K. H. PANOFSKY, LEE AAMODT and H. F. YORK: *Phys. Rev.*, **78**, 825 (1950); A. G. CARLSON, J. E. HOOPER and D. T. KING: *Phyl. Mag.*, **41**, 701 (1950).

([28]) R. FINKELSTEIN: *Phys. Rev.*, **72**, 415 (1947); M. VERDE: *Ric. Scient.*, **17**, 2031 (1947).

([29]) H. W. LEWIS, J. R. OPPENHEIMER and S. A. WOUTHUISEN: *Phys. Rev.*, **73**, 127 (1948).

where we assume [30]

$$\left(\frac{\mathrm{d}W}{\mathrm{d}l}\right)_J = \delta = \text{const} \cong 1.48 \cdot 10^8 \text{ eV} .$$

The balance will yield

$$\frac{\partial g^{\pm}}{\partial l} = \frac{1}{24}\frac{s}{q}\left(\frac{W}{q}\right)^{-s-1}[7H_0 \exp(-\alpha l) \pm 3P_0 \exp(-\beta l)] - B\frac{g^{\pm}}{Wl} + \delta\frac{\partial g^{\pm}}{\partial W} . \tag{12}$$

The solution is

$$g^{\pm}(W, l) = R(W, l)\left[7\frac{H_0}{P_0}\Phi_{\alpha}(W, l) \pm 3\Phi_{\beta}(W, l)\right] , \tag{13}$$

where

$$R(W, l) = \frac{P_0}{24}\frac{s}{q}\left(\frac{\delta}{q}\right)^{-s-1}\left(\frac{W}{\delta l}\right)^{Bl/(W+\delta l)} , \tag{14}$$

$$\Phi_{\varrho}(W, l) = \int_0^l \exp(-\varrho x) x^{Bl/(W+\delta l)}\left(\frac{W}{\delta} + l - x\right)^{Bl/(W+\delta l)-s-1} \mathrm{d}x . \tag{15}$$

These results hold for $W \geqslant W_0 = qE_{\pi}$. If $W < W_0$, equation (12) reads

$$\frac{\partial g_{<}^{\pm}}{\partial l} = -B\frac{g_{<}^{\pm}}{Wl} + \delta\frac{\partial g_{<}^{\pm}}{\partial W} , \tag{16}$$

since no mesons of such energy are created directly. The solutions of (16) which join smoothly the solution (13) (valid for $W \geqslant W_0$) are

$$g_{<}^{\pm}(W, l) = R(W, l)\left[7\frac{H_0}{P_0}\Phi_{\alpha}(W_0, l) \pm 3\Phi_{\beta}(W_0, l)\right] . \tag{17}$$

The expressions for the total mesonic component are

$$g(W, l) = 14\frac{H_0}{P_0}R(W, l)\Phi_{\alpha}(W, l) , \qquad g_{<}(W, l) = 14\frac{H_0}{P_0}R(W, l)\Phi_{\alpha}(W_0, l) .$$

These results hold for magnetic latitudes higher than the latitude φ for which the cut-off energy for protons E_q equals the critical energy E_{π} for the production of mesons (1·2).

---

[30] The ionization loss is thought to be about $2.08 \cdot 10^7$ eV for one cm of Hg. Considering $\sigma = 2.27 \cdot 10^{-26}$ cm², $l = 1$ corresponds to about 72 g/cm², thus giving the assumed value of δ.

4·3. – Positive excess of the mesonic component.

The positive excess is a good check on any theory on the mechanism of meson production. The usual measure of the positive excess is

$$\varepsilon(W, l) = 2\,\frac{g^+(W, l) - g^-(W, l)}{g^+(W, l) + g^-(W, l)}\,;$$

the differential positive excess so defined is a function of the energy of mesons and of the altitude. Our theory yields, by using (13) (16),

for $W \geqslant W_0$ $$\varepsilon(W, l) = \frac{6}{7}\,\frac{P_0}{H_0}\,\frac{\Phi_\beta(W, l)}{\Phi_\alpha(W, l)}\,;$$

and for $W \leqslant W_0$ $$\varepsilon(W, l) = \frac{6}{7}\,\frac{P_0}{H_0}\,\frac{\Phi_\beta(W_0, l)}{\Phi_\alpha(W_0, l)}\,.$$

The positive excess for $W < W_0$ should be constant: obviously this result derives from assuming σ constant for $E \geqslant E_\pi$ and zero for $E < E_\pi$. Actually σ will certainly not vanish for $E < E_\pi$, but will go to zero gradually. So our value of $\varepsilon(W, l)$ is an upper bound for $W < W_0$: a lower bound would be obtained by applying in this energy interval the formulas valid for $W > W_0$.

4·4. – Effects of the multiple production of mesons.

In the collision of nucleons of high energy (above some 10 GeV) production of mesons with multiplicity higher than one can occur. These processes are less important than those with multiplicity one for cosmic rays in the atmosphere: however they might exert an appreciable influence on some quantities (e.g. the positive excess of the mesonic component).

To evaluate the importance of multiple processes, we have computed the influence on the distribution of mesons of the following production with multiplicity 2:

$$P + P = \begin{cases} P + P + \pi^0 + \pi^0 \\ P + P + \pi^+ + \pi^- \\ P + N + \pi^0 + \pi^+ \\ N + N + \pi^+ + \pi^+ \end{cases} \qquad N + N = \begin{cases} N + N + \pi^0 + \pi^0 \\ N + N + \pi^+ + \pi^- \\ N + P + \pi^0 + \pi^- \\ P + P + \pi^- + \pi^- \end{cases}$$

$$\left.\begin{matrix} P + N \\ N + P \end{matrix}\right\} - \begin{cases} P + N + \pi^0 + \pi^0 \\ P + N + \pi^+ + \pi \\ P + P + \pi^0 + \pi^- \\ N + N + \pi^0 + \pi^+ \end{cases}.$$

Equal probability is assigned to the various possibilities in each collision process. One obtains the following equations for the proton and neutron distributions in the atmosphere:

$$(18)\quad \begin{cases} -\dfrac{\partial P(E,l)}{\partial l} = P(E,l) - \dfrac{9}{8\varepsilon}\displaystyle\int_{E/\varepsilon}^{\infty} P(E',l)\,\frac{E}{E'^2}\,\mathrm{d}E' - \frac{7}{8\varepsilon}\int_{E/\varepsilon}^{\infty} N(E',l)\,\frac{E}{E'^2}\,\mathrm{d}E' , \\ -\dfrac{\partial N(E,l)}{\partial l} = N(E,l) - \dfrac{9}{8\varepsilon}\displaystyle\int_{E/\varepsilon}^{\infty} N(E',l)\,\frac{E}{E'^2}\,\mathrm{d}E' - \frac{7}{8\varepsilon}\int_{E/\varepsilon}^{\infty} P(E',l)\,\frac{E}{E'^2}\,\mathrm{d}E' ; \end{cases}$$

their solutions are:

$$(19)\quad \begin{cases} P(E,l) = \dfrac{1}{2}\,E^{s}[H_0\exp(-\alpha l) + P_0\exp(-\beta_2 l)] \\ N(E,l) = \dfrac{1}{2}\,E^{-s}[H_0\exp(-\alpha l) - P_0\exp(-\beta_2 l)] \end{cases} \quad \text{where} \quad \begin{cases} a = 1 - \dfrac{2\varepsilon^s}{s+1} = 0.574 \\ \beta_2 = 1 - \dfrac{\varepsilon^s}{4(s+1)} = 0.947 . \end{cases}$$

The corresponding equations for the distribution of mesons produced in double processes are:

$$(20)\quad \begin{cases} \dfrac{\partial g_2^{\pm}(W,l)}{\partial l} = \dfrac{s}{8}\left(\dfrac{2W}{q}\right)^{-s-1}[9H_0\exp(-\alpha l) \pm 3P_0\exp(-\beta_2 l)] - \\ \qquad\qquad - B\,\dfrac{g_2^{\pm}(W,l)}{Wl} + \delta\,\dfrac{\partial g_2^{\pm}(W,l)}{\partial W}, \qquad \text{for } W \geqslant \dfrac{W_0}{2} , \\ \dfrac{\partial g_2^{\pm}(W,l)}{\partial l} = -B\,\dfrac{g_2^{\pm}(W,l)}{Wl} + \delta\,\dfrac{\partial g_2^{\pm}(W,l)}{\partial W}, \qquad \text{for } W \leqslant \dfrac{W_0}{2} . \end{cases}$$

Their solutions read:

$$\begin{cases} g_2^{\pm}(W,l) = \dfrac{3}{2^{s+1}}\,R(W,l)\left[9\,\dfrac{H_0}{P_0}\,\Phi_{\alpha}(W,l) \pm 3\Phi_{\beta_2}(W,l)\right], & W \geqslant \dfrac{W_0}{2} \\ g_2^{\pm}(W,l) = \dfrac{3}{2^{s+1}}\,R(W,l)\left[9\,\dfrac{H_0}{P_0}\,\Phi_{\alpha}\left(\dfrac{W_0}{2},l\right) \pm 3\Phi_{\beta_2}\left(\dfrac{W_0}{2},l\right)\right], & W \leqslant \dfrac{W_0}{2} . \end{cases}$$

It is easy to verify that the positive excess calculated on the ground of meson production of multiplicity 2 is much smaller than the one for multiplicity 1. On the other hand the probability of the « double » processes increases with energy. We shall assume that in a certain interval of energy no processes of multiplicity greater than 2 occur: then the number $g(W,l)$ of mesons of energy W observed at a depth l can be written as a sum of the number of mesons created, with the probability $a(W,l)$, in double processes and of the number of mesons created, with the probability $1 - a(W,l)$, in single processes

$$g(W,l) = g^{+}(W,l) + g^{-}(W,l) = [1 - a(W,l)]g_1(W,l) + a(W,l)g_2(W,l) .$$

The differential positive excess is given by

$$(21) \qquad \varepsilon(W, l) = 2\,\frac{g^+(W, l) - g^-(W, l)}{g^+(W, l) + g^-(W, l)} =$$

$$= 2\,\frac{[1 - a(W, l)][g_1^+(W, l) - g_1^-(W, l)] + a(W, l)[g_2^+(W, l) - g_2^-(W, l)]}{[1 - a(W, l)]g_1(W, l) + a(W, l)g_2(W, l)}.$$

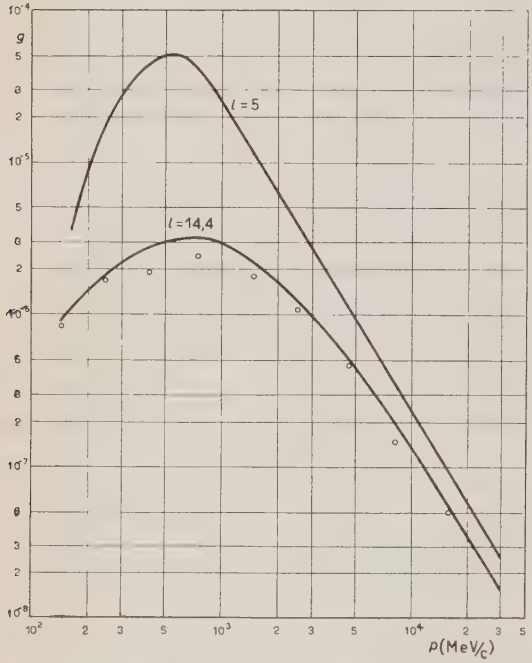

Fig. 2. – Spectral distribution of mesons at different dephts (at sea level and at 360 g/cm²).
○ Wilson

where the function $a(W, l)$ can be determined from experimental results (see the following number).

4·5. – Numerical calculations and comparison with experiments.

Fig. 2 gives the curves for spectral distribution of the mesonic component for $l = 14.4$ (sea level) and for $l = 5$ (about 8 000 m a. s. l.): E_π has been taken equal to 3 GeV to have a latitude effect beginning at $\varphi = 45°$ in agreement with experiment. The curves are very similar to the experimental ones obtainable by extrapolating the results of HALL [31] (experiments performed at Mount Evans, about 4 350 m) and of SCHEIN and coworkers [32] (experiments performed at 5-6 000 m) for the high altitude part and using the results of WILSON [33] and BLACKETT [34] for the low altitude part. The comparison of the two curves shows also the well established increase of the number of slow mesons with altitude.

---

[31] D. B. HALL: *Phys. Rev.*, **66**, 321 (1944).
[32] M. SCHEIN, O. E. WOLLAN and G. GROTZINGER: *Phys. Rev.*, **58**, 1027 (1940).
[33] J. G. WILSON: *Nature*, **158**, 414 (1946).
[34] P. M. S. BLACKETT: *Proc. Roy. Soc.*, A **159**, 1 (1937); see L. LEPRINCE-RINGUET and J. CRUSSARD: *Journ. de Phys. et Rad.*, **8**, 207 (1937).

Numerical integration on the energy spectrum of mesons for different values of l has yielded the number of mesons at different altitudes. Mesons have been classified as fast ($W > 0.33$ GeV) and as slow ($W < 0.33$ GeV) to compare our results with the experimental curves of Rossi ([35]). Fig.s 3 and 4 show the results obtained. H_0, the only parameter yet indetermined, has been chosen to give the correct number of fast mesons at sea level: the data on the distribution of fast mesons are more exact than those for slow mesons. Fig. 3 shows that the theoretical absorption is slightly steeper than the experimental one: the position of the maximum is at 200 g/cm², in good agreement with experiments. The agreement is certainly satisfactory, if one considers the simplifying assumptions of the theory (one-dimensional approximation, assumption on the cross section, etc.) and the uncertainty of the experimental data.

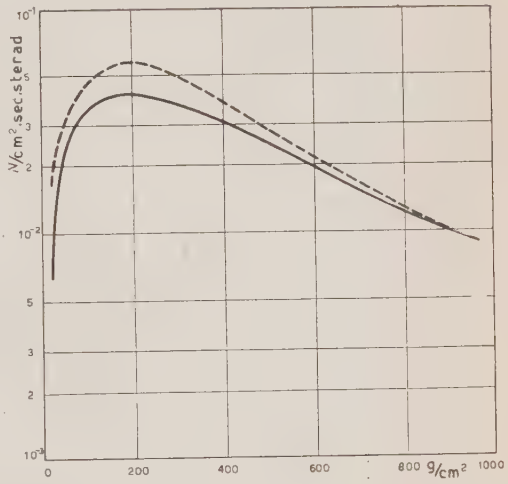

Fig. 3. – Distribution of fast mesons in the atmosphere.
——— Experimental curve (Rossi)
- - - Theoretical curve.

The value found for H_0 ($2.8 \cdot 10^{16}$ cm^{-2}s^{-1}sterad^{-1} eV$^{1.8}$) has been used to calculate the distribution of slow mesons: fig. 4 gives the results. The number of slow mesons is slightly smaller than the experimental one: however the simplifying assumptions on the cross section reduce appreciably the probability of production of slow mesons and, on the other side, experimental data are quite uncertain.

The results obtained allow us to determine the parameter λ which measures efficiency of production of mesons by the nucleons contained in α-particles and heavier nuclei. Indeed the experimental results ([36]) on the spectrum and the nature of particles (protons and nuclei) arriving at the top of the

([35]) B. Rossi: *Rev. Mod. Phys.*, **20**, 537 (1948).

([36]) The observations on the *particles* incident at the top of the atmosphere can be interpreted by assuming an integral spectrum of the type $2.4 \cdot 10^{16} \cdot E^{-2.8}$, and considering the protons to be a bit more than 70% of the incident particles (equal to about 30% of the total number of nucleons).

atmosphere give the values

$$P_0 = 1.68 \cdot 10^{16} \text{ cm}^{-2} \text{ s}^{-1} \text{ sterad}^{-1} \text{ eV}^{1.8}$$

$$H_0 = 2.84 \cdot 10^{16} \text{ cm}^{-2} \text{ s}^{-1} \text{ sterad}^{-1} \text{ eV}^{-1.8};$$

since equation (4) holds, the value already found for H_0 gives $\lambda = 0.39$.

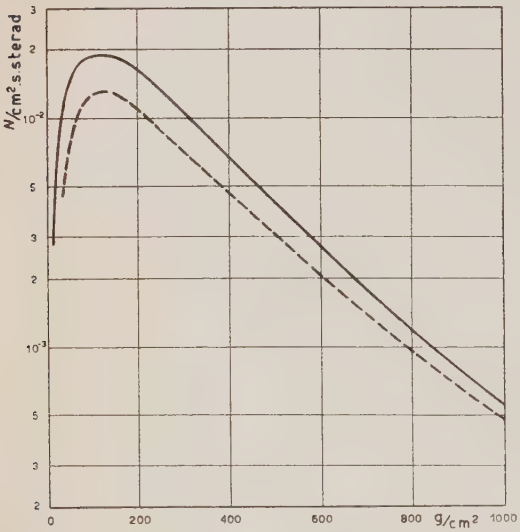

Fig. 4. – Distribution of slow mesons in the atmosphere.

——— Experimental curve (Rossi)

– – – – Theoretical curve.

This result is very useful in interpreting the experimental data on the positive excess of the mesonic component. The existence of this excess was proved experimentally by various authors [37] and particularly by the direct experiments of Bernardini and coworkers [38]: these measurements seem to indicate a value of 15 ($\pm$ 5) % for the integral excess (cut-off energy 0.3 $\div$ 0.5 GeV) at sea level. The first measurement [39] of the positive excess of mesons for given energy showed a rather uncertain decrease of the differential excess with increasing energy: later results of Brode [40], of the group of Padova [41], of Wilson and Owen [42] and of Caro, Parry and Rathgeber [43] show a noticeable increase of the positive excess with energy up to 5 GeV while, at higher

---

[37] H. Jones: *Rev. Mod. Phys.*, **11**, 235 (1939); D. J. Hughes: *Phys. Rev.*, **57**, 592 (1940).

[38] G. Bernardini, M. Conversi, E. Pancini, E. Scrocco and G. C. Wick: *Phys. Rev.*, **68**, 109 (1945).

[39] M. Conversi, E. Pancini and O. Piccioni: *Nuovo Cimento*, **3**, 372 (1946); N. Nereson: *Phys. Rev.*, **73**, 365 (1948).

[40] R. B. Brode: *Bull. Am. Phys. Soc.*, **5**, 24 (1949); Como Confer. Sept. 1949.

[41] P. Bassi, E. Clementel, I. Filosofo and G. Puppi: Como Confer. Sept. 1949.

[42] J. G. Wilson: Como Confer. Sept. 1949; B. G. Owen and J. G. Wilson: *Proc. Phys. Soc.*, A **64**, 417 (1951).

[43] D. E. Caro, J. K. Parry, and A. D. Rathgeber: *Nature*, **165**, 689 (1950).

energies, the accurate measurements of WILSON and OWEN show a decrease of the excess.

Fig. 5 shows the theoretical curves for the positive excess due to single and double meson production and also the experimental curves of WILSON and OWEN. Below 5 GeV the first theoretical curve agrees well with the

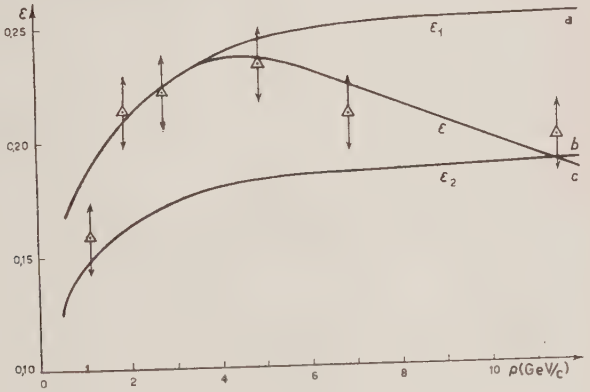

Fig. 5. – Differential positive excess at sea level.
△ Wilson.

experimental one, indicating that mesons in this energy interval have been created by nucleons (with an energy $\leqslant 25$ GeV) by single processes. The decrease of the positive excess of mesons of energy higher than 5 GeV indicates instead that nucleons of energy higher that 25 GeV create mesons by multiple processes with multiplicity increasing with energy. Assuming that only single and double processes occur up to a certain energy, formula (21) holds. Up to energies of 11 GeV, it is possible to determine the function $a(W)$ in it to obtain a fair agreement between theoretical and experimental results; above 11 GeV this is not possible any more, indicating that at these energies multiplicities higher than two are present. Since the average energy W of a meson is connected with the energy of a generating primary by the relation

$$E = (1 - a)\frac{W}{q} + 2\frac{W}{q}a = \frac{W}{q}(1 + q),$$

we can obtain the dependence of the average multiplicity on the energy of the incident nucleon

$$K(E) = 2a + (1 - a) = a + 1.$$

This is illustrated in fig. 6 ([44]). The calculations seem to show that in the collision of two nucleons the production of mesons is practically single up to energies of 25 GeV; while, for energies between 25 and 70 GeV, double production is important and is actually prevalent beyond a certain point. For energies above ~ 70 GeV the multiplicity is higher.

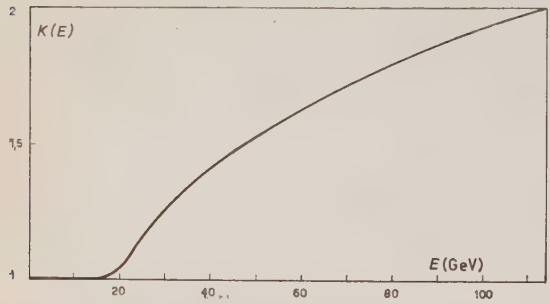

Fig. 6. – Dependence of the production multiplicity on the energy of the incident nucleon.

Fig. 7 shows that on passing from $l = 14.4$ (sea level) to $l = 5$ (360 g/cm^2) the positive excess does slightly increase. This result of our calculation agrees even quantitatively with the measurements of Quercia, Rispoli and Sciuti ([45]) at high altitudes. Even more significant is the agreement of our theory with the results of these authors ([46]) on the dependence of the positive excess on the direction of the mesons.

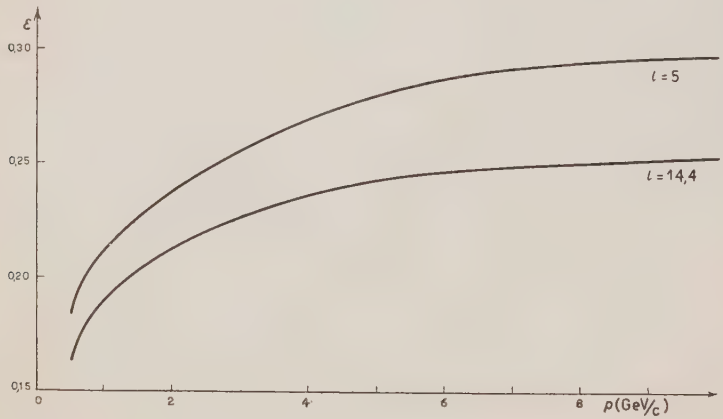

Fig. 7. – Differential positive excess at sea level and at 360 g/cm^2.

([44]) In determining the function $K(E)$ we have not considered the ionization losses of mesons, from their production quota to sea level. Owing to this simplification the values of E, in the figure corresponding to K, are to low of a few GeV.

([45]) I. F. Quercia, B. Rispoli and S. Sciuti: *Nuovo Cimento*: 5, 397 (1948); see M. Conversi: *Phys. Rev.*, **76**, 311 (1949).

([46]) I. E. Quercia, B. Rispoli and S. Sciuti: *Nuovo Cimento*, **7**, 715 (1950).

All our calculations have been done on the assumption of a very particular mechanism of energy transfer from the incident nucleon to the scattered one and to the mesons produced. Though our results depend on the assumptions made, we believe that reasonable modification of them will not produce substantial changes. Furthermore, since experimental data are uncertain, our considerations are purely indicative.

5. – The electronic component.

5·1. – General remarks.

The electromagnetic component of cosmic rays is generated by different processes: the most important is now considered to be the disintegration of the neutretto into two photons.

Since it appears plausible that the number of neutrettos produced in the interaction between nucleons is comparable with the number of charged mesons, it is obvious that this process should be the main source of the electromagnetic component, expecially at high altitudes. Important contributing effects, however, are the disintegration of μ-mesons and their knock-on collisions on the electrons of the air. On the other hand, the knock-on of protons, the direct production of γ-rays in stars or in collisions between nucleons and the absorption of π^- mesons by nucleons, according ([47]) to BRUNO and to MARSHAK, do not give an appreciable contribution and are not considered in our calculations.

5·2. – Disintegration of the neutretto.

The assumption of isotropic emission of the two photons in the center of mass system gives the value $W_\pi/2$ for the average energy of each photon. The number of photons produced between l and $l + \mathrm{d}l$ is then given by

$$\mathrm{d}_l\gamma(W, l)\,\mathrm{d}W = 4\mathrm{d}_l g^0(2W, l)\,\mathrm{d}W\,.$$

Assuming that π^0 disintegrate immediately after creation, equation (9) gives the following average spectrum of formation:

$$\mathrm{d}_l\gamma(W, l)\,\mathrm{d}W = \frac{5}{3}\,sH_0\left(\frac{2W}{\varepsilon^*}\right)^{-s-1}\exp\left(-\alpha l\right)\frac{\mathrm{d}W}{\varepsilon^*}\,\mathrm{d}l\,.$$

([47]) R. E. MARSHAK and A. S. WIGHTMAN: *Phys. Rev.*, **76**, 114 (1949); B. BRUNO: *Ark. Phys.*, **1**, 19 (1949).

Naturally this holds only for latitudes such that $E_q \leqslant E_\pi$; then the minimum value of W in the spectrum of photons is $\varepsilon^* E_\pi/2$.

Under these boundary conditions the theory of showers ([48]) in Arley's ([49]) approximation yields the following electronic integral-spectrum

$$
(22)\quad \left\{
\begin{aligned}
\Pi(E,t) = {} & \left\{ \frac{B_0}{E_j^{s+1}} \left[\frac{E_j}{s} \frac{\exp[\lambda_1(s)t] - \exp[-a\alpha t]}{\lambda_1(s) + a\alpha} - \frac{\exp[\lambda_2(s)t] - \exp[-a\alpha t]}{\lambda_2(s) + a\alpha} \right] + \right. \\
& + \left[\frac{\exp[\lambda_1(s)t]}{\lambda_1(s)} \cdot \frac{1 - \exp[-\lambda_1(s)\varrho]}{\lambda_1(s) + a\alpha} + \frac{\exp[-a\alpha t]}{a\alpha} \cdot \frac{1 - \exp[a\alpha\varrho]}{\lambda_1(s) + a\alpha} - \right. \\
& \left. \left. - \frac{\exp[\lambda_2(s)t]}{\lambda_2(s)} \cdot \frac{1 - \exp[-\lambda_2(s)\varrho]}{\lambda_2(s) + a\alpha} + \frac{\exp[-a\alpha t]}{a\alpha} \cdot \frac{1 - \exp[a\alpha\varrho]}{\lambda_2(s) + a\alpha} \right] \right\}.
\end{aligned}
\right.
$$

For details see paper IV.

5·3. – Electrons from μ-mesons disintegration and knock-on electrons.

It is almost certain ([50]) that $\mu^\pm$ mesons disintegrate in one electron (+ and —) and two neutrinos. The spectra of the decay electrons give for the mean energy E' in the reference system of the meson a value between 35 and 40 MeV: the most probable value is 36 MeV. In the laboratory system $\overline{E} = 36\,(W/\mu_0) = \chi\, W$; then the spectrum of formation of the decay electron is:

$$
\pi(E,t)\,\mathrm{d}E\,\mathrm{d}t = \frac{B}{Et}\, g\left(\frac{E}{\chi}, at\right) \mathrm{d}E\,\mathrm{d}t\,.
$$

The problem of the shower originated from this source has been solved in paper IV by means of Mellin transforms and the saddle point method, both for energies higher and lower then the critical energy E_j of the air.

Similarly one could evaluate the contribution to the electromagnetic component from the knock-on of μ-mesons: however the formula for the highest energy given to the electron shows that the contribution of slow mesons can be forgotten.

The calculations for fast mesons do not need to be carried out, since the

([48]) B. Rossi and K. Greisen: *Rev. Mod. Phys.*, **13**, 240 (1941).

([49]) N. Arley: *Proc. Roy. Soc.*, A **168**, 519 (1938).

([50]) E. P. Hincks and B. Pontecorvo: *Phys. Rev.*, **75**, 698 (1949); R. B. Leighton, C. D. Anderson and A. J. Seriff: *Phys. Rev.*, **75**, 1432 (1949); J. D. Davies, W. O. Lock and H. Muirhead: *Phyl. Mag.*, **40**, 1250 (1950).

ratio of the intensity of the electromagnetic component for knock-on to those for decay, for the same spectrum of generating mesons, is already known ([51]).

5·4. – Numerical valuations.

Fig. 8 compares our results with the measurements of POMERANTZ ([52]) and with the curve of ROSSI ([35]): the agreement between theory and experiment is satisfactory. The dotted curve gives the partial contribution of neutrettos: the depth corresponding to the maximum of the curve agrees with experiment and its position is not very sensitive to the values chosen for the parameters; the intensity of the curve near the maximum almost equals the total intensity and the difference of the two logically increases towards low altitude.

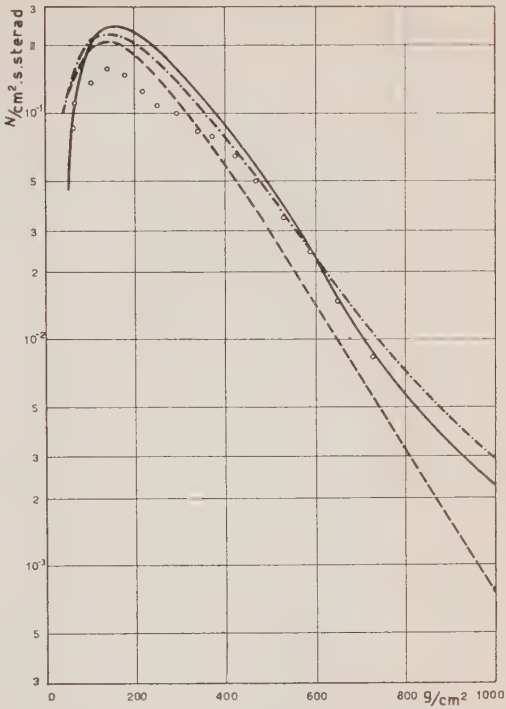

Fig. 8. – Distribution of the electronic component in the atmosphere.

– · – · – Theoretical curve
– – – – Partial contribution of nutrettos.
——— Rossi
○ ○ ○ Pomerantz

The calculations show that slow mesons are much less important than fast ones.

([51]) B. ROSSI and S. J. KLAPMAN: *Phys. Rev.*, **61**, 414 (1942); G. BERNARDINI, B. N. CACCIAPUOTI and B. QUERZOLI: *Nuovo Cimento*, **3**, 349 (1946); L. JANOSSY: *Cosmic Rays* (Oxford, 1948), page 247.

([52]) M. A. POMERANTZ: *Phys. Rev.*, **75**, 69 and 1721 (1949); **77**, 830 (1950).

6. – Latitude effects.

6·1. – Latitude effect of the nucleonic component.

We have to integrate equations (6′) of the nucleonic shower under proper initial conditions. Let $E_\varphi > E_\gamma$ be the cut-off energy of the earth's field at the magnetic latitude φ: the initial conditions read

$$\begin{cases} P(E, 0) = \left(P_0 + \lambda \dfrac{H_0^*}{2}\right) E_\varphi^{-s} & (0 < E < E_\varphi) \\ P(E, 0) = \left(P_0 + \lambda \dfrac{H_0^*}{2}\right) E^{-s} & (E_\varphi \leqslant E)\,. \end{cases}$$

$$\begin{cases} N(E, 0) = \lambda \dfrac{H_0^*}{2} E_\varphi^{-s} & (0 < E < E_\varphi) \\ N(E, 0) = \lambda \dfrac{H_0^*}{2} E^{-s} & (E_\varphi \leqslant E)\,. \end{cases}$$

A detailed study of equations (6′) under these conditions was carried out in paper III. $H(E, l) = P(E, l) + N(E, l)$ and $K(E, l) = P(E, l) - N(E, l)$ satisfy the equations:

$$(23) \qquad \begin{cases} -\dfrac{\partial H(E, l)}{\partial l} = H(E, l) - \dfrac{(a+b)}{\varepsilon} E \displaystyle\int_{E/\varepsilon}^{\infty} H(E', l) \frac{\mathrm{d}E'}{E'^2} \\ -\dfrac{\partial K(E, l)}{\partial l} = K(E, l) - \dfrac{(a-b)}{\varepsilon} E \displaystyle\int_{E/\varepsilon}^{\infty} K(E', l) \frac{\mathrm{d}E'}{E'^2}\,, \end{cases}$$

with the new boundary conditions

$$(24) \qquad \begin{cases} H(E, 0) = H_0 E_\varphi^{-s} & (0 < E < E_\varphi) \\ H(E, 0) = H_0 E^{-s} & (E_\varphi \leqslant E); \end{cases} \qquad \begin{cases} K(E, 0) = P_0 E_\varphi^{-s} & (0 < E < E_\varphi) \\ K(E, 0) = P_0 E^{-s} & (E_\varphi \leqslant E)\,. \end{cases}$$

Therefore we simply have to study equations of the type:

$$(25) \qquad \frac{\partial F(x, y)}{\partial y} + F(x, y) = \frac{\sigma x}{\varepsilon} \int_{x/\varepsilon}^{\infty} F(\xi, y) \frac{\mathrm{d}\xi}{\xi^2}\,,$$

with boundary conditions

$$F(x, 0) = A_0 x_0^{-s} \quad (0 < x < x_0); \qquad F(x, 0) = A_0 x^{-s} \quad (x \geqslant x_0)\,.$$

The solution $F(x, l)$ can be written in polynomial form

$$F(x, y) = A_0 x^{-s} \exp\left[\left(\frac{\sigma\varepsilon^s}{s+1} - 1\right) y\right] \qquad (x > x_0)$$

$$F(x, y) = A_0 x^{-s} \exp(-y)\left[x^s/x_0^s - 1 + \exp\frac{\sigma y \varepsilon^s}{s+1}\right] \qquad (\varepsilon x_0 < x < x_0)$$

$$F(x, y) = A_0 x^{-s} \exp\left[\left(\frac{\sigma\varepsilon^s}{s+1} - 1\right) y\right] + P_0 x_0^{-s} \exp(-y)\left[1 + \sum_{n=1}^{\nu} \frac{\sigma^n y^n}{n!} + \right.$$

$$\left. - \sum_{n=1}^{\nu} \frac{\sigma^n y^n}{n!\,(n-1)!} \frac{\mathrm{d}^{n-1}}{\mathrm{d}p^{n-1}} \left\{\left(\frac{1}{p} + \frac{1}{s-p}\right) \exp(a_n p)\right\}_{p=-1} \cdot \frac{x_0^s}{x^s} \sum_{n=0}^{\nu} \frac{\sigma^n y^n \varepsilon^{sn}}{n!\,(s+1)^n}\right] .$$

$$(\varepsilon^{\nu+1} x_0 < x < \varepsilon^{\nu} x_0;\ \nu \geqslant 1).$$

The results of the numerical calculations are given in figs. 9, 10, 11. Fig. 9 represents the ratios

$$R_P(E_\pi, l_0) = \frac{P_\varphi(E_\pi, l_0)}{P_{>\varphi_0}(E_\pi, l_0)} ,$$

$$R_N(E_\pi, l_0) = \frac{N_\varphi(E_\pi, l_0)}{N_{>\varphi_0}(E_\pi, l_0)} ,$$

$$R_H(E_\varphi, l_0) = \frac{H_\varphi(E_\pi, l_0)}{H_{>\varphi_0}(E_\pi, l_0)} ,$$

between the number of fast nucleons at the latitude φ and the number of nucleons of the same type at latitudes greater than φ_0 (45°) where the effect of the cut-off is not felt any more. The curves have been calculated for $l_0 = 14.4$ and $l_0 = 5$. At sea level the ratios are practically the same for the various types of nucleons, but this is not so at higher altitudes where the values of R_N become appreciably greater than those of R_P.

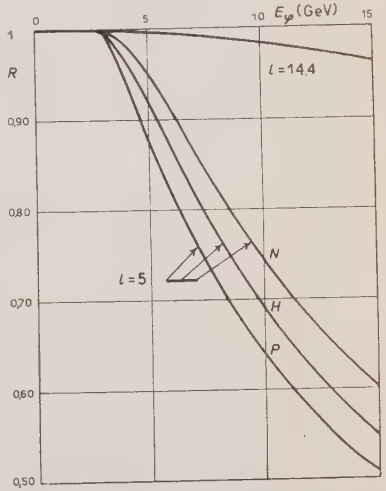

Fig. 9. – Ratios between the total number of nucleons with $E \geqslant E_\pi$ at latitude φ and at latitudes $\geqslant 45°$.

Fig. 10 represents, for $l_0 = 14.4$, the ratios

$$S_P(E; l, \varphi) = \frac{P_\varphi(E, l_0)}{P_{>\varphi_0}(E, l_0)} , \qquad S_N(E; l_0, \varphi) = \frac{N_\varphi(E, l_0)}{N_{>\varphi_0}(E, l_0)} ,$$

$$S_H(E; l_0, \varphi) = \frac{H_\varphi(E, l_0)}{H_{>\varphi_0}(E, l_0)} ,$$

between the distribution functions $P_\varphi(E, l_0)$, $N_\varphi(E, l_0)$, $H_\varphi(E, l_0)$ for the values 5, 10 and 15 GeV of the cut-off energy and the corresponding distributions without cut-off. Fig. 11 represents the same ratios for $l = 5$.

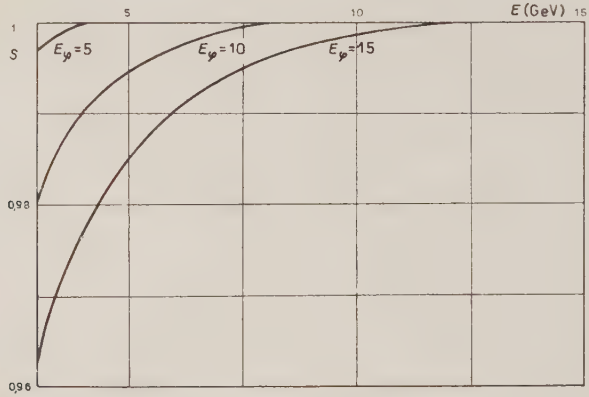

Fig. 10. Ratio between the integral spectrum of nucleons at latitude φ and the corresponding spectrum at latitudes $\geqslant 45^\circ$ ($l_0 = 14.4$).

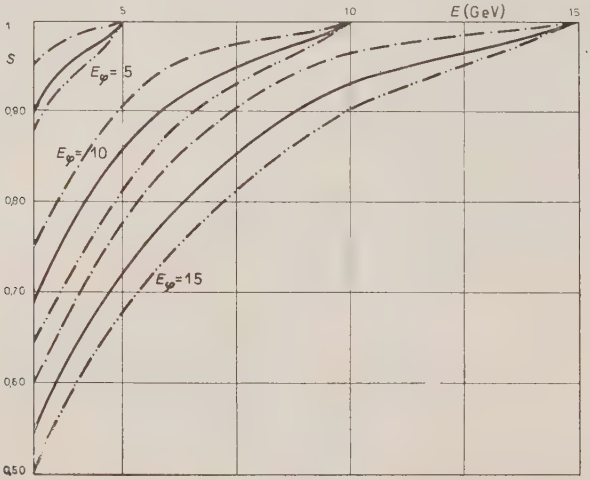

Fig. 11. – Ratio between the integral spectrum of nucleons at latitude φ and the corresponding spectrum at latitudes $\geqslant 45^\circ$ ($l_0 = 5$).
– H —··— P —·—·— N.

The curves of fig.s 10 and 11 have been used to study the latitude effect of the mesonic component. The magnitude of the effect at sea level is 4% at 0°. The effect increases appreciably with the altitude and at ~ 8000 m

is 40% for the neutrons and 50% for the protons: this implies an increase of the mean free path for absorption, in passing from the northern latitudes to the equator, greater for neutrons than for protons. Fig. 1 shows that the absorption curve for fast neutrons differs from the exponential, at depths smaller than 300 g/cm², when no cut-off is present: at the equator this will occur even at greater dephts.

These results are in qualitative agreement with experiment ([53]), but no careful check is possible since the exponential data are as yet few and rather uncertain: the available data on slow neutrons cannot be used in this connection.

APPAPILLAI and MAILVAGANAM ([54]) did not find at sea level and $\varphi = 30°$ any latitude effect on the generating component of hard showers; but the uncertainty of their data can mask an effect of 4%. ROSSI *et al.* ([55]) have found at 20° and 300 g/cm² an effect of $\sim 20\%$ for protons of energy > 5 GeV and of $\sim 50\%$ for protons of energy > 0.4 GeV.

We should conclude that the latitude effect that we predict for the nucleonic component is rather high: the same holds if we compare our results with the experimental findings of WINCKLER and coworkers ([56]) and of WHYTE ([57]). Other theories and particularly MESSEL's one give the same result: MESSEL ([8]) suggested that the exponent chosen for the primary spectrum might be too high. Recent experiments confirm this.

6·2. – Latitude effect of the mesonic component.

The latitude dependence of the spectral and of the absorption curves and of the positive excess of mesons is a good check on any scheme for the production of mesons. The utility of this check has been proved by various authors and particularly by M. FERRETTI SFORZINI ([58]) who has shown that the latitude effect of the meson component is incompatible with high multiplicity productions.

To carry out the calculations we start from the formulas for the distribution in the atmosphere of the various nucleonic components (protonic, neutronic and total) at different latitudes (see preceding number) and from

---

([53]) J. STAKER: *Phys. Rev.*, **80**, 52 (1950); J. A. SIMPSON and E. HUNGERFORD: *Phys. Rev.*, **77**, 847 (1950).

([54]) V. APPAPILLAI and A. W. MAILVAGANAM: *Nature*, **162**, 887 (1948).

([55]) A. J. MC MAHON, B. ROSSI and W. F. BURDITT: *Phys. Rev.*, **80**, 157 (1950).

([56]) J. R. WINKLER, T. STIK K. DWIGHT, and R. SABIN: **79**, 656 (1950).

([57]) G. N. WHYTE: *Phys. Rev.*, **78**, 321 (1950).

([58]) M. FERRETTI SFORZINI: *Nuovo Cimento*, **7**, 196 (1950), **8**, 909 (1951).

the general formulas for the distribution of mesons given in **4**. One obtains:

$$g^{\pm}(W, l) = \left(\frac{W}{l}\right)^{B/(\delta l + W)} \int_0^l x^{B/(\delta l + W)} [W + \delta(l - x)]^{-B/(\delta l + W)} \cdot S^{\pm}[x,\ W + \delta(l - x)]\, \mathrm{d}x,$$

where:

$$S^{\cdot} = \frac{\mathrm{d}_l g^{\pm}}{\mathrm{d}W \cdot \mathrm{d}l}, \qquad \mathrm{d}_l g^{+} = \left(\frac{5}{12}\, p + \frac{1}{6}\, n\right)\frac{\mathrm{d}W}{q}\, \mathrm{d}l, \qquad \mathrm{d}_l g^{-} = \left(\frac{1}{6}\, p + \frac{5}{12}\, n\right)\frac{\mathrm{d}W}{q}\, \mathrm{d}l.$$

Two arbitrary constants are contained in these formulas: the fraction ε^* of the energy of the incident nucleon transferred to the mesons created in the

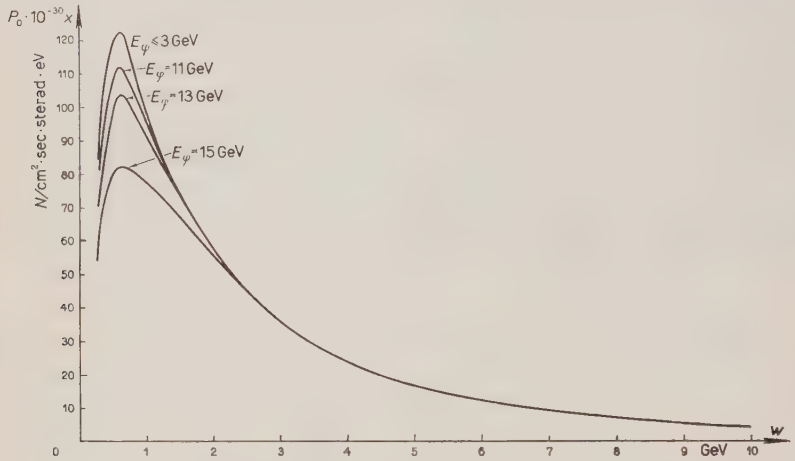

Fig. 12. – Differential mesonic spectrum at sea level at different latitudes.

collision with another nucleon; and the critical energy E_π for the production of mesons. The calculations which do not involve the geomagnetic effects are fairly insensitive to the numerical values of these parameters; instead the results for the geomagnetic effect for mesons show a critical dependence on the values of ε^* and E_π and allow one to determine them rather accurately. The best results are obtained assuming $E_\pi = 3$ GeV, $\varepsilon^* = 0.25$ and keeping 125 g/cm² as the value of the absorption coefficient for the nucleonic component.

Fig. 12 gives the computed energy spectra of mesons at sea level and in the vertical direction corresponding to latitudes identified by different values of the cut-off energy E_π: the latitude effect appears most relevant for mesons of energy smaller than a few GeV.

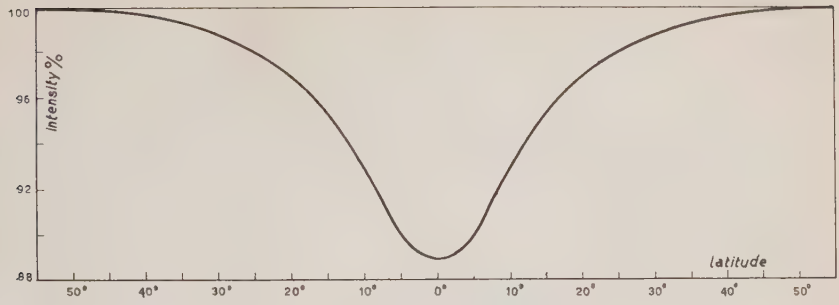

Fig. 13. – Latitude effect of the mesonic component (at sea level).

Fig. 13 gives the percentual latitude effect on the total number of mesons (energy $\geqslant 0.2$ GeV) obtained from the computed spectra at the various latitudes using VALLARTA's theory [59] for the correspondence between cut-off

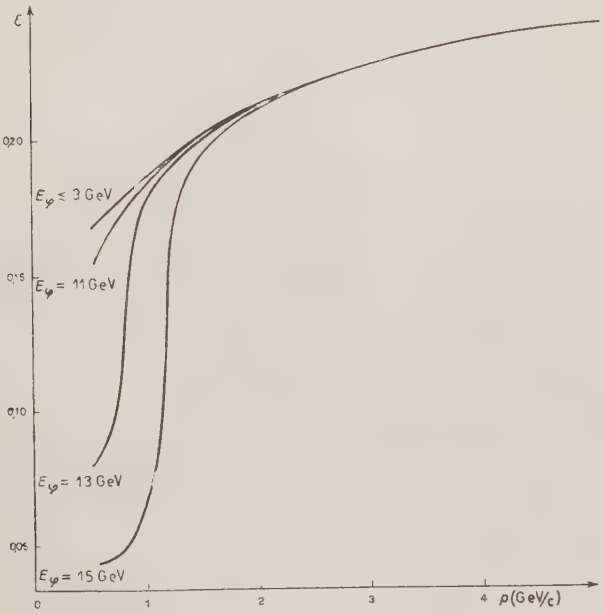

Fig. 14. – Differential positive excess at different latitudes (at sea level).

[59] D. J. X. MONTGOMERY: *Cosmic Ray Physics* (Princeton, 1949), page 55.

energy and magnetic latitudes. The theoretical curve has the characteristic behaviour of the experimental curve and the numerical values agree farly well (60).

Fig. 14 gives the curves for the differential positive excess of the mesonic component at sea level for different values of the cut-off energy: the results are normalized to keep account of α-particles and heavier nuclei in the primary radiation (see 4·5). The magnetic field lowers the positive excess for low energy mesons.

Most experimental data as yet available give the latitude effect on the integral intensity of the mesonic component and not the dependence of the effect on the energy of mesons. A strict comparison of energy spectra of mesons at different latitudes determined under the same experimental conditions, as well as the comparison of the curves for the differential positive excess at different latitudes, could be of great use in checking the adequacy of our scheme as well as of any theory on the mechanism of production of the mesonic component. Also the study at different latitudes of the dependence of the energy spectrum and of the curve of the differential positive excess on meson direction would yield interesting data.

Conclusions.

We have seen that the measurements on the distribution of the different components of cosmic rays in the atmosphere are compatible with what one knows on the composition of the primary radiation and on the processes through which the nucleonic component transforms into the mesonic and electromagnetic components.

The good agreement with experiment of the curves that we have computed with simple assumptions shows that the current ideas on cosmic ray processes are substantially correct: the phenomena not considered (e.g. V particles production) and the eventual processes as yet unknown are not very important in the total energy balance. Our results allow us also to draw some conclusion on the interaction between particles; in particular our scheme agrees well with the hypothesis of single meson production up to energies of a few times 10 GeV and of multiplicity slowly increasing with increasing energy of the interacting nucleons, in fairly good agreement with FERMI's theory.

(60) D. J. X. MONTGOMERY: *Cosmic Ray Physics* (Princeton, 1949), page 127.

RIASSUNTO

Partendo dai risultati sperimentali relativi alla composizione della radiazione cosmica primaria, viene sviluppata una teoria fenomenologica di tutti i processi che hanno luogo attraverso l'atmosfera. In particolare si calcola: *a*) la distribuzione della componente nucleonica (protonica e neutronica) veloce; *b*) la distribuzione della componente mesonica, il suo spettro energetico e il suo eccesso positivo a diverse altezze; *c*) la distribuzione della componente elettronica. Vengono poi studiati accuratamente gli effetti di latitudine dovuti al taglio del campo magnetico terrestre. Tutti i risultati teorici ottenuti sono confrontati con i più recenti dati sperimentali.

Luminescenza di soluzioni per effetto di raggi γ rivelata mediante un fotomoltiplicatore 931 A.

A. Ciccone

Istituto di Fisica dell'Università - Pisa

(ricevuto il 25 Ottobre 1951)

Riassunto. — Nella presente nota si riferisce su esperienze eseguite al fine di studiare la luminescenza di soluzioni per effetto di raggi γ, e l'intensità della luminescenza al variare della concentrazione; si riportano due possibili spiegazioni qualitative del fenomeno della luminescenza.

1. – Introduzione.

Molti liquidi organici, quando sono allo stato di grande purezza, eccitati con radiazioni di alta energia (raggi α, β, γ, neutroni, ecc.) emettono una debolissima luminescenza che diventa assai più sensibile se nel liquido sono disciolte piccolissime dosi di speciali sostanze come antracene, fenantrene, naftalina, terfenile, carbazolo, ecc.

Questa luminescenza dipende dalla specie della sostanza in soluzione, dalla sua concentrazione e dalla natura del solvente adoperato. Per lo studio di tali luminescenze male si prestano i soliti metodi spettroscopici o spettrografici a causa della debolissima intensità di esse. Ottimamente invece si prestano i fotomoltiplicatori per la loro grandissima sensibilità e per il carattere quantitativo dei risultati che se ne possono ricavare.

Ageno e collaboratori [1] hanno studiato la luminescenza prodotta dai raggi γ in una soluzione di naftalina in xilolo sia in funzione della concentrazione, sia in funzione dello spessore della soluzione; Reynold [2], Kallmann [3]

---

[1] M. Ageno, M. Chiozzotto e R. Querzoli: *Acc. dei Lincei*, **6**, 626 (1949).
[2] G. Reynold: *Nucleonics*, **6**, 69 (1950).
[3] H. Kallmann: *Phys. Rev.*, **78**, 621 (1950).

hanno esaminato la luminescenza di liquidi organici puri, e di soluzioni eccitati con diverse sorgenti di alta energia; REYNOLD, HARRISON, SALVINI [4] hanno studiato la luminescenza di liquidi organici puri, di soluzioni in determinate concentrazioni e di liquidi organici in cui erano state disciolte quantità diverse di due sostanze luminescenti. I numeri che questi autori riportano, rappresentano ciò che essi definiscono « efficiency » di questi liquidi.

Più organico è il lavoro di KALLMANN e FURST [5] i quali hanno studiato sia la luminescenza di soluzioni diluitissime di antracene, carbazolo e terfenile in xilolo in funzione della concentrazione, sia il comportamento dell'intensità della luminescenza di alcune soluzioni per aggiunta di un'altra sostanza luminescente. Questi autori suggeriscono inoltre un'interpretazione dei fenomeni osservati basata sul trasporto dell'energia di eccitazione dalle molecole del solvente alle molecole del soluto.

È da notare, peraltro, che la maggior parte delle misure eseguite in questo campo [6] non sono facilmente confrontabili le une con le altre.

In questo articolo si riportano i primi risultati di una serie di misure intese a investigare in modo sistematico e, per quanto possibile, esauriente le caratteristiche di liquidi luminescenti. I risultati qui riportati si riferiscono a soluzioni in xilolo di alcune sostanze che ho potuto procurarmi in ottime condizioni di purezza. Per questo studio mi è stato prezioso l'appoggio dell'Istituto di Chimica Farmaceutica della nostra Università (*).

2. – Dispositivo sperimentale.

Tra i vari tipi di fotomoltiplicatori i più adatti per il nostro uso sono l'1P28, il 931A, l'1P22, i quali differiscono fra di loro perchè utilizzano superficie fotocatodiche aventi curve di risposta spettroscopica diverse l'una dall'altra; io ho potuto avere a mia disposizione un 931A. Questo ha una superficie fotocatodica di antimonio-cesio [7] e una zona di sensibilità spettroscopica compresa fra 4000 e 5000 Å con un massimo intorno a 4500 Å. Esso servirà dunque, per rivelare luminescenze le cui lunghezze d'onda sono comprese in questo intervallo.

Il primo problema è stato quello di mettere il fotomoltiplicatore (FM) in condizioni di massimo rendimento. È noto che per usare un FM si possono seguire due metodi: o la registrazione e il conteggio dei singoli impulsi, o la

---

[4] G. REYNOLD, F. B. HARRISON e G. SALVINI: *Phys. Rev.*, **78**, 488 (1950).

[5] H. KALLMANN e M. FURST: *Phys. Rev.*, **79**, 858 (1950); *Nucleonics*, **7**, 69 (1950).

[6] Cfr. per es., G. REYNOLD: loc. cit. [2]; G. REYNOLD e collaboratori: loc. cit. [4].

(*) Al Direttore prof. R. DE FAZI, all'assistente prof. CARBONI e al dott. SEGNINI, esprimo i miei più sentiti ringraziamenti.

[7] J. W. COLTMAN: *The Scintillation Counter* (Proc. of the I.R.E.).

misura della corrente media mediante un galvanometro. Ho usato questo secondo metodo adoperando un galvanometro Deprez d'Arsonval la cui sensibilità, ad un metro della scala dallo specchio, era di $1{,}8 \cdot 10^{-9}$ A per mm.

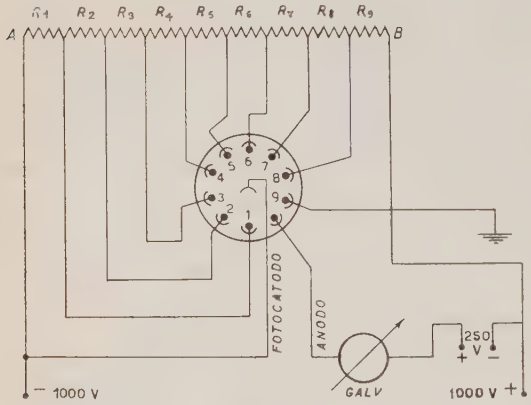

Fig. 1.

La fig. 1 rappresenta lo schema elettrico adoperato; le tensioni erano mantenute costanti con appropriati stabilizzatori.

Per avere un buon funzionamento del FM conviene proteggerlo da variazioni di temperatura; per questo motivo esso è stato racchiuso in una scatola di lamierino d'ottone, a doppia parete, con il fotocatodo in corrispondenza di una piccola finestra rettangolare (praticata in una delle pareti) alla quale si accosta un diaframma in ottone pure sfinestrato in corrispondenza (fig. 2).

Per evitare radiazioni estranee provenienti dall'ambiente, la scatola è stata racchiusa in una cassa di legno ($90 \times 35 \times 29$ cm^3, spessore cm 3) annerita internamente.

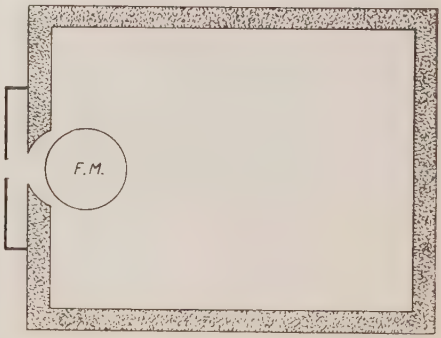

Fig. 2.

Le connessioni fra il FM e gli alimentatori sono state effettuate in modo da garantire un perfetto isolamento e da prevenire qualsiasi infiltrazione di luce.

Come è noto il FM presenta, anche nella perfetta oscurità, una debole corrente «corrente di zero», la quale, se non si prendono speciali precauzioni può superare in intensità la corrente segnale da misurare.

Per questo si prendono in considerazione le differenze d'intensità, ma se si ricerca grande sensibilità, bisogna, naturalmente, che la corrente di zero sia ridotta a un valore molto basso. Ciò si otterrebbe facilmente raffreddando il FM con una miscela di ghiaccio e sale, o con anidride carbonica e acetone, ma riconobbi che questi metodi, per le mie esperienze, portavano ad altri inconvenienti e quindi ho preferito operare alla temperatura ambiente.

Varie prove dimostrarono che la corrente di zero, in buona parte era dovuta a dispersione per imperfetto isolamento, ma con opportuni accorgimenti si è riusciti a ridurre la corrente di zero a $0{,}3 \cdot 10^{-8}$ A raffreddando il FM alla temperatura di zero gradi centigradi, a $2{,}4 \cdot 10^{-8}$ A alla temperatura ambiente di 13 °C, e a $4{,}3 \cdot 10^{-8}$ A alla temperatura estiva di 27 °C; in ogni esperimento la tensione fra un dinodo e il successivo era di 100 V.

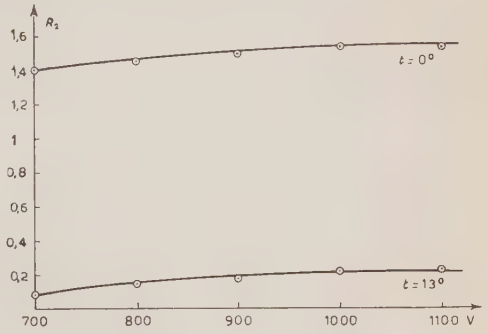

Fig. 3.

Una valutazione delle buone condizioni sperimentali così realizzate, è stata ottenuta nel modo seguente: inviando sul fotocatodo una radiazione luminosa d'intensità determinata, si leggeva una deviazione al galvanometro; la differenza tra questa lettura e quella corrispondente alla corrente di zero esprimeva l'effetto della radiazione. Il rapporto tra questa differenza e la corrente di zero si può assumere come una misura della sensibilità del FM ([8]).

Questa luce d'intensità determinata e fissa era fornita da una lampadina alimentata da una corrente d'intensità molto piccola (tale da rendere il filamento appena luminoso) che veniva mantenuta esattamente costante.

La lampadina era posta ad una distanza di 15 cm da un diaframma collocato immediatamente davanti alla finestra della scatola (fig. 2) e avente un foro del diametro di 3 mm: essa era sistemata in modo che la sua luce cadesse perpendicolarmente sulla superficie del fotocatodo.

Nei grafici della fig. 3 è riportata la sensibilità del FM in funzione della tensione fra i dinodi estremi (punti A e B di fig. 1) per due diverse temperature.

Essi mostrano che al crescere della tensione la sensibilità cresce lentamente e suggeriscono una tensione di 100, 110 V, fra un dinodo e il successivo, come la più opportuna.

3. – Risultati sperimentali.

Si sono preparate due soluzioni in xilolo, una di naftalina e una di acenaftene, entrambe prodotti purissimi rispettivamente delle Case Merck e Fraenkel, alla concentrazione di 0,18 g/cm^3. Lo xilolo è stato, per maggiore precauzione, privato da eventuali tracce di umidità e ridistillato in laboratorio.

([8]) M. Ageno, M. Chiozzotto e R. Querzoli: *Nuovo Cimento*, **6**, 621 (1949).

Le vaschette contenenti le soluzioni sono state appositamente da me costruite con vetri a pareti sottilissime (circa 3/10 di mm) ed hanno una larghezza di mm 19 ed una altezza di cm 5; esse potevano adattarsi vicinissime alla finestra della scatola di ottone che conteneva il FM.

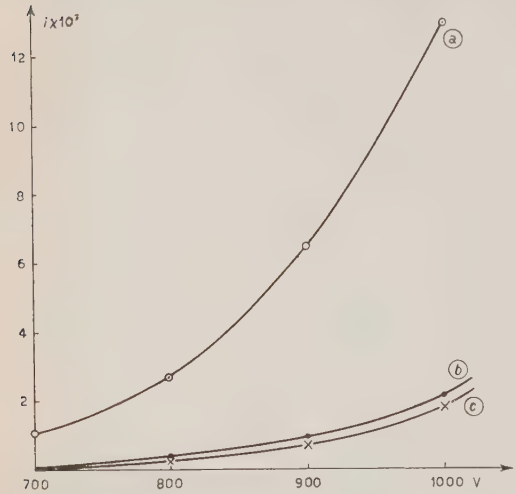

Fig. 4. - *a*) cristallo di antracene; *b*) soluzione di acenaftene in xilolo; *c*) soluz. di naftalina in xilolo.

La sorgente, un sale di Radio di circa un millicurie, è stato sistemato in una scatoletta di alluminio dello spessore di 8/10 di mm, onde assorbire i raggi β. Essa irradiava le sostanze in esame attraverso un foro di 3 mm praticato in un blocchetto di piombo protettivo.

Si è dapprima studiata la luminescenza di un cristallo di antracene molto trasparente, di g 3,76, il quale veniva collocato con una faccia immediatamente davanti alla finestra del FM, mentre sulle rimanenti facce veniva rivestito con un sottile foglio di stagnola per raccogliere anche la luce emessa nelle altre direzioni.

Come misura del potere luminescente del cristallo si è assunta la differenza tra la corrente anodica misurata con e senza la sorgente radioattiva. Il grafico *a* della fig. 4 è stato ottenuto riportando il potere luminescente in funzione della tensione applicata tra *A* e *B* (fig. 1). Gli altri due grafici *b* e *c* si riferiscono rispettivamente alle soluzioni (7,520 g, concentrazione 0,18 g/cm³) di acenaftene e di naftalina e sono stati riportati per confronto con il grafico *a*. Uguale geometria in tutti e tre i casi.

Al fine di verificare se la luminescenza emessa dal cristallo sotto l'azione della radiazione γ, fosse effettivamente responsabile dell'effetto osservato, ho ritenuto opportuno, come prima prova, fotografare lo spettro della luce emessa. Ciò è stato fatto usando un Hilger E2. Lo spettrogramma riprodotto nel testo rivela una banda compresa fra 4000 e 5000 Å, con un massimo d'intensità intorno a 4460 Å. Essa è la più intensa delle tre bande rivelate fotograficamente da L. Roth [9] usando un cristallo di antracene e radiazioni di alta energia.

---

[9] L. Roth: *Phys. Rev.*, **75**, 983 (1949). Cfr. pure F. B. Harrison e G. Reynold: *Phys. Rev.*, **79**, 732 (1950).

Per ottenere il mio spettrogramma, che è del resto assai poco intenso, sono state necessarie ben 72 ore di esposizione, mentre con il FM si ottengono immediatamente effetti notevoli.

Ulteriori prove analoghe a quelle di AGENO e collaboratori [1] eseguite per accertare che l'azione registrata dal FM è dovuta esclusivamente alla luminescenza sono:

1) togliendo il cristallo o la vaschetta con la soluzione e lasciando davanti alla finestra del FM la sola sorgente dei raggi γ non si è notato alcun aumento della corrente di zero. Ciò dimostra che i raggi γ non hanno azione diretta sul fotocatodo;

2) interponendo fra il cristallo o la vaschetta irradiati, e la finestra del FM un cartoncino nero la corrente anodica si è ridotta alla corrente di zero. Ciò dimostra che il contributo degli elettroni estratti dal cristallo o dalla soluzione per azione dei raggi γ incidenti è addirittura trascurabile;

3) sostituendo al cristallo o alla vaschetta con la soluzione una lastrina di piombo di spessore tale da emettere sotto l'azione dei raggi γ un numero di elettroni Compton maggiore di quello emesso dal cristallo o dalla soluzione in esame, non si è notato alcun aumento della corrente di zero.

Assunta arbitrariamente come unità di misura per la corrente di luminescenza quella fornita dal cristallo di antracene alla tensione di 900 V fra gli estremi *A* e *B* (fig. 1), sono state eseguite misure comparative su una massa di g 7,520 di soluzione in xilolo rispettivamente di naftalina e acenaftene alla concentrazione di 0,18 g/cm³. Successivamente si sono effettuate misure sulle quantità di xilolo puro e delle sostanze organiche che entrano come componenti in 7,520 g di soluzione.

Le misure relative ai liquidi e alle sostanze organiche eseguite in condizioni geometriche identiche sono riportate nella seguente tabella.

TABELLA I.

SOSTANZE	Grammi	Corrente di luminescenza
Cristallo di antracene	3,760	1
Soluzione di naftalina in xilolo	7,520	0,107
Xilolo puro	5,972	0,012
Naftalina in microcristalli	1,548	0,066
Soluzione di Acenaftene in xilolo	7,520	0,138
Xilolo puro	6,000	0,013
Acenaftene in cristallini	1,520	0,071

Da essa risulta che tanto lo xilolo quanto la naftalina e l'acenaftene, irradiati separatamente, presentano una debolissima luminescenza, la quale cresce quando essi sono uniti in soluzione.

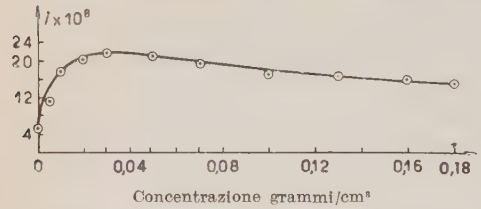

Fig. 5. - Soluzione di acenaftene in xilolo.

Si è anche esplorato il comportamento della intensità della luminescenza delle soluzioni al variare della concentrazione.

Il grafico della fig. 5 rappresenta l'intensità della corrente di luminescenza in funzione della concentrazione.

Come si vede, una piccolissima quantità di acenaftene è sufficiente per produrre un netto aumento della luminescenza (praticamente nulla per lo xilolo puro); questa aumenta rapidamente al crescere della concentrazione, raggiunge un massimo e poi lentamente decresce per concentrazioni via via crescenti [10].

È stato anche esaminato il comportamento di una soluzione di naftalina in xilolo (0,18 g/cm³) al fine di poter stabilire un confronto diretto tra le misure di altri autori e quelle qui riportate in fig. 6. L'andamento della nostra curva è lievemente diverso da quello trovato da altri autori [11]. Appare infatti, dalla fig. 6, che per concentrazioni maggiori di 1,5 % l'intensità della luminescenza rimane praticamente costante, mentre quella degli autori menzionati ha un andamento crescente.

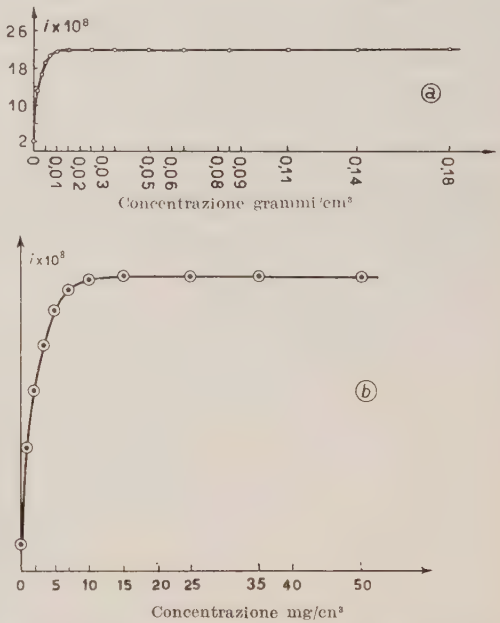

Fig. 6 - *a*) soluzione di naftalina in xilolo; *b*) particolare della curva.

---

[10] Alla concentrazione 0,18 g/cm³, la soluzione di acenaftene o di naftalina è praticamente satura.

[11] M. Ageno e collaboratori: loc. cit [1]; H. Kallmann e M. Furst: *Phys. Rev.*, **81**, 853 (1951).

Dei fatti osservati si possono dare, a mio avviso, due spiegazioni, se pure qualitative.

La prima può ottenersi, penso, seguendo l'analogia con certi fenomeni di assorbimento, nella regione del primo ultrarosso, da parte di varie sostanze disciolte in tetracloruro di carbonio [12] [13]. Si può allora pensare che la luminescenza provenga quasi esclusivamente dalle molecole disciolte e si presenti così intensamente nelle soluzioni, perchè i movimenti delle molecole, di qualunque natura esse siano, si effettuano più liberamente, essendo queste maggiormente allontanate.

La seconda spiegazione possibile, analoga a quella suggerita da H. KALLMANN e FURST [5], si può basare su un'analogia con i fenomeni di fluorescenza sensibilizzata (WOOD, RASETTI), pensando che la luminescenza sia prevalentemente prodotta dalle molecole del solvente, ma si manifesti intensamente solo quando, per l'aggiunta del soluto, le molecole del solvente consegnano a quelle in esso disciolte, la loro energia di eccitazione.

Non sembra che al momento attuale si disponga di elementi sufficienti per accreditare l'una o l'altra spiegazione o, eventualmente, qualche altra diversa da esse.

Sono allo studio soluzioni di altre sostanze organiche in xilolo, benzolo ed altri liquidi.

Ringrazio il prof. CONVERSI per le utili discussioni avute sull'argomento.

---

[12] L. BERTI: *Nuovo Cimento*, **5**, 44 (1948).
[13] A. CICCONE: *Nuovo Cimento*, **5**, 489 (1948); **6**, 500 (1949); **7**, 373 (1950).

SUMMARY (*)

The paper reports experiences performed in order to study the luminescence of solutions due to γ-rays, and the intensity variation of luminescence with changing concentration. Two possible qualitative explanations of the luminescence are reported.

(*) *Editor's translation.*

Argon Isotopes in Natural Gases.

G. Boato and G. Careri

Istituto di Fisica dell'Università, Centro di studio per la Fisica Nucleare del C.N.R. - Roma

M. Santangelo

Istituto Nazionale di Geofisica - Roma

(ricevuto il 6 Novembre 1951)

Summary. — The Argon isotopic composition has been measured in many italian fumeroles and soffioni. A remarkable enrichment of A^{40} has been found, certainly due to the K^{40} decay in the inner of the earth. With the help of these data, the problem of the origin of atmospheric Argon is considered.

Introduction.

Natural gases have been studied for a long while to get informations on the inner of the earth. Chemical analyses of natural gases (volcanic gases, fumeroles, drill-hole gases and so on) have been made by many authors (1), but as far as we know the isotopic composition has not yet been considered.

Rare gases are always present in some amount in natural gases. Attention must be stressed to rare gases as invaluable sources of information on constitution, origin and evolution of the earth atmosphere.

Argon (2) isotopes are very interesting in this respect. The K^{40} disintegration was postulated by von Weizsäcker (3) to explain the great amount

(1) For a review of these data see: U. Sborgi: *Ann. di Chim. Appl.*, **32**, 395 (1942).

(2) The Argon content in the atmosphere is 0,93% in volume. Its isotopic composition, as given by A. O. Nier: *Phys. Rev.*, **77**, 789 (1950), is

A^{36}	0.337 ± 0.001 %
A^{38}	0.063 ± 0.001 %
A^{40}	99.600 ± 0.001 %

(3) C. F. von Weizsäcker: *Phys. Zeits.*, **38**, 623 (1937).

of A^{40} in the atmosphere. As a matter of fact K^{40} (which is contained in natural Potassium as 0.0119 %) has been shown later to decay not only by β disintegration, but also [4] by K-capture, the final product of this second process being just A^{40}. Furthermore Potassium content in the earth has been shown [5] to be in such a large amount to justify the A^{40} content in the atmosphere.

A question still open is the mechanism by which A^{40} accumulated in the atmosphere [6]. There is still some doubt whether a great amount of the actual A^{40} was already contained in the primitive atmosphere, or whether it was continuously evolving in the geological time. In this respect the A^{40}/A^{36} ratio in natural gases is a source of information for the A^{40} amount which continually goes in the atmosphere.

Experimental part.

We starked our work in volcanic gases. It is a difficult task to capture true volcanic gases avoiding air contamination. A few attempts have been made to catch gases from Etna, Stromboli and Vulcano, introducing a vacuum tight tank as deep as possible in the vulcano gaps. A device was used to open and to close the tank right inside the gap, in order to prevent any air contamination. In all collected samples the enrichment factor

$$\eta = [A^{40}\ A^{36}]_{\text{gas}}\ [A^{40}\ A^{36}]_{\text{atmosphere}}$$

was so close to one to believe the collected smokes were not really coming from the inside of the volcano, but probably were some circulating air in the gaps.

For this reason we left volcanic gases for fumeroles and drill holes where the capture is much easier and safer (expecially for the experimentalist). As two samples provided by the interest of the Larderello Corporation were found [7] to have a η value larger than one, we collected further samples from the most important italian fumeroles and « soffioni » [8].

---

[4] F. C. Thompson and S. Rowlands: *Nature*, **152**, 103 (1943).

[5] H. E. Tatel: *Journ. Geoph. Res.*, **55**, 329 (1950); F. Birch: *Journ. Geoph. Res.* **56**, 107 (1951).

[6] J. H. J. Poole, C. F. G. Delaney: *Nature*, **167**, 680 (1951); A. Rostagni: *Geof. pura e applicata*, **18**, 128 (1950).

[7] G. Boato, G. Careri, G. Nencini and M. Santangelo: *Ann. di Geofisica*, **4**, 111 (1951).

[8] « Soffioni » are high temperature and pressure steam wells, somewhat like geysers. Some of them carries to the atmosphere a hundred tons of water vapour per hour. For details see: P. Ginori Conti: *Journ. Chem. Educ.*, **4**, 281 (1927); U. Sborgi: *Atti della Reale Acc. d'Italia*, **5**, 667 (1934).

« Soffioni » samples have been collected and purified by the Larderello Corporation. Fumerole gases have been collected by us with a bell immersed in the bubbling water. Water and carbon dioxide, the most abundant components (9), were both adsorbed on the spot. Rare gases were extracted in the laboratory in the usual way. A quantity of nearly 100 cm³ at 20 mmHg, suitable for isotopes analysis, was obtained working on one cubic meter of original gases at standard conditions.

A Nier-type mass spectrometer built in this laboratory (10) was used for isotopes analysis. For every sample the full mass spectrum in the range 35

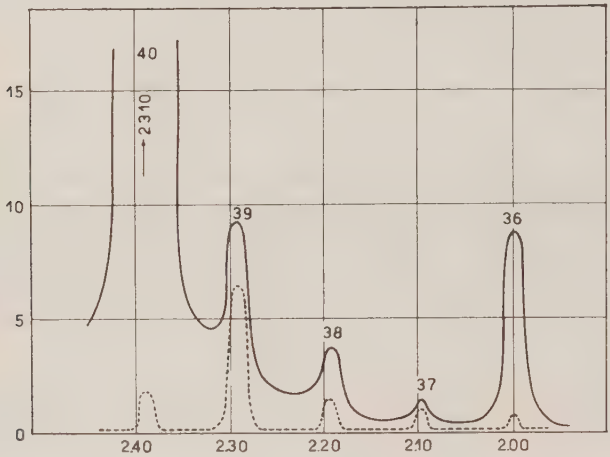

Fig. 1. - The typical mass spectrum of atmospheric Argon, and the background (dotted curve) in the mass range 36 to 40. It is a plot of the ion current in arbitrary units versus the magnet current in Ampere.

to 41 has been measured and compared with an atmospheric Argon sample used as a standard. In this mass range the background had a constant value after the copper analyser tube had been heated at 200 °C for a few days. The background has been always measured before and after a sample has been introduced, and subtracted in the proper way. Due to the high in-

(9) Except for water, always present as vapour or also in condensed form, carbon dioxyde constitutes 90-99% of these gases. No appreciable oxygen quantities are generally found, instead Nitrogen and rare gases are always present. Other gases, like Hydrogen, Hydrogen sulfide, Methane, are sometimes present in small amount as reported in reference (1).

(10) G. CARERI and G. NENCINI: *Nuovo Cimento*, **7**, 64 (1950).

tensity of mass 38 background peak, the Argon measurements have been limited to the 36 and 40 peaks. Magnetic scanning was used with an 1500 V accelerated ion beam. Molecular flow was surely established, an important condition to make quantitative analysis without a calibration of the spectrometer. As a proof of the good performance of our instrument, we obtained for the A^{40}/A^{36} ratio in atmospheric Argon 294 ± 3, to be compared with the Nier's 296 ± 1, obtained with a carefully calibrated instrument. A typical mass spectrum of ours is reported in fig. 1.

Results of our analyses are reported in table I. The quoted error is mainly due to the reproducibility, as for this purpose some samples have been measured again after a few months.

TABLE I.

SOURCE	$[A^{40}/A^{36}]_{gas}/[A^{40}/A^{36}]_{atm.}$
FUMEROLES	
Agnano (Napoli)	1.15 (*a*)
Pozzuoli (Napoli)	1.12
Bullicame (Viterbo)	1.00
Montemiccioli (Volterra)	1.99
Rapolano (Siena)	1.26
SOFFIONI	
Larderello N. 1 (*b*) (Pisa)	1.22
Larderello » 2 »	1.19
Larderello » 3 »	1.16
Larderello » 4 »	1.24
Larderello » 5 »	1.28
Castelnuovo N. 1 »	1.12
Castelnuovo » 2 »	1.40
Serrazzano N. 1 »	1.60
Serrazzano » 2 »	1.71
Travale »	1.21
Sasso »	1.25
Lagoni Rossi »	1.45
Lago Tassinaie »	1.25
Monterotondo »	1.45

(*a*) Experimental error on the enrichment factor $\pm 4\%$.
(*b*) A progressive number has been used to identify different neighbor sources.

Discussion of the results.

With a glance at table I, one sees the observed enrichment to be sometimes very remarkable, compared with the usual variations of isotopic composition of elements in the earth.

The A^{40}/A^{36} ratio in all samples is never less than the atmospheric one, and this seems quite reasonable from the following considerations. The atmosphere of to-day is generally assumed to be completely of secondary origin ([11]), namely the result of the earth outgassing from the time when gravitational field and termal conditions were such to prevent gas excaping far from our planet. Although some outgassing still remains to-day, and volcanic phenomena are an example of it, the most important quantity of gases has been developed probably during the earth's solidification.

Let us consider Argon isotopes A^{40} and A^{36}. Due to the same chemical properties and the light mass difference, we can think they have had the same story in the process of earth outgassing. Also without any guess about the A^{40}/A^{36} value in the atmosphere at the beginning of the earth, one must say, as a result of K^{40} decay into A^{40}, that ratio has always been less in the atmosphere than in the inside of the earth. In other words, the A^{40}/A^{36} ratio in the atmosphere has alway been rising, but with some delay with respect to the inside of the earth.

Obviously one must always consider only the average value of the ratio A^{40}/A^{36} in the inside of the earth. In spite of our results, it can also happen that some natural gases have a η value less than one, and this is due to the non homogeneous Potassium distribution. The figures of table I show remarkable variations of η depending on the gas source.

We believe this is due to the non uniform geological constitution of the surface crust, to the different path of the gas coming to the surface and also to some air contamination inside the earth. It is difficult to day to explain these variation without a knowledge of the gas path, and also of data concerning η of the same source in different times.

To answer the question about the mechanism of A^{40} accumulation in the atmosphere, one should extend this kind of analysis to all the earth's surface, to know more about the quantity of natural gases excaping up to day. It is however interesting to point out that the Soffioni of Larderello supply about $4.4 \cdot 10^6$ grams of A^{40} per year, to be compared with $6.6 \cdot 10^{19}$ grams ([12]), which

---

([11]) H. JEFFREYS: *The Earth* (Cambridge, 1929), p. 312; H. BROWN: *The Atmospheres of the Earth and Planets* (Chicago, 1950), p. 260.

([12]) F. A. PANETH: *Neue Wege exact. Naturerk.*, pag. 1 (1939).

is the total A^{40} content in the atmosphere. Although it is not possible to think that such an intense outgassing happens all aroud the earth, the above figures allow us to believe that a remarkable amount of A^{40} is still flowing in the atmosphere.

Acknowledgment.

Thanks are due to Prof. E. AMALDI for stimulating discussions on this problem. We also express our appreciation to Dr. LENZI, Head of Larderello Corp. Chemical Department, who kindly provided us with some samples of rare gases.

RIASSUNTO

La composizione isotopica dell'Argon è stata misurata in un gran numero di fumarole e di soffioni italiani. Si è trovato un notevole arricchimento in A^{40}, sicuramente dovuto al decadimento del K^{40} contenuto nell'interno della Terra. Alla luce di queste misure viene considerato il problema della genesi dell'Argon atmosferico.

Theory and Use of Statistical Methods in the Determination of Symmetry and Structure of Crystals (*).

A. J. C. Wilson

Viriamu Jones Laboratory, University College, Cardiff, Great Britain

(ricevuto il 7 Novembre 1951)

Summary. — Centres of symmetry, mirror planes, and rotation axes can be recognized in suitable cases through a statistical study of the intensities of the X-ray reflexions. The number of essentially distinct space groups that can be determined by X-ray methods is thus raised from about 60 to 215, out of a total of 219. Statistical methods may also be of use in the study of pseudosymmetry. Applications to ephedrine and haemoglobin are described briefly.

Certain symmetry elements in crystals (lattice centring, glide planes, screw axes) may be readily recognized by the systematic absences they produce among the X-ray reflexions. Others (centrosymmetry, mirror planes, rotation axes) have no such obvious effect on the X-ray reflexions, and until recently were thought to be undetectable by X-ray methods. For crystals with poorly developed external forms, therefore, there was often considerable doubt about the proper assignment of crystal class and space group. Recently, however, it has been shown that a statistical study of the intensities of the X-ray reflexions will often reveal the presence of the second type of symmetry element, and the number of crystals of uncertain symmetry can be correspondingly reduced.

If the contributions made to the structure factor by the various atoms of a non-centrosymmetric structure are plotted on an Argand diagram an

---

(*) A paper given at the Second International Congress of Crystallography, Stockholm, 1951.

irregular polygon is formed, bearing a striking resemblance to illustrations of Brownian motion (fig. 1). The line representing the resultant structure factor can have any length from zero up to a maximum equal to the sum of

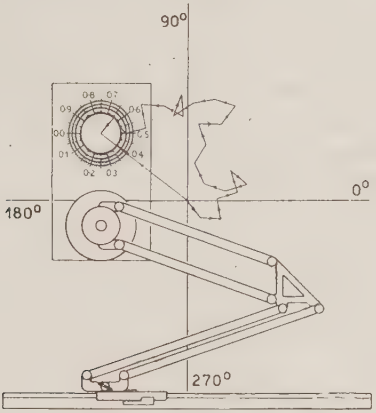

Fig. 1. – Contributions of individual atoms added vectorially to form the structure factor of a non-centrosymmetric crystal. The broken line is closely analogous to illustrations of Brownian motion. (The device shown is a draughting machine modified for the rapid and convenient graphical calculation of structure factors (1).)

the atomic scattering factors. Except for crystals with few atoms in the unit cell or for very low values of $\sin\theta$, however, the probability of the structure factor coming anywhere near this maximum is very small. In various ways (2) (3), one being the analogy with Brownian motion just mentioned, it can be shown that the average value of the intensity of reflexion, $I \equiv F^2$, is equal to the sum of the squares of the atomic scattering factors, Σ, and that the probability of I lying between I and $I + \mathrm{d}I$ is

$$P(I)\,\mathrm{d}I = \Sigma^{-1} \exp\left[-I/\Sigma\right]\mathrm{d}I\,. \tag{1}$$

Integration (4) shows that the fraction of the intensities less than or equal to I is given by

$$N(I) = 1 - \exp\left[I/\Sigma\right]. \tag{2}$$

(1) D. C. Phillips: *Journ. Sci. Instrum.*, in course of publication.

(2) A. J. C. Wilson: *Nature*, **150**, 152 (1942).

(3) A. J. C. Wilson: *Research*, **2**, 246 (1949); *Acta Cryst.*, **2**, 318 (1949).

(4) E. R. Howells, D. C. Phillips and D. Rogers: *Research*, **2**, 338 (1949); *Acta Cryst.*, **3**, 210 (1950).

The variance, the mean square deviation of I from its mean value Σ, is easily seen to be Σ^2, and in fact a more exact expression can be derived (5), free from restriction on the number of atoms in the cell:

$$V = \Sigma^2 - \Sigma_4 ,$$

where Σ_4 is the sum of the fourth powers of the atomic scattering factors.

For centrosymmetric crystals the situation is rather different, as the atoms occur in pairs whose combined contribution to the structure factor is restricted to the real axis. The mean value of I still remains Σ, but by analogy with one-dimensional Brownian motion or otherwise it can be shown (3) that the probability distribution of the intensities is now given by

$$P(I)\,\mathrm{d}I = (2\pi\Sigma I)^{-1/2} \exp\left[-I/2\Sigma\right] \mathrm{d}I , \tag{4}$$

the fraction of intensities less than I is

$$N(I) = \operatorname{erf}\left(I/2\Sigma\right) , \tag{5}$$

where $\operatorname{erf} x$ is the error function, and the variance is $2\Sigma^2$, or more exactly

$$V = 2\Sigma^2 - 3\Sigma_4 . \tag{6}$$

Expressions (4), (5) and (6) are quite different from (1), (2) and (3) in their mathematical form, and experience with over a dozen substances has shown that distinct indications of the presence or absence of a centre of symmetry can be obtained by their intelligent use. The qualification intelligent is important, because some judgement is required in deciding (i) whether the substance is sufficiently complex, and (ii) whether a sufficient number of reflexions has been estimated to make the application of statistical methods justifiable.

One substance to which the methods have been applied is the alkaloid ephedrine. The fact that the mean intensity of reflexion is equal to Σ may first be used to place the relative estimated intensities on an absolute scale. Since thermal vibration reduces the intensities of reflexion by the factor $\exp\left[-2B\sin^2\theta/\lambda^2\right]$, a graph of $\log\left(\langle I\rangle/\Sigma\right)$ against $\sin^2\theta$ will be a straight line, whose intercept on the ordinate axis gives the factor required to convert the estimated relative intensities to the absolute scale, and whose slope gives the effective value of the temperature parameter B. (The effective value may be increased above that for temperature alone by crystal imperfections.)

---

(5) A. J. C. Wilson: *Research*, **4**, 141 (1951).

Three such graphs are shown in fig. 2; they are linear within the experimental error and determine the absolute scale within a few percent. Fig. 3 shows $N(z)$ as a function of z (where $z = I/\Sigma$) for the same two zones, together with the theoretical curves from equation 3 (lower curve) and 6 (upper curve). There is no doubt that the 010 projection of this substance is centrosymmetric.

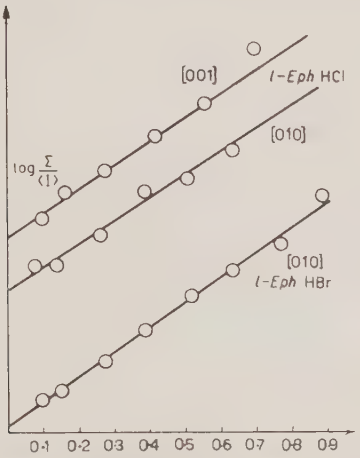

Fig. 2. Graph of $\log(\Sigma/\langle I \rangle)$ as a function of $\sin^2\theta$ for two zones of ephedrine hydrochloride and one zone of ephedrine hydrobromide. The plots are closely linear, and from their intercepts the factors required to place the arbitrary visual estimates of intensity on an absolute scale can be found. Their slopes give the effective Debye temperature factors.

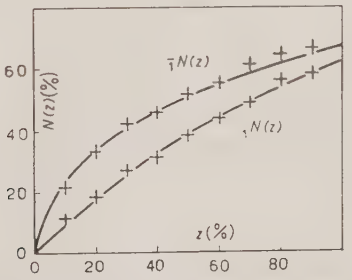

Fig. 3. – Fraction (in %) of reflexions with intensity less than z % of the average value. The curves are theoretical, the upper one for a centrosymmetric crystal or projection, the lower one for a non-centrosymmetric crystal or projection. The experimental points are for two zones of ephedrine hydrochloride, and show that the 010 zone corresponds to a centrosymmetric projection, and the 001 zone to a non-centrosymmetric projection. The space group $P2_1$ is thus confirmed.

and that the 001 projection is non-centrosymmetric, confirming the space group $P2_1$.

The differences in intensity distribution may be applied either to the general reflexion *hkl* for the detection of real centres of symmetry, or, as has just been described, to zones of reflexions for the determination of centrosymmetric projections. In projections, however, the statement that the average intensity is equal to Σ has certain exceptions ([6]), and these make possible the statistical determination of symmetry elements that cause atoms to coincide in projection. For example, in projection on to a mirror plane the atoms coincide in pairs, and for the corresponding zone of reflexions only the crystal must be regarded as containing half the actual number of atoms, each having a doubled atomic scattering factor. Since the scattering factors are squared in Σ, the average intensity in this zone is doubled. In general, when the atoms in projection coincide in groups of n, the average intensity in the corresponding zone or row is multiplied by n. Comparison of zone or row averages with each other or with the general average thus makes possible the detection of a considerable number of symmetry elements. The use of statistical methods and systematic absences together make possible the unambiguous determination of 215 of the 219 effectively distinct space groups ([7]), whereas the latter alone determine unambiguously only about 60.

An interesting possibility not yet fully explored is the study of pseudosymmetry. If a structure is pseudocentrosymmetric in the atomic positions one would expect the distribution curve to change from the type of equation (5) to the type of equation (2), and the variance to decrease from $2\Sigma^2$ toward Σ^2, as batches of reflexions of successively larger mean $\sin\theta$ are examined. (Other types of pseudocentrosymmetry might produce the opposite variation). Through the kindness of Mr. E. R. Howells and Dr. M. F. Perutz I am able to reproduce two $N(z)$ distribution curves for the 100 projection of horse methaemoglobin (fig. 1). The upper curve shows the theoretical distribution for a centrosymmetric crystal, and the experimental points for the low-order reflexions are in good agreement with it. The lower curve is the theoretical distribution for a non-centrosymmetric crystal, and the experimental points for the higher-order reflexions are in fair agreement with it, though there is some irregularity. These curves confirm the conjecture, based on other evidence, that this projection of methaemoglobin is pseudocentrosymmetric, though it cannot actually be centrosymmetric.

The limited time allowed for this paper makes it impossible to discuss the practical methods of carrying out the statistical investigations. I shall there-

---

([6]) A. J. C. Wilson: *Research*, **3**, 48 (1950); *Acta Cryst.*, **3**, 258 (1950).

([7]) D. Rogers: *Research*, **2**, 342 (1949); *Acta Cryst.*, **3**, 455 (1950).

fore close by summarizing: in many cases the statistical methods make possible the conversion of relative intensity data to the absolute scale, make

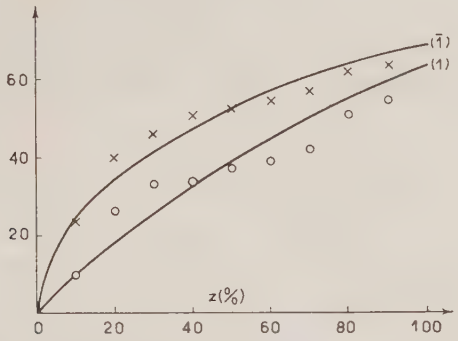

Fig. 4. – $N(z)$ curves for horse methaemoglobin, 100 projection. The crosses are from low-angle reflexions (spacings greater than 6 Å), and the circles for higher-angle (spacings less than 6 Å). The curves are theoretical. The projection is thus actually non-centrosymmetric, in accordance with the space group, but would appear centrosymmetric if examined at low resolution.

possible the detection of symmetry elements not revealed by systematic absences, and may give indications of pseudo-symmetry (not necessarily pseudo-centrosymmetry). Knowledge of the absolute scale and pseudosymmetry can be very helpful in the early stages of structure determination.

RIASSUNTO (*)

I centri di simmetria, i piani di simmetria, e gli assi di rotazione si possono spesso identificare con lo studio statistico delle intensità delle riflessioni dei raggi X. Il numero dei gruppi spaziali nettamente distinti che può essere determinato con l'impiego dei raggi X si eleva così da circa 60 a 215 su un totale di 219. I metodi statistici possono anche essere impiegati nello studio della pseudosimmetria. Si descrivono brevemente alcune applicazioni del metodo all'efedrina e all'emoglobina.

(*) *Traduzione a cura della Redazione.*

Cosmic Ray Evidence on the μ-meson Magnetic Moment.

D. C. Peaslee (*)

Washington University, St. Louis, Missouri (**)

(ricevuto il 1° Dicembre 1951)

Summary. — A survey is made to determine what information is provided by the intensity-depth relation of cosmic rays underground on the possibly anomalous character of the μ-meson magnetic moment. Energy losses due to ionization, bremsstrahlung and electron pair creation by normal and anomalous Dirac particles are discussed. It is concluded that if the magnetic moment in terms of the Bohr magneton is $\mu_0(1 + \delta)$, the only limitation provided by present experience at depths of 3000 m w.e. or less is $|\delta| \lesssim 1$.

1. – Introduction.

The intensity versus depth relation of cosmic rays underground can be interpreted solely in terms of electromagnetic interaction of the μ-meson [1], down to depths of 3000 meters water equivalent. Agreement with observation is obtained by assuming energy losses appropriate to a normal Dirac particle. The question arises whether this agreement is sufficient evidence that the μ-meson has a normal magnetic moment, since particles of anomalous moment have exceptional radiative properties at high energy. A negative answer is indicated by the following argument. According to present views, only particles of compound structure have anomalous moments. This compound structure may involve one or more (virtual) particles with a maximum associated Compton wavelength λ_0. The anomalous moment effects will then be cut off for processes involving momentum transfers $\Delta p \gtrsim \hbar/\lambda_0$ in the rest

(*) Now at Columbia University, New York.

(**) Assisted by the joint program of the ONR and AEC.

(1) S. Hayakawa and S. Tomonaga: *Prog. Theor. Phys.*, **4**, 287 (1949).

system of the original particle. For example, on this account the anomalous moment terms are of little interest with regard to divergences in quantum electrodynamics, since they will have a negligible effect unless it is assumed that there exists a truly elementary particle with anomalous moment; but such a particle would represent almost as grave a philosophical difficulty as the divergences themselves.

2. – Ionization losses.

The cross section for energy loss by electron knock-on of a normal μ-meson goes as $\ln E_\mu$; the anomalous moment introduces a term proportional to E_μ, which should dominate at high energies except for the cutoff mentioned above. If the magnetic moment is $(1 + \delta)\mu_0$, with μ_0 the normal moment, the cross section (2) for knock-on with transfer of energy εE_μ to the electron in the laboratory system is, for $E_\mu \gg \mu c^2$,

$$\sigma(E_\mu, \varepsilon)\,\mathrm{d}\varepsilon = \delta^2 \pi r_\mu^2 (1/\varepsilon - 1)\,\mathrm{d}\varepsilon\,, \tag{1}$$

where $r_\mu = e^2/\mu c^2$ is the «classical radius» of the meson. The integrated cross section for energy loss is clearly proportional to E_μ if no cutoff is imposed. For the cutoff the longest Compton wavelength involved is presumably that of the μ-meson; thus in the center of gravity system

$$1 \gtrsim \Delta p/\mu c = (2p/\mu c) \sin (1/2)\theta\,, \tag{2}$$

where the momentum p in the c.g. system is simply related to E_μ and m, the electron rest mass. The cutoff (2) may be inserted in (1) by means of the relation $\varepsilon \sim \sin^2 (1/2)\theta$; the integrated cross section for energy loss then becomes

$$\sigma(E_\mu) = \delta^2 (1/2) \pi r_\mu^2 \begin{cases} E_\mu & E_\mu \lesssim 0.8\ \mu^2 c^2/m\,, \\ \mu^2 c^2/m & E_\mu \to \infty\,. \end{cases} \tag{3}$$

These asymptotic forms indicate a maximum energy loss per unit path lengt of $|\,\partial E/\partial x\,| \lesssim 1.9 \cdot 10^{-2}$ MeV cm²/g. Of course the normal ionization loss is present in any case and will be dominant for $|\,\delta \ll 10$, which is the only limitation imposed by experimental agreement with intensity-depth curves calculated for $\delta = 0$.

The ionization produced by a fast neutron can also be crudely estimated in this way. Here the cutoff wavelength is presumably that of a π-meson;

---

(2) H. C. Corben and J. Schwinger: *Phys. Rev.*, **58**, 953 (1940).

the maximum energy loss occurs at $E_N \sim 0.5[m_\pi M/m]c^2 \simeq 1.3 \cdot 10^2$ GeV and is about $5 \cdot 10^{-3}$ MeV cm^2/g, less than 1% of conventional «minimum ionization».

3. – Bremsstrahlung.

The anomalous bremsstrahlung can be treated by the well known method of virtual quanta ([3-5]). The leading term in the anomalous cross section is

$$\sigma(E_\mu, \varepsilon)\,\mathrm{d}\varepsilon = \delta^4\alpha(Zr_\mu)^2(1-E)\,\mathrm{d}\varepsilon \int_{\varepsilon\mu c^2/(1-\varepsilon)}^{E_\mu} \mathrm{d}E_\nu \int_{r_{\min}}^{r_{\max}} \mathrm{d}r/r\,, \tag{4}$$

with $\alpha = 1/137$. The integrals in (4) describe the Compton scattering in the meson rest system of a virtual photon of energy E_ν from the nuclear Coulomb field; the lower energy limit is obtained from transformations relating the initial and final Compton scattering energies, and the meson rest system with the laboratory system. The radial integral is characteristic of the Weizsäcker-Williams method; when no special restrictions are imposed $r_{\max} \sim \lambda_\mu E_\mu/E_\nu$, where λ_μ is the Compton wavelength of the meson. The lower limit $r_{\min}$ is roughly equal to the cutoff (nuclear) radius R of the Coulomb field or λ_μ, whichever is larger; for the μ-meson $R = \lambda_\mu Z^{1/3}$ to a good approximation, while in the electron case $\lambda > R$ for all Z. Thus the integral over r is $\ln(gE_\mu/E_\nu Z^{1/3})$, where g is a number of order unity; without cutoff, the integral over E_ν is of order E_μ, so that the integrated cross section for energy loss is of order E_μ^2.

If the cutoff wavelength for the anomalous terms is taken to be that of the μ-meson, the energy integral is to be extended only over $E_\nu \lesssim \mu c^2$ and becomes

$$\int_{\varepsilon\mu c^2/(1-\varepsilon)}^{\mu c^2} \mathrm{d}E_\nu \ln\,(gE_\mu\, E_\nu Z^{1/3}) \sim \begin{cases} \left(\dfrac{1-(3/)2\,\varepsilon}{1-\varepsilon}\right) \ln\,(gE_\mu/Z^{1/3}\mu c^2) & \varepsilon \leqslant 2/3\,, \\ 0 & \varepsilon \geqslant 2/3\,. \end{cases} \tag{5}$$

This cutoff therefore causes a reduction to normal type bremsstrahlung; and further reduction to the form ln (const) for very high E_μ is brougth about in the usual way by electron shielding of the nuclear Coulomb field, which cuts it off at $r_{\max} \sim a_0 Z^{-1/3}$, with a_0 the Bohr radius. The integrated cross

---

([3]) C. F. v. Weizsäcker: *Zeits. f. Phys.*, **88**, 612 (1934).
([4]) S. B. Batdorf and R. Thomas: *Phys. Rev.*, **59**, 621 (1941).
([5]) J. L. Powell: *Phys. Rev.*, **75**, 32 (1949).

section for energy loss by anomalous bremsstrahlung is thus of order

$$\sigma(E_\mu) \sim 0.12\delta^4\alpha(Zr_\mu)^2E_\mu \ln(gF)$$

$$F = \begin{cases} E_\mu/Z^{1/3}\mu c^2 \\ 3.8\cdot 10^4/Z^{2/3}\,, \end{cases} \tag{6}$$

where the smaller value of F is always to be chosen. The corresponding cross section for normal bremsstrahlung, always present in addition, is $\alpha(Zr_\mu)^2E_\mu \ln gF$. Because of the δ^4 dependence, the anomalous bremsstrahlung is a somewhat more sensitive index than the ionization loss; in view of the agreement with $\delta = 0$ down to 3000 m.w.e., $|\delta|$ can certainly not be as large as 10, but a value of order 1 is not excluded. Intensity measurements at depths $\gg 10^3$ m.w.e. would in principle determine the bremsstrahlung loss more precisely and might reduce the upper limit on $|\delta|$.

4. – Pair production.

A similar discussion applies to the process of electron pair creation, which for mesons is comparable in importance to bremsstrahlung and would considerably exceed bremsstrahlung for a particle as heavy as the proton. An estimate of the normal cross section for energy loss by pair creation (the anomalous cross section can again be neglected for $|\delta| \lesssim 1$) is given by the Weizsäcker-Williams method for $E_\mu \gg \mu c^2$:

$$\sigma_{\text{pair}} \sim (2/\pi)\,\alpha \int \sigma_\nu \mathrm{d}E_\nu \int_{r_{\min}}^{r_{\max}} \mathrm{d}r/r\,, \tag{7}$$

where σ_ν is the cross section for electron pair creation by a photon of energy E_ν. For high E_μ, the range of E_ν greatly exceeds $183\,Z^{-1/3}\,mc^2$, so that the constant high-energy value can be used for σ_ν throughout. In this case $r_{\min}$ is determined by the longest Compton wavelength involved, which is that of the electron; and $r_{\max}$ is $\lambda_\mu E_\mu/E_\nu$. Integrating E_ν only over the range for which $r_{\max} \geqslant r_{\min}$, one has

$$\sigma_{\text{pair}} \sim (8/\pi)(\alpha Z r_0)^2(m/\mu)gE_\mu \ln(183Z^{-1/3})\,, \tag{8}$$

where r_0 is the electron classical radius and m its mass. Taking $g \sim 1$, the ratio of pair production to bremsstrahlung at high energies is

$$R = \sigma_{\text{pair}}/\sigma_{\text{brems}} \sim (2/\pi)\alpha\left(\frac{mr_0^2}{\mu r_\mu^2}\right)\frac{\ln(183\,Z^{-1/3})}{\ln(3.8\cdot 10^4\,Z^{-2/3})} \sim (\alpha/\pi)(\mu/m)\,. \tag{9}$$

The dependence of R on (μ/m) shows that pair creation is negligible in comparison with bremsstrahlung for a primary electron, is of comparable importance for a meson, and is probably the dominant effect for a proton. With $R \sim 0.5$ for a μ-meson, the energy loss per unit path length due to both pair production and bremsstrahlung is about $2 \cdot 10^{-6} E_\mu$ cm²/g, which is to be compared with the roughly constant ionization loss of about 2 MeV cm²/g. Therefore only the effects of normal ionization loss need be considered for mesons with $|\delta| \lesssim 1$ at underground depths of 10^3 m w.e. or less.

RIASSUNTO (*)

Si compie un'indagine per determinare quali informazioni si possano trarre dalla relazione intensità-profondità dei raggi cosmici sotto terra sul carattere eventualmente anomalo del momento magnetico dei mesoni μ. Si discutono le perdite d'energia dovute alla ionizzazione, alla bremsstrahlung, e alla creazione di coppie di elettroni da parte di particelle di Dirac normali e anomale. Si conclude che, se il momento magnetico espresso in magnetoni di Bohr è $\mu_0(1 + \delta)$, la sola limitazione fornita dalle presenti esperienze a profondità di 3.000 m_{H_2O} o minori, è $|\delta| \lesssim 1$.

(*) *Traduzione a cura della Redazione.*

IL NUOVO CIMENTO Vol. IX, N. 1 1 Gennaio 1952

Cosmic Rays Underground.

D. C. Peaslee (*)

Washington University, St. Louis, Missouri (**)

(ricevuto il 1° Dicembre 1951)

Summary. — Cosmic rays underground are treated as entirely caused by the electromagnetic interactions of μ-mesons. Simple approximations are given for the underground spectra of μ-mesons, virtual photons, soft showers, and nucleons. Comparison with experimental data is satisfactory on the absolute rate of slow neutron and nuclear star production, and on the charge ratio of star primaries, if the charged primaries are at least half protons. Disagreement is found with the observed variation of star production with depth. Comparison with observation suggests that the cross section for nuclear excitation by γ-rays decreases on the average more slowly than $1/E$ from its large measured value $\sigma_\gamma/A \sim 1 \cdot 10^{-28}$ cm^2 per nucleon at $E = 200 \div 300$ MeV. This mechanism therefore predominates over meson-proton knock-on in production of the underground nucleonic component. Measurement of slow neutron or star production over large differences in depth would yield more detailed information on the behavior of σ_γ/A at high energies. Measurement of the size-frequency distribution of soft showers at high energies would yield information about the production of neutral π-mesons.

1. – Introduction.

Of the cosmic radiation at sea level, only μ-mesons and neutrinos can penetrate to depths of about 20 meters water equivalent or more. There are accordingly only three sources of underground cosmic rays: i) electromagnetic interactions of μ-mesons; ii) non-electromagnetic interactions of μ-mesons; iii) neutrinos. Only the first of these is of any importance, and can be used

(*) Now at Columbia University, New York.

(**) Assisted by the joint program of the ONR and AEC.

exclusively to interpret the intensity-depth curve down to 3.000 m w.e. (1). If this is assumed as the minimum mean free path for a non-electromagnetic interaction, the corresponding cross section is $\sigma \lesssim 5 \cdot 10^{-30}$ cm^2 per nucleon. Direct measurements (2) have indicated $\sigma \lesssim 2.3 \cdot 10^{-30}$ cm^2 for fast mesons; and the value calculated from the specifically nuclear potential (3) necessary to explain the capture of slow negative mesons is $\sigma \sim 10^{-39} (p/\mu c)^2$ cm^2, where p is the meson momentum and μ its rest mass. The same formula in the same units holds for excitation by neutrino absorption, considered as an inverse β-decay process, where p is now the neutrino momentum.

Thus only the electromagnetic interactions of μ-mesons will be considered below; and the accompanying note indicates that it will be sufficient to consider the meson as a normal Dirac particle, even if this is not quite the case.

2. – Underground meson spectrum.

The vertical cosmic ray intensity as a function of depth shows a considerable change in slope ad about 300 m w.e.: at shallower depths it varies (4) roughly as $d^{-1.5}$, at greater depths as $d^{-2.5}$. This has been interpreted (5,6) as reflecting a competition between nuclear absorption and μ-decay for the parent π-meson high in the atmosphere. In the π-meson rest system, the μ-meson kinetic energy is negligible in comparison with its rest mass; therefore in the laboratory system $E_\mu/\mu c^2 \sim E_\pi/m_\pi c^2$. Accordingly the relative probability of π-μ decay is

$$(1) \qquad P(E_\mu) = \{(m_\pi c^2/E_\pi)1/\tau c\} / \{\varrho/\lambda + (m_\pi c^2/E_\pi)1/\tau c\} = B/(E_\mu + B) ,$$

$$B = \lambda \mu c/\varrho\tau ,$$

where λ is the mean free path for absorption by air nuclei of a π-meson of energy E_π and mean life τ in its rest frame, and ϱ is the air density at the average height of production of μ-mesons.

If the π-mesons are originally distributed according to a power law $E_\pi^{-\gamma-1}$, the integrated μ-meson intensity will vary with depth as $d^{-\gamma}$ far above and $d^{-\gamma-1}$ far below the critical depth corresponding to the energy loss B. This statement assumes a linear energy loss with depth by the μ-mesons, which

(1) S. Hayakawa and S. Tomonaga: *Prog. Theor. Phys.*, **4**, 287 (1949).
(2) E. Amaldi and G. Fidecaro: *Nuovo Cimento*, **7**, 535 (1950).
(3) J. A. Wheeler: *Rev. Mod. Phys.*, **21**, 133 (1949).
(4) V. C. Wilson: *Phys. Rev.*, **53**, 337 (1938).
(5) K. I. Greisen: *Phys. Rev.*, **73**, 521 (1948).
(6) S. Hayakawa: *Prog. Theor. Phys.*, **3**, 199 (1949).

is justified because the critical depth is considerably less than 10^3 m w.e., where bremsstrahlung losses first begin to become important. The average value obtained from intensity-depth measurements is $\gamma = 1.65$, which is in accord with the observation [7] that the high energy differential spectrum of vertical mesons at sea level can be fitted by $(E_\mu + E_s)^{-2.6}$, where $E_s \sim 20\ \mu c^2$ is roughly the ionization loss by mesons arriving from the top of the atmosphere. It is also in agreement with the value $\gamma = 1\frac{2}{3}$ recently deduced [8] for the primary radiation at high energies.

For depths at which linear energy loss is valid, the differential vertical spectrum underground is

$$(2)\qquad \begin{cases} n_v(E_\mu)\,\mathrm{d}E_\mu = n_0 P(E_\mu + \sigma d)\,\mathrm{d}E_\mu [E_\mu + \sigma d]^{-\gamma-1} \\ \gamma = 1.65 \\ n_0 = 2.0(\mu c^2)^{1.65}\ \mathrm{cm}^{-2}\,\mathrm{s}^{-1}\,\mathrm{sterad}^{-1}\,, \end{cases}$$

where $\sigma \sim 2\mu c^2/\mathrm{m\ w.e.}$ and d is the depth measured from the top of the atmosphere. The low energy mesons at sea level that deviate from this formula will all have been absorbed at less than 10 m w.e. underground, and decay in flight is negligible. The coefficient n_0 is evaluated by fitting (2) to the sea level measurements [9] at $E_\mu = 10\mu c^2$, where $P \sim 1$. To discuss the integral spectra, crude approximations will be used throughout to preserve a perspicuous analytic form at the expense of precision, which is not to be expected to a high degree in any case. The total vertical intensity obtained by integrating (2) is

$$(3)\qquad I_v(d) = \int_0^\infty n_v(E_\mu)\,\mathrm{d}E_\mu = n_0 J_v(d)/\gamma(\sigma d)^\gamma\,,$$

where it is clear that $J_v \to 1$ as $\sigma d/B \to 0$, and $J_v \to \gamma/[(\gamma+1)\sigma d]$ as $\sigma d/B \to \infty$. The simplest form with these properties is

$$(3a)\qquad J_v(d) \sim P[(1 + 1/\gamma)\sigma d]\,,$$

which will be assumed as a lowest order approximation (in excess).

Under the form (3*a*) the depth D of the « knee » in the intensity – depth curve is related to the constant B by

$$(4)\qquad B \sim D(1 + 1/\gamma) \sim 10^3\ \mu c^2\,,$$

(7) L. Jánossy: *Cosmic Rays* (Oxford, 1948), p. 171.
(8) H. V. Neher: *Phys. Rev.*, **83**, 649 (1951).
(9) B. Rossi: *Rev. Mod. Phys.*, **20**, 537 (1948).

using $D \sim 300$ m w.e. Detailed calculations ([10,11]) show that at angle θ to the vertical

$$B(\theta) \sim B/\cos\theta \,. \tag{5}$$

The source of local secondary radiation underground is the total meson spectrum integrated over all angles θ of deviation from the vertical. Assuming only ionization (linear) energy loss at depths $d < 10^3$ m w.e., one has

$$I_\theta(d) = I_v(d/\cos\theta) = [n_0/\gamma(\sigma d)^\gamma][(\cos\theta)^\gamma J_v(d/\cos\theta)] \,, \tag{6}$$

where by (3*a*) and (5) J_v is actually independent of θ, and the integral of (6) over all angles becomes

$$I(d) = 2\pi n_0 P[(1 + 1/\gamma)\sigma d]/\gamma(\gamma + 1)(\sigma d)^\gamma \,. \tag{7}$$

It is also desirable to have an expression for the differential spectrum $n(E_\mu)$ integrated over all angles; a simple approximation of suitable general form is

$$n(E_\mu)\,\mathrm{d}E_\mu = \frac{2\pi n_0\,\mathrm{d}E_\mu}{[E_\mu + (\gamma+1)^{1/\gamma}\sigma d]^{\gamma+1}}\, P[(1 + 1/\gamma)\sigma d] \,, \tag{8}$$

which has the properties that it integrates to (7) and agrees asymptotically with the direct angular integration of (2) in the limiting cases $E_\mu \to 0, \infty$. With the insertion of numerical values given above, these become

$$I(d) = 0.92\, d^{-1.65}[1 + 2.7\cdot 10^{-3}\, d]^{-1}\ \mathrm{cm^{-2}\,s^{-1}} \,, \tag{7a}$$

and the normalized form

$$i(E_\mu)\,\mathrm{d}E_\mu = \frac{1}{I}\, n(E_\mu)\,\mathrm{d}E_\mu = 13.7\, d^{1.65}[E_\mu + 3.6\, d]^{-2.65}\,\mathrm{d}E_\mu \,, \tag{8a}$$

where E_μ is in units of μc^2 and d in m w.e. Equations (7*a*) and (8*a*) are the basis of the remaining discussion.

3. – Secondary soft radiation.

Soft showers are initiated by electron knock-on and bremsstrahlung; μ-meson decay is negligible in the dense medium underground. As indicated in the accompanying note, electron pair creation by μ-mesons is similar in character to bremsstrahlung and about half as large in magnitude. The cor-

---

([10]) K. Greisen: *Phys. Rev.*, **76**, 1718 (1949).
([11]) K. Greisen: private communication.

responding cross sections per atom for energy loss are in simplest approximation

$$(9)\qquad \begin{cases} \sigma_K(E)\,\mathrm{d}E = 2\pi r_0^2 Z(mc^2)\,\mathrm{d}E/E^2 \\ \sigma_B(E)\,\mathrm{d}E = 4\alpha(Zr_\mu)^2 E_\mu \ln(3.8\cdot 10^4 Z^{-2/3})\,\mathrm{d}E/E \\ \sigma_P(E)\,\mathrm{d}E = 0.5\,\sigma_B(E)\,\mathrm{d}E \\ \sigma(E,\,E_\mu) = \sigma_K + \sigma_B + \sigma_P\,, \end{cases}$$

where E, E_μ are the shower and meson energies, respectively, and r_0 and r_μ are the classical radii of electron and meson. In σ_P there is cancellation of two factors of 2 from the fact that two showers are initiated, each on the average with half the energy of an equivalent bremsstrahlung shower. For showers of energy E the production rate $R_s(E)$ in $\mathrm{g^{-1}\,s^{-1}}$ is given by

$$(10)\qquad [R_s(E)/I(d)]\,\mathrm{d}E\left\{\begin{matrix}\mathrm{CaCO_3}\\ \mathrm{Pb}\end{matrix}\right\} =$$

$$= (N_0/A)\int_{\dot{E}}^{\infty}\sigma(E,\,E_\mu)\,\mathrm{d}E\,i(E_\mu)\,\mathrm{d}E_\mu \sim \left\{\begin{matrix}7.1-.027E\\ 5.7-.12E\end{matrix}\right\}\cdot 10^{-4}\,\mathrm{d}E/E^2\,,$$

with E and d in μc^2 and m.w.e. The two sets of coefficients in the brackets correspond to $CaCO_3$ and Pb, respectively, and will be carried throughout as typical of light and heavy materials. If the measured size-frequency distribution should show any pronounced excess above these curves, it would presumably constitute evidence for a strong nuclear source of soft showers, such as the decay of neutral π-mesons. This excess would be apparent only for showers of energy $E > m_\pi c^2$.

Since the cross section for nuclear excitation by γ-rays appears to be rather high, it is desirable to have an expression for the average photon spectrum accompanying an underground meson. The photons are both virtual and real, arising respectively from the Coulomb field of the meson and the soft showers. The virtual photon spectrum accompanying the average meson is

$$(11)\qquad \gamma'(E_\nu)\,\mathrm{d}E_\nu = \frac{2}{\pi}\,\alpha(\mathrm{d}E_\nu/E_\nu)\int_{\dot{E}_\nu}^{\infty}\ln(E_\mu/E_\nu)\,i(E_\mu)\,\mathrm{d}E_\mu = \frac{2}{\pi}\,\alpha(\mathrm{d}E_\nu/E_\nu L)(E_\nu).$$

The integral $L(E_\nu)$ occurs repeatedly, and the following forms are found numerically:

$$(12)\qquad L_\nu(E) \sim \begin{cases} 0.86\ln(3.6\,d/E_\nu) & E_\nu < 3.6\,d \\ 0.61(0.5 + E_\nu/3.6\,d)^{-1.65} & E_\nu > 3.6\,d\,, \end{cases}$$

where the low- and high-energy expressions do not coincide in the intermediate region $E_\nu \sim 3.6d$. The logarithmic term is in error by less than 10% for $.002 < E_\nu/d < 2$ and suffices for most purposes; the second formula is needed only for rare events of very high energy. For the real photons the approximation is used that a shower initiated by an event of energy E' has a path length ([12]) for γ-rays of energy E_ν that is $X(E_\nu)\,\mathrm{d}E_\nu = 0.57 X_0 E'\,\mathrm{d}E_\nu/E_\nu^2$ where X_0 is the radiation length of the material traversed, $X_0^{-1} \quad 4\alpha(Zr_0)^2 N_0/A \times$ $\times \ln(183 Z^{-1/3})$. The corresponding spectrum of real photons per average meson is

$$(13)\quad \gamma''(E_\nu)\,\mathrm{d}E_\nu = 0.57(X_0 N_0/A)(\mathrm{d}E_\nu/E_\nu^2)\int_{E_\nu}^{\infty} i(E_\mu)\,\mathrm{d}E_\mu \int_{E_\nu}^{E_\mu} E'\sigma(E', E_\mu)\,\mathrm{d}E' \sim$$

$$\sim (\mathrm{d}E_\nu/E_\nu^2)\left[\begin{Bmatrix} 1.1\cdot 10^{-2} \\ 1.9\cdot 10^{-2}\end{Bmatrix} L(E_\nu) + 1.4\cdot 10^{-4} d(2.5 y^{-.65} - y^{-1.65})\right],$$

$$y = (1 + E_\nu/3.6d)\,,$$

where as usual the brackets refer to $CaCo_3$ and Pb, and E_ν, d are measured in μc^2 and m.w.e. In evaluating (13), the rough approximation is made that the average value of E_μ in the integral of type L is $\bar{E}_\mu \sim 3.6d$.

Because of the different dependence on E_ν, the virtual photons are dominant for energies $E_\nu \gtrsim 5\,\mu c^2 \sim 0.5$ GeV, the real photons at lower energies. For nuclear excitation, proton knock-on makes some contribution, so that the average distribution of secondary electrons per meson might also be computed. This distribution would be given by $0.76\,\gamma''(E_\beta)$ and for energies $E_\beta \gtrsim \mu c^2$ would be only a few percent so intense as the primary meson component; since the energy region above 100 MeV is the most interesting for consideration of nuclear excitation, the secondary electron component will be neglected throughout.

4. – Nuclear excitation.

Nuclear excitation of energy E by proton knock-on occurs at a rate $R_k(E)$ g^{-1} s^{-1}, where

$$(14)\quad R_k(E)\,\mathrm{d}E/I(d) = 2\pi r_0^2 (N_0 Z/A)(m/\mu)(m/M)(\mathrm{d}E/E^2)\int_E^{\infty} i(E_\mu)\,\mathrm{d}E_\mu =$$

$$= \begin{Bmatrix} 3.9 \\ 3.1\end{Bmatrix}\cdot 10^{-7}(\mathrm{d}E/E^2)[1 + E/3.6d]^{-1.65}.$$

([12]) B. Rossi and K. Greisen: *Rev. Mod. Phys.*, **13**, 240 (1941).

This rate represents a minimum estimate, since it can only be increased by the knock-on of virtual π-mesons ([13]); since the π-mesons are present only a fraction of the time, however, equation (14) should probably be correct in order of magnitude. The excitation rate by γ-rays is $R_\gamma(E)$ g^{-1} s^{-1}, with

$$R_\gamma(E)\,\mathrm{d}E/I(d) = N_0\gamma(E)\sigma_\gamma(E)/A\,, \tag{15}$$

where $\gamma(E) = \gamma'(E) + \gamma''(E)$, and $\sigma_\gamma(E)/A$ is the effective cross section per nucleon for γ-excitation.

Recent measurements ([14,15]) indicate that in the range $E_\gamma \sim 200 \div 300$ MeV the total cross section for excitation is of order $N_0\sigma_\gamma/A \sim 10^{-4}$ g^{-1} cm^2, a remarkably high value. At these energies comparison of (14) and (15) shows that R_γ exceeds R_k by an order of magnitude. Hence measurement of size-frequency distribution of nucleon cascades underground would yield information about the behavior of σ_γ at energies above the limits of presents machines; such measurements would in principle extend up to energies where $\sigma_\gamma(E)$ starts to fall off faster than $1/E$.

As an index of nuclear excitation one may consider the average number of slow neutrons m_s produced per unit length (in g/cm^2) when a meson traverses an underground absorber. This number is

$$m_s(d) = \int_{E_s}^{\infty} [Y(R_k + R_\gamma)/I(d)](E/E_s)\,\mathrm{d}E\,, \tag{16}$$

where $E_s \sim 0.1\ \mu c^2$ is the average of a « slow » neutron relative to its bound state, and the yield Y is the fraction of initial excitation energy that is eventually converted into slow neutrons. Certainly $Y < 1$, and $Y \gtrsim 0.1$ seems probable as a lower limit. Two possible types of variation will be assumed for σ_γ:

$$N_0\sigma_\gamma(E)/A = \begin{cases} 10^{-4} & \text{(17}a\text{)} \\ 10^{-4}(2/E)\,, & \text{(17}b\text{)} \end{cases}$$

in both cases $E \geqslant 2$, and $\sigma_\gamma(E) \equiv 0$ for $E < 2$. Measurement of m_s as a function of d would be evidence as to which of equations (17) is closer to the truth.

For comparison with observation it is convenient to define $\sigma_s(d)/A$, an effective cross section per nucleon of slow neutron production; and for pro-

---

([13]) C. Franzinetti: *Nuovo Cimento*, **7**, 384 (1950).
([14]) S. Kikuchi: *Phys. Rev.*, **81**, 1060 (1951); *Bull. Am. Phys. Soc.*, **26** (3), 7 (1951).
([15]) R. D. Miller: *Phys. Rev.*, **82**, 260 (1951).

duction in Pb at $d = 30$ m w.e.,

$$\sigma_s(30)/A = m_s(30)/N_0 = \begin{cases} 82\,Y \cdot 10^{-29} \text{ cm}^2 & (18a) \\ 18\,Y \cdot 10^{-29} \text{ cm}^2 . & (18b) \end{cases}$$

A preliminary measured value [16] can be fitted by (18*a*) with $Y \sim 0.5$, but (18*b*) would require $Y \sim 2$, which is impossible. This is an indication that at high energies the excess of R_γ over R_k becomes even greater than the order of magnitude found for excitation around 200÷300 MeV. The underground nucleonic component is therefore primarily due to γ-excitation of nuclei and only secondarily to proton knock-on.

5. – Stars in emulsion underground.

Nuclear stars in emulsion have been measured underground [17] at depths $d = 33$, 44, 70 m w.e. from the top of the atmosphere. Very little trend with depth is evident, and the formula

$$R_*(d) \sim 2.0 \cdot 10^{-7}\, d^{-.67} \text{ g}^{-1}\,\text{s}^{-1} \qquad (19)$$

represents about the maximum decrease with depth consistent with the stated errors. The average of all the measurements is

$$R_*(55) \sim 1.5 \cdot 10^{-8} \text{ g}^{-1}\,\text{s}^{-1} . \qquad (20)$$

About 4% of the primaries appear to be charged. The observed stoppings of slow π-mesons cannot be readily interpreted, as it is not clear to what extent the slow π's are locally produced in the material immediately surrounding the emulsion. A π-meson with a residual range of 100 μ of emulsion has a 90% chance of decay in a path length of 3 meters. It therefore seems likely that the observed rate is strongly influenced by apparatus geometry.

The energy required for a star of 3 or more prongs is taken [18] as $E \gtrsim 1.4\,\mu c^2$. The stars are produced directly by μ-mesons (knock-on and virtual quanta), by soft showers (real quanta), and by nucleons in locally produced cascades. For the nucleon cascades, a crude diffusion treatment is developed in the Appendix, which results in the following approximate

---

[16] R. D. Sard: private communication.
[17] E. P. George and J. Evans: *Proc. Phys. Soc.*, **63**, 1248 (1950).
[18] R. Brown *et al.*: *Phil. Mag.*, **40**, 862 (1949).

path lengths for neutrons and protons of energy E initiated by an event of energy E_0:

$$(21)\qquad \begin{cases} \lambda_n(E, E_0)\,\mathrm{d}E \sim 0.42\,\lambda_g E_0(\mathrm{d}E/E^2)[1 + 3E_c/(E_c + 1.6E)] \\ \lambda_p(E, E_0)\,\mathrm{d}E \sim 0.42\,\lambda_g E_0\,\mathrm{d}E/[E(E + E_c)]\,, \end{cases}$$

where the ionization loss by a proton per geometric mean free path λ_g is $E_c = \begin{cases} 1.4\ \mu c^2 \\ 3.0\ \mu c^2 \end{cases}$ for $\begin{cases} \mathrm{CaCO_3} \\ \mathrm{Pb} \end{cases}$. The average number of nucleons of energy E accompanying a meson is then

$$(22)\qquad N_{n,p}(E)\,\mathrm{d}E = \mathrm{d}E \int_E^\infty \{\lambda_{n,p}(E, E_0)[R_k(E_0) + R_\gamma(E_0)]/I(\bar{d})\}\,\mathrm{d}E_0\,.$$

In the emulsion the rate of star production is somewhat less than the rate of nuclear excitation, since a nucleus with sufficient energy to produce a star of 3 or more prongs does not always do so. For an order-of-magnitude estimate it is assumed that the average rate of visible stars is 1/2 the rate of excitation to energies $\gtrsim 1.4\ \mu c^2$, regardless of the mode of excitation. Then the star rates with meson, γ-ray, neutron and proton primaries are

$$(23)\qquad \begin{cases} R_{*\mu} = (1/2)\int_{1.4}^\infty [R_k(E) + R_{\gamma'}(E)]\,\mathrm{d}E \\ R_{*\gamma} = (1/2)\int_{1.4}^\infty R_{\gamma''}(E)\,\mathrm{d}E \\ R_{*n,p} = (1/2)I(\bar{d})(N_0\sigma_g/A)\int_{1.4}^\infty N_{n,p}(E)\,\mathrm{d}E\,, \end{cases}$$

where $N_0\sigma_g/A = 1.0 \cdot 10^{-2}$ cm²/g is the average geometrical cross section of emulsion.

In evaluating $R_{*n,p}$ in (23), it is sufficient to regard the factors external to $\lambda_{n,p}$ as relatively slowly varying with E, so that the correction terms involving E_c can be approximated by averaging over $\lambda_{n,p}(E, E_0)$ alone, for $1.4 \leqslant E < \infty$. With $E_c = 1.4\ \mu c^2$, this yields

$$(24)\qquad \begin{cases} \lambda_n(E, E_0)\,\mathrm{d}E \sim 1.68 \cdot 0.42\,\lambda_g E_0\,\mathrm{d}E/E^2 \\ \lambda_p(E, E_0)\,\mathrm{d}E \sim 0.69 \cdot 0.42\,\lambda_g E_0\,\mathrm{d}E/E^2 \end{cases}$$

so that 30% of the star producing nucleonic component consists of protons.

This extimate, although only order of magnitude, indicates that the proton component is not to be ignored. With this approximation, expressions (23) are evaluated under assumptions (17*a*) and (17*b*), resulting in table I. The fractions of the total star rate due to each source are given, as well as the fraction of charged primaries $f_c = f_\mu + f_\pi$.

TABLE I.

	$R_*(55)$	Variation $30 \div 70$ m w.e.	f_μ	f_γ	f_n	f_p	f_c
Approx. (17*a*)	$2.8 \cdot 10^{-8}$ g^{-1} s^{-1}	$d^{-.87}$	.09	.09	.58	.24	.33
Approx. (17*b*)	$0.7 \cdot 10^{-8}$ g^{-1} s^{-1}	$d^{-1.31}$	.19	.15	.47	.19	.38

Comparison with the observations (19), (20) leads to the following conclusions. The absolute star production rate suggests that the truth is intermediate to approximations (17*a*) and (17*b*); that is, the relatively large value observed for $\sigma_p A$ at $E \quad 200 \div 300$ MeV is maintained over a considerable energy range, falling off more slowly than $1/E$. This has the corollary that meson-proton knock-on is of generally negligible importance as an intermediate mechanism in production of underground cosmic rays. The fraction of charged primaries is relatively insensitive to assumptions and is about 35%, of which at least half appear to be protons. The variation in depth cannot be made to agree with the very small experimental value, and an assumption intermediate to (17*a*) and (17*b*) would yield something like d^{-1} as the most probable calculated variation.

The variation in depth would be more significant if it could be determined at greater depths, such as shown in table II. The values of f_c are also included and are seen to show very little variation.

TABLE II.

	$R_*(a)$	$f_c(a)$	$R_*(b)$	$f_c(b)$
d — 100 m w.e.	$1.5 \cdot 10^{-8}$ g^{-1} s^{-1}	.31	$3.0 \cdot 10^{-9}$ g^{-1} s^{-1}	.35
150	$1.0 \cdot 10^{-8}$ g^{-1} s^{-1}	.31	$1.7 \cdot 10^{-9}$ g^{-1} s^{-1}	.33
200	$.71 \cdot 10^{-8}$ g^{-1} s^{-1}	.30	$1.1 \cdot 10^{-9}$ g^{-1} s^{-1}	.31
300	$.46 \cdot 10^{-8}$ g^{-1} s^{-1}	.30	$.64 \cdot 10^{-9}$ g^{-1} s^{-1}	.29

6. – Summary and conclusions.

Cosmic rays underground are considered as due to the electromagnetic interaction of μ-mesons. Tractable approximate expressions are obtained for i) the flux of underground μ-mesons; ii) size-frequency distribution of soft showers; iii) rate of nuclear excitation and production of slow neutrons; iv) production of nucleon cascades and stars in emulsion.

The dominant feature in nuclear effects is the large cross section σ_γ/A for γ-excitation of the nucleus, which has been measured to be of order $1 \cdot 10^{-28}$ cm^2 per nucleon at E 200 to 300 MeV. Comparison with measurements on slow neutrons and star production underground indicates that σ_γ/A falls off more slowly than $1/E$ for higher energies and hence remains relatively large over a wide range. Other modes of nuclear excitation, such as meson-proton knock-on become negligible in comparison.

The agreement calculation with observation is satisfactory except for the depth dependence of nuclear stars; this difficulty would be illuminated by measurements at greater depths than hitherto attempted, for which calculated values are given. Measurement of nuclear excitation by means of stars or slow neutrons over wide depth intervals would yield more definite information about the variation of σ_γ/A at high energies.

Measurement of the size-frequency distribution, of soft showers at energies of a few hundred MeV and above would also provide information on the cross section for neutral π-meson production at these energies. In all such applications, the underground μ-mesons are being utilized essentially as a naturally provided betatron of low intensity but unlimited energy range.

The author takes pleasure in thanking Professor R. D. Sard for an introduction to these problems and for many interesting and helpful discussions.

Appendix

In the absence of ionization loss, the diffusion equation for a nucleon cascade reads

$$\partial N(E, x)/\partial x = -N(E, x) + \int_{\dot{E}}^{\infty} G(E, E')N(E', x)\,\mathrm{d}E' , \tag{A1}$$

where N is the nucleon density and x the distance in units of γ_0, the geometric mean free path. For the reproduction function a convenient phenomeno-

logical form is

$$G(E, E')\,\mathrm{d}E' = (n+2)(n+1)(E'-E)^n E'^{-n-1}\,\mathrm{d}E' , \tag{A2}$$

where the normalization insures energy conservation in a nuclear collision process with E' the incident energy and E the energy parameter of the emitted particles. Here n is the single adjustable parameter, since there is only one experimental fact to be reproduced; namely, that the mean free path for absorption of the atmospheric N-component is $2\lambda_p$. The Mellin transform of (A1) is

$$\begin{cases} \partial N(s,x)/\partial x = \left[-1 + \dfrac{(n+2)!\,s!}{(n+s+1)!}\right] N(s,x) = [-1 + 2C(s)]N(s,x) , \\ N(s,x) = \displaystyle\int_0^\infty (E/E_0)^s N(E,x)\,\mathrm{d}E . \end{cases} \tag{A3}$$

For an initial power spectrum $N(E, 0) = E^{-s-1}$ with $s = 1.65$, the value $n = 2.5$ makes the bracketed coefficient in (A3) become $-1/2$ in accordance with observation.

For energies at which ionization loss by the protons becomes important, the equations become

$$\begin{cases} \partial N_n(E,x)/\partial x = -N_n(E,x) + \displaystyle\int_E^\infty G(E,E')[(1/2)N_n(E',x) + (1/2)N_p(E',x)]\,\mathrm{d}E' \\ \partial N_p(E,x)/\partial x = -N_p(E,x) + \displaystyle\int_E^\infty G(E,E')[(1/2)N_n(E',x) + (1/2)N_p(E',x)]\,\mathrm{d}E' + \\ \qquad\qquad + E_c\,\partial N_p(E,x)/\partial E , \end{cases} \tag{A4}$$

where E_c is the (assumed constant) ionization loss per mean free path. The factor of 1/2 inside the integrals assumes equal probability for neutron and proton emission in nuclear collisions. Since these equations are difficult to solve, consider the easier set obtained by inserting an additional factor (E/E_0) in the ionization loss term. This will cause a considerable underestimate of ionization losses but is at least more realistic than (A3). The transformed equations are then

$$\begin{cases} \partial N_n(s,x)/\partial x = -N_n(s,x) + C(s)[N_n(s,x) + N_p(s,x)] , \\ \partial N_p(s,x)/\partial x = -N_p(s,x) + C(s)[N_n(s,x) + N_p(s,x)] - \\ \qquad\qquad - (s+1)(E_c/E_0)N_p(s,x) . \end{cases} \tag{A5}$$

The solution with $N_p(s, 0) = N_n(s, 0) = 1$ corresponding to an initiating event of energy E_0, which reduces to the solution of (A3) if $E_c = 0$, is

$$\begin{cases} \left.\begin{matrix} N_n(s,x) \\ N_p(s,x) \end{matrix}\right\} = \left\{\begin{matrix} C/(\mu+1) \\ 1 - C/(\mu+1) \end{matrix}\right\} \exp[-\mu x] , \\ \mu(s) = C(s) - 1 - \delta/2 + \sqrt{C^2 + \delta^2/4} , \qquad \delta = (s+1)E_c/E_0 = (s+1)\delta_0 . \end{cases} \tag{A6}$$

The total path length at energy E is the inverse Mellin transform of $\int_0^\infty N(s, x)\,\mathrm{d}x$ and can be approximated by the residue at s_0, which has the algebraically largest real part of any pole position. For $\delta = 0$, this pole of $1/\mu(s)$ is at $s_0 = 1$; and $s_0 = 0.95$ even for $\delta_0 = 10$, so that $s_0 \sim 1$ can be taken as a good approximation throughout. The residue at s_0 is considerably more sensitive to δ_0; but simple numerical approximations good to 10% in the range $\delta_0 = 0$ to 10 are

$$\text{(A7)} \qquad \begin{cases} \lambda_n(E, E_0)\,\mathrm{d}E = 0.42\,\lambda_g[1 + 3\,\delta_0'(1 + 1.6\,\delta_0)]E_0\,\mathrm{d}E/E^2\,, \\ \lambda_p(E, E_0)\,\mathrm{d}E = [0.42\,\lambda_g 1/(1 + \delta_0)]E_0\,\mathrm{d}E/E^2\,, \end{cases}$$

where the geometrical path length λ_g is introduced explicitly.

The path lengths (A7) are based on an approximation that reduces the actual ionization loss by a factor $\bar{E}(E)/E_0 < 1$, where $\bar{E}(E)$ is the average energy of a nucleon cascade in passing from energy E_0 to E. The crudest estimate is $\bar{E} \sim E$; in higher approximation this will be corrected by factors of order $\ln(E_0/E)$, etc., which are secondary in order of magnitude. Using just the lowest approximation, one has $\delta_0 \to \delta_0 E_0/E$, with the simple result

$$\text{(A8)} \qquad \begin{cases} \lambda_n(E, E_0)\,\mathrm{d}E \sim 0.42\,\lambda_g[1 + 3\,E_c\,(E_c + 1.6\,E)]E_0\,\mathrm{d}E/E^2\,, \\ \lambda_p(E, E_0)\,\mathrm{d}E \sim 0.42\,\lambda_g E_0\,\mathrm{d}E/E(E + E_c)\,. \end{cases}$$

RIASSUNTO (*)

I raggi cosmici nel sottosuolo sono trattati come dovuti esclusivamente alle interazioni elettromagnetiche dei mesoni μ. Si danno delle semplici approssimazioni per gli spettri sotterranei dei mesoni μ, dei fotoni virtuali, degli sciami molli e dei nucleoni. Il confronto coi dati sperimentali è soddisfacente per quanto riguarda la misura assoluta della produzione dei mesoni lenti e delle stelle nucleari, e il rapporto di carica dei primari producenti stelle, se i primari carichi elettricamente sono almeno per metà protoni. Non c'è accordo con la dipendenza osservata della produzione di stelle dalla profondità. Il confronto con l'osservazione fa pensare che la sezione d'urto per l'eccitazione nucleare da parte dei raggi γ decresca in media più lentamente di $1/E$ dal suo notevole valore misurato $\sigma_\gamma/A \sim 1 \cdot 10^{-28}$ cm^2 per nucleone a $E = 200 \div 300$ MeV. Questo meccanismo predomina quindi, nella produzione della componente nucleonica, nel sottosuolo su quello di knock-on mesone-protone. Misure di neutroni lenti o di produzione di stelle a grandi differenze di profondità fornirebbero maggiori chiarimenti sul comportamento di σ_γ/A alle alte energie. Misure della distribuzione ampiezza-frequenza degli sciami molli alle alte energie fornirebbero dati sulla produzione di mesoni π neutri.

(*) *Traduzione a cura della Redazione.*

NOTE TECNICHE

A New Resistor Network for the Integration of Laplace's Equation.

E. PERSICO

Istituto di Fisica dell'Università - Roma

(ricevuto il 7 Novembre 1951)

Summary. — This paper develops the theory of an improved type of resistor network, for the numerical calculation of an harmonic function (in two dimensions, or in three with axial symmetry) with given values on the boundary. The advantage of this type of apparatus on those hitherto described is that it takes into account terms of an higher order in h (h — side of the mesh), so permitting a much better accuracy with the same value of h. It is shown that, also for the usual type of network, the reasoning based on the analogy with the electrolytic tank is misleading, and that the correct method of calculation leads, in the case of axial symmetry, to values of the resistances which, in the vicinity of the axis, differ by an appreciable amount from those adopted by preceding Authors. A method is indicated for imposing the boundary condition on a curved line not passing through the junctions of the network.

1. – Introduction.

As it is well known, the problem of solving numerically Laplace's equation $\Delta V = 0$ with given boundary conditions is of paramount importance in many fields of physics and engineering. Since an analytical solution can be found only in a minority of cases, three methods have been developed for an approximate numerical determination of the function V: the *relaxation method* [1], the *electrolytic tank* and the *resistor network*. The first is a method of nume-

[1] R. V. SOUTHWELL: *Relaxation Methods in Engineering Science* (Oxford, 1940); *Relaxation Methods in Theoretical Physics* (Oxford, 1946). See also: G. LIEBMANN: *Adv. in Electronics*, **2**, 101 (1950), where a neat account can be found also of the methods of the electrolytic tank and of the resistor network.

rical computation whose approximation can be pushed as far as desired, but at the cost of a considerable sum of work and time. The last two methods, based on electrical analogies, once constructed the necessary apparatus enable to solve a variety of problems with little labor and accuracy sufficient in most practical cases. It has been pointed out recently (2) that the resistor network can give results much more accurate than an electrolytic tank and presents many advantages over the latter.

The resistor network so far considered is a net of electrical resistors disposed according to the pattern of fig. 1: they have all the same value if the equation in cartesian coordinates

$$\frac{\partial^2 V}{\partial x^2} + \frac{\partial^2 V}{\partial y^2} = 0 \,, \tag{1}$$

must be solved: they have instead values graded according to a certain law if the equation to be solved is

$$\frac{\partial^2 V}{\partial r^2} - \frac{1}{r}\frac{\partial V}{\partial r} + \frac{\partial^2 V}{\partial z^2} = 0 \,, \tag{2}$$

that is, the equation satisfied by an harmonic function of the *cylindrical* coordinates r, z, ϑ, in the case of axial symmetry (V independent of ϑ). This is, for instance, the equation of the electric (or magnetic) potential in an electron lens. It can be shown that the electric potential v at any junction of the net (which can be measured by means of a potentiometer) equals the value of the function V at the corresponding point of the field, provided that the fourth order derivatives of V, in the case of (1), or the *third* order ones, in the case of (2), can be neglected.

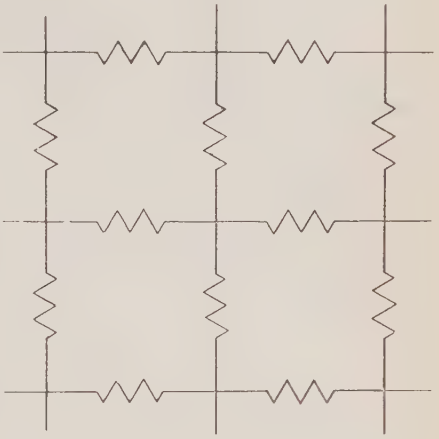

Fig. 1.

In this paper we will show that the accuracy can be much improved by adding to the network appropriate resistors along the diagonals, as shown in fig. 2. In this type of network the lowest derivatives that are disregarded are those of eighth order in the case of (1) (cartesian coordinates) and of the *fourth* order (but with a very small coefficient) in the case of (2) (cylindrical coordinates). It is found that, in the case of (1), the diagonal resistances must be four times larger than the others; in the case of (2), the law is more complicated, and, besides, also the non-diagonal resistances must be recalculated by means of recurrence formulae. But these calculations, made once and for all, enable to construct any resistance network of this type: these results are collected in a numerical table (tab. I).

Of course the increase in accuracy obtained in the network with diagonals would be deceptive if the boundary conditions (which we take of the Dirichlet

(2) G. LIEBMANN: *Brit. Journ. Appl. Phys.*, **1**, 92 (1950).

type $V = V_c$) were not realised with a corresponding exacteness. Since the boundary line, along which must be $V = V_c$, in general will not pass exactly through the junctions, a method is indicated, more accurate than that hitherto employed, by which the junctions nearest to the boundary will assume automatically potential values differing from V_c by the appropriate small amounts (n. 6).

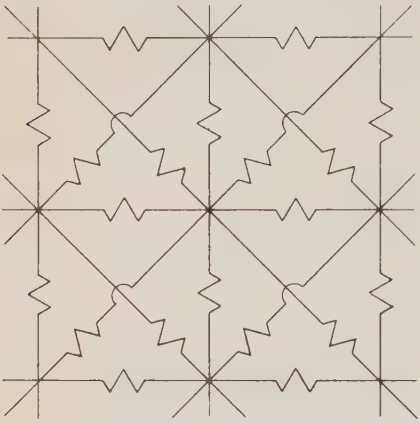

Fig. 2.

We have based our calculations on Taylor developments, avoiding any resort to the analogy with the electrolytic tank which, in our opinion, is misleading. In fact, if our method is applied to the ordinary network (without diagonals) for cylindrical coordinates, it is found (n. 4) that the resistances must be graded according to a law differing from that adopted by de Packh [3] and by Liebmann [2]: the difference is negligible at points far from the axis $r = 0$, but not so in the vicinity of the latter. For the resistances along the axis, we find a definite value intsead of the infinite value given by de Packh's formula.

Our values of the resistances for the network without diagonals for cylindrical coordinates are also collected in table I.

2. – Diagonal network for cartesian coordinates.

In this section we suppose thathe unknown function $V(x, y)$ satisfies equation (1) (cartesian coort dinates). We immagine drawn in the xy plane a lattice of square meshes of side h, whose corners correspond to the junctions of the resistor network. Let P_0 (fig. 3) represent any of these junctions (not contiguous to the boundary). For the sake of simplicity, we have suppressed from this drawing as well as from the following ones all the resistors except those connected to the junction P_0, and have represented these

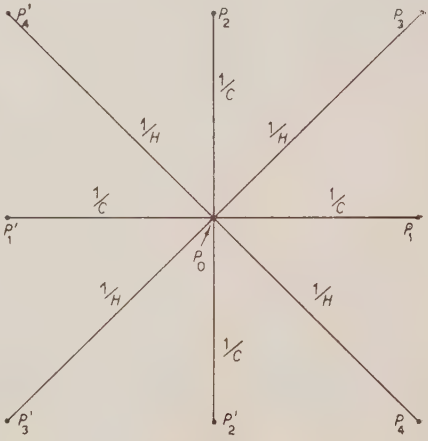

Fig. 3.

(3) D. C. de Packh: *Rev. Sci. Instr.*, **18**, 798 (1947).

with straigth lines instead of the customary symbol. The resistances along the horizontal and the vertical sides will have all the same value $1/C$, those along the diagonals the value $1/H$ (so C ad H mean the *conductances*: they are the same throughout the network). The potentials of the junctions P_0, P_1, P_1', ..., will be denoted by v_0, v_1, v_1',..., and the values of the V function at the corresponding points of the xy plane will be called V_0, V_1, V_1', ... The differences $v_0 - V_0$, $v_1 - V_1$, etc., will be the « errors ». It is impossible to give a general expression for the errors, but an insight on the accuracy of the method can be gained by evaluating the error $\varepsilon = v_0 - V_0$ at P_0, when the errors at all eight neighbouring junctions are assumed to be zero.

Kirchhoff's law applied to the junction P_0 gives

$$C(v_1 + v_1' + v_2 + v_2' - 4v_0) + H(v_3 + v_3' + v_4 + v_4' - 4v_0) = 0\,, \tag{3}$$

and therefore, if $v_1 = V_1$, $v_1' = V_1'$, etc., $v_0 = V_0 + \varepsilon$,

$$\varepsilon = \frac{C(V_1 + V_1' + V_2 + V_2' - 4V_0) + H(V_3 + V_3' + V_4 + V_4' - 4V_0)}{4(C + H)}\,. \tag{4}$$

Now V_1, V_1', etc., can be expressed as a Taylor series by means of V and its derivatives at P_0: denoting by h_x, h_y the coordinates of a point with respect to P_0, the series can be written

$$V - V_0 = \sum_1^\infty{}_n \left(h_x \frac{\partial}{\partial x} + h_y \frac{\partial}{\partial y}\right)^n V\,, \tag{5}$$

(where it is understood that the derivatives are to be taken at P_0). In developing this formula we must take into account that, because of (1),

$$\left(\frac{\partial}{\partial y}\right)^2 = -\left(\frac{\partial}{\partial x}\right)^2 \tag{6}$$

(if applied to V or any of its derivatives) and therefore, for any integer k,

$$\left(\frac{\partial}{\partial y}\right)^{2k} = (-1)^k \left(\frac{\partial}{\partial x}\right)^{2k}\,. \tag{7}$$

Applying (5) to the eight points for which h_x, h_y have the values $0, \pm h$, and substituting in (4), we find that many terms cancel out and we are left with

$$V_1 + V_1' + V_2 + V_2' - 4V_0 = 4 \sum_1^\infty{}_m \frac{h^{4m}}{(4m)!} \frac{\partial^{4m} V}{\partial x^{4m}}\,,$$

$$V_3 + V_3' + V_4 + V_4' - 4V_0 = 4 \sum_1^\infty{}_m (-4)^m \frac{h^{4m}}{(4m)!} \frac{\partial^{4m} V}{\partial x^{4m}}\,.$$

Therefore, if we disregard all derivatives higher than the eighth, formula (4) reduces to

$$\varepsilon = \frac{1}{4(C+H)} \left[\frac{h^4}{6} (C-4H) \frac{\partial^4 V}{\partial x^4} + \frac{h^8}{10\,080} (C+16H) \frac{\partial^8 V}{\partial x^8} \right]. \tag{8}$$

From this expression it is seen that we can get rid of the fourth order part of the error by making

$$C = 4H\,, \tag{9}$$

that is, giving the *diagonal resistances a value four times that of the others*. The principal part of the error then becomes

$$\varepsilon = \frac{h^8}{10\,080} \frac{\partial^8 V}{\partial x^8} = \frac{h^8}{10\,080} \frac{\partial^8 V}{\partial y^8}\,. \tag{10}$$

This value must be compared with the error in a network of the usual type, without diagonals. We can find the latter by putting $H = 0$ in (8), which gives for the principal part of the error, without diagonals,

$$\varepsilon = \frac{h^4}{24} \frac{\partial^4 V}{\partial x^4} = \frac{h^4}{24} \frac{\partial^4 V}{\partial y^4}\,. \tag{11}$$

It may appear that, with the cost of the materials used for the diagonal resistors, one could instead enlarge the usual type network and so adopt a smaller value of h, but it is readily seen that h would be reduced only by a factor $\sqrt{2}$, and therefore ε by a factor 4. The advantage gained by reducing the error from the *fourth* to the *eighth* order is in general much more considerable (except, of course, in regions where V happens to be very well represented by a polynomial of the third degree). Besides, it is to be expected that the doubling of the number of resistors connected to each junction contributes to a better smoothing out of the random errors caused by the resistors tolerances.

3. – Diagonal network for cylindrical coordinates.

We turn now to equation (2) and proceed along the same line of the preceding section, except that the values of the resistances of a mesh depend on the distance of it from the (horizontal) axis $r = 0$. So the eight resistors connected to any junction P_0 (with $r \neq 0$) are of five different values, as shown in fig. 4, where the letters C, G, G', H, H' denote, as before, the conductances. The values of each of these quantities is a function of r, that is of the order number $n = r/h$ of the row. The row $n = 0$ will be considered later (n. 5): for the moment we suppose $n \neq 0$.

Kirchhoff's equation (3) for the junction P_0 is now replaced by

$$\begin{aligned} C(v_1 + v_1' - 2v_0) + G(v_2 - v_0) + G'(v_2' - v_0) + \\ + H(v_3 + v_4' - 2v_0) + H'(v_4 + v_3' - 2v_0) = 0 \end{aligned}$$

and if $v_0 = V_0 + \varepsilon$, $v_1 = V_1$, etc., the error is given by

$$\varepsilon = \frac{I}{2C + G + G' + 2(H + H')}, \tag{12}$$

where we have called I the quantity

$$I = C(V_1 + V_1' - 2V_0) + G(V_2 - V_0) + G'(V_2' - V_0) + \\ + H(V_3 + V_4' - 2V_0) + H'(V_4 + V_3' - 2V_0). \tag{12'}$$

To calculate this expression we develop $V_1 - V_0$, $V_1' - V_0$, etc., with formula (5) (where x and y must now be replaced by z and r) limited to the fourth

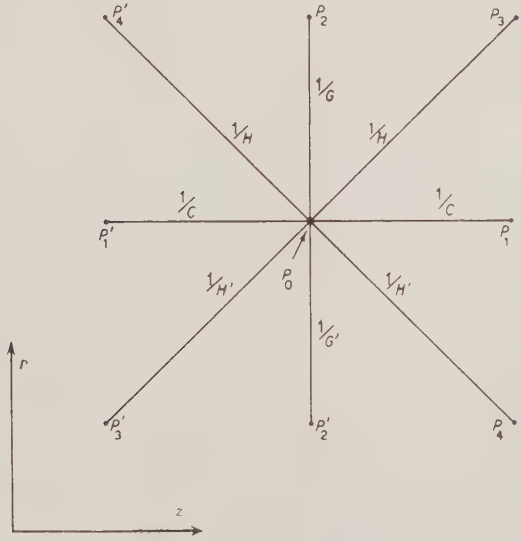

Fig. 4.

order terms. Then the numerator I of (12) comes out as a rather cumbersome expression containing the eight derivatives (at P_0)

$$V_r, \quad V_{rr}, \quad V_{rrr}, \quad V_{rrrr}, \quad V_{zz}, \quad V_{zzr}, \quad V_{zzrr}, \quad V_{zzzz}, \tag{13}$$

$\left(\text{where } V_r \equiv \left(\frac{\partial V}{\partial r}\right)_{P_0}, \text{ etc.}\right)$. These quantities are not independent, being related by equation (2) and those which can be deduced from it by differentiation, namely

$$\begin{cases} V_{zz} = -V_{rr} - V_r/r \\ V_{zzr} = -V_{rrr} - V_{rr}/r + V_r/r^2 \\ V_{zzrr} = -V_{rrrr} - V_{rrr}/r + 2V_{rr}/r^2 - 2V_r/r^3 \\ V_{zzzz} = V_{rrrr} + 2V_{rrr}/r - V_{rr}/r^2 + V_r/r^3. \end{cases} \tag{14}$$

By means of these formulae we can eliminate from the expression of I all derivatives with respect to z, and we are left with the following formula, where the derivatives are all independent (and $n = r/h$)

$$
(15)\quad \left\{\begin{aligned} I = {} & \left[G - G' + \left(2 - \frac{1}{n} + \frac{1}{n^2} - \frac{11}{12n^3}\right) H - \left(2 + \frac{1}{n} + \frac{1}{n^2} + \frac{11}{23n^3}\right) H' + \right. \\ & \left. + \left(-\frac{1}{n} + \frac{1}{12n^3}\right) C \right] h V_r + \\ & + \left[G + G' + \left(-\frac{2}{n} + \frac{11}{6n^2}\right) H + \left(\frac{2}{n} + \frac{11}{6n^2}\right) H' - \left(2 + \frac{1}{6n^2}\right) C \right] \frac{h^2}{2!} V_{rr} + \\ & + \left[G - G' - \left(4 + \frac{2}{n}\right) H + \left(4 - \frac{2}{n}\right) H' + \frac{C}{n} \right] \frac{h^3}{3!} V_{rrr} + \\ & + [G + G' - 8H - 8H' + 2C] \frac{h^4}{4!} V_{rrrr}. \end{aligned}\right.
$$

Now, if we suppose already determined the conductances G', H' of the $(n-1)$-th row, we can determine C, G, H (conductances of the n-th row) so as to eliminate the first, second and third part of I (and therefore of ε). In fact, putting equal to zero the coefficients of V_r, V_{rr}, V_{rrr}, we get the following three linear equations in the three unknowns C, G, H:

$$
(16)\quad 12n^3 G + (24n^3 - 12n^2 + 12n - 11) H - (12n^2 - 1) C = \\ = 12n^3 G' + (24n^3 + 12n^2 + 12n + 11) H' ,
$$

$$
(17)\quad 6n^2 G - (12n - 11) H - (12n^2 + 1) C = -6n^2 G' - (12n + 11) H' ,
$$

$$
(18)\quad nG - (4n + 2) H + C = nG' - (4n - 2) H' .
$$

We start the solution by eliminating C. It is convenient at this point to introduce the following abbreviations:

$$
L_n = 24n^3 + 36n^2 - 16n + 9 , \qquad P_n = 24n^3 - n ,
$$
$$
M_n = 48n^3 + 24n^2 + 16n - 9 , \qquad N_n = 12n^3 + 6n^2 + n .
$$

Then the equations for G and H take the form

$$
P_n G - L_n H = P_n G' + L_{-n} H' ,
$$
$$
N_n G - M_n H = -N_{-n} G' + M_{-n} H' ,
$$

and their solution is

$$
(19)\quad G = \frac{-(L_n N_{-n} + P_n M_n) G' + (-L_{-n} M_n + L_n M_{-n}) H'}{L_n M_n - P_n M_n} ,
$$

$$
(20)\quad H = \frac{-P_n (N_n + N_{-n}) G' + (P_n M_{-n} - N_n L_{-n}) H'}{L_n N_n - P_n M_n} .
$$

Once calculated G and H, formula (18) gives

$$C = nG' - nG - (4n-2)H' + (4n+2)H \,. \tag{21}$$

These formulae enable to calculate, step by step, all the conductances of the network when those of the first row are given. In n. 5 we shall show how the first row of « vertical » and « diagonal » conductances (that is, G and H for $n = 0$) can be calculated once the value of the conductances along the axis (C for $n = 0$) has been arbitrarily chosen. In this way, using formulae (35), (36), (19), (20), (21), we have computed the values (to five significant figures) of all the resistances of the first 26 rows, assuming for those along the axis the arbitrary value $1/C_0 = 100\,000$ ohm: the results are collected in table I. Of course all resistances could be multiplied by an arbitrary constant.

TABLE I. – *Values of the resistances.*

n	With diagonals			Without diagonals	
	$1/C$	$1/G$	$1/H$	$1/C$	$1/G$
0	100 000	14 706	71 428	100 000.0	25 000.0
1	6 578.9	4 612.5	18 248	15 625.0	10 135
2	3 321.5	2 713.4	10 714	7 865.3	6 214.5
3	2 221.3	1 924.1	7 620.8	5 245.9	4 466.9
4	1 667.3	1 491.4	5 921.1	3 934.8	3 483.4
5	1 334.2	1 217.9	4 843.3	3 147.9	2 853.9
6	1 111.9	1 029.3	4 098.2	2 623.2	2 416.7
7	953.01	891.40	3 552.0	2 248.5	2 095.5
8	833.81	786.11	3 134.4	1 967.4	1 849.6
9	741.12	703.09	2 804.8	1 748.8	1 655.3
10	667.02	635.94	2 537.8	1 573.9	1 497.9
11	606.31	580.51	2 317.3	1 430.9	1 367.8
12	555.80	533.97	2 132.1	1 311.6	1 258.5
13	513.03	494.35	1 974.3	1 210.7	1 165.3
14	476.34	460.20	1 838.2	1 124.3	1 085.0
15	444.60	430.47	1 719.7	1 049.3	1 015.1
16	416.78	404.35	1 615.5	983.74	953.64
17	392.24	381.21	1 523.3	925.88	899.19
18	370.49	360.59	1 441.0	874.43	850.62
19	351.01	342.07	1 367.1	828.50	807.03
20	333.47	325.37	1 300.5	787.02	767.64
21	317.61	310.22	1 240.0	749.51	731.95
22	303.18	296.42	1 184.9	715.46	699.44
23	290.01	283.80	1 134.5	684.36	669.70
24	277.93	272.20	1 088.2	655.86	642.34
25	266.83	261.52	1 045.6	629.60	617.16

If the resistances are chosen according to this law, in formula (15) all terms disappear except those of the fourth order and the error becomes

$$\varepsilon = \alpha \frac{h^4}{24} \frac{\partial^4 V}{\partial r^4} \tag{22}$$

where

$$\alpha = \frac{2C + G + G' - 8(H + H')}{2C + G + G' + 2(H + H')} . \tag{23}$$

The values of α for a few values of n are given in table II. It will be noted that they are very small and tend to zero when n increases, as it is to be expected because, very far from the axis, conditions approach those of the cartesian coordinates (n. 2).

TABLE II.

$n =$	1	2	5	10	15	20
$\alpha =$	0.0529	0.0016	— 0.0034	— 0.0015	— 0.0009	— 0.0006

4. – The network for cylindrical coordinates without diagonals.

Now we shall avail ourselves of the calculations of the preceding section for deducing the theory of the network without diagonals in a better approximation than that adopted by de PACKH and LIEBMANN.

Formula (15), in the case of a network without diagonals, that is with $H = H' = 0$, becomes

$$I = \left[G - G' + \left(-\frac{1}{n} + \frac{1}{12n^3}\right) C\right] h V_r + G + \left[G + G' \left(2 + \frac{1}{6n^2}\right) C\right] \frac{h^2}{2!} V_{rr} + \tag{24}$$

$$+ \left[G - G' + \frac{C}{n}\right] \frac{h^3}{3!} V_{rrr} + [2C + G + G'] \frac{h^4}{4!} V_{rrrr} .$$

If G' is given, we can determine C and G so as to suppress the first and second order terms. This leads to the system of linear equations

$$12n^3 G + (-12n^2 + 1) C = 12n^3 G' ,$$
$$6n^2 G - (12n^2 + 1) C = -6n^2 G' ,$$

whose solution is

$$C = -\frac{24n^3}{Q_{-n}} G' , \tag{25}$$

$$G = -\frac{Q_n}{Q_{-n}} G' , \tag{26}$$

where

$$Q_n = 24n^3 + 12n^2 + 2n - 1 . \tag{27}$$

For the first row ($n = 0$) we shall find in n. 5 that we must take $G = 4C_0$, where C_0 is the value arbitrarily chosen for the conductances along the axis. Assuming $1\ C_0 = 100\,000$ ohms, we have calculated step by step, using (25) and (26), all the resistances of the first 26 rows: they are collected in table I along with those for the diagonal network.

For high values of n we may neglect the last two terms in (27), and then formulae (25) and (26) reduce to

$$C = \sim \frac{2n}{2n-1} G' , \qquad G = \sim \frac{2n+1}{2n-1} G' ,$$

that is

$$C = \sim 2nK , \tag{28}$$

$$G = \sim (2n+1)K , \tag{29}$$

where K is an arbitrary constant. These are the formulae adopted by DE PACKH and LIEBMANN. On the axis, they give $1/C = \infty$. The difference between these values and those calculated from (25) and (26) is far from being negligible in the first two or three rows, as is shown in fig. 5. In this we have indicated the values of the resistances $1/C$, $1/G$ from our formulae and, in parentheses, those from de Packh's approximation, assuming for the arbitrary constant such a value ($K = 3.177\ C_0$) as to give coincidence when n tends to infinity.

The error in the network without diagonals can be calculated from (24) (reduced to the third and fourth order terms) and (12) with $H = H' = 0$. It comes out

$$\varepsilon = \frac{-1}{48n^3 + 2n} \left(\frac{h^3}{6} \frac{\partial^3 V}{\partial r^3} + \frac{h^4}{24} \frac{\partial^4 V}{\partial r^4} \right) . \tag{30}$$

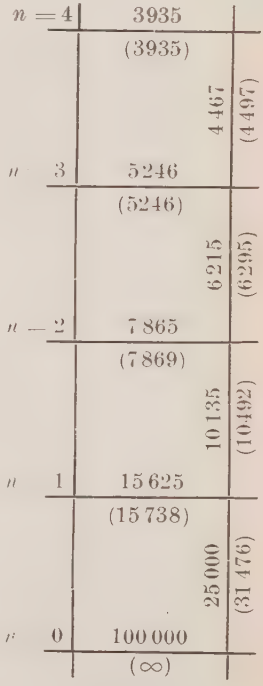

Fig. 5.

Comparing this formula with (22) we see that the diagonals not only suppress entirely the third order error, but eliminate practically even the fourth order one, by introducing in it the very small factor α.

5. – The first row of resistors ($n = 0$).

The calculations of the last two sections are not valid for $n = 0$, that is for the first row of resistors near the axis $r = 0$. We must start again the reasoning, taking into account that, if V is regular on the axis (as we shall assume) all its derivatives of odd order with respect to r are zero for $r = 0$. This permits expressing V at any point by means of its values on the axis:

in fact, denoting these values by $f(z)$ $V_{r=0}(z)$, we have the development, well known in electron optics [4]

$$V(z, r) = f(z) - \frac{1}{4} f''(z) r^2 + \frac{1}{64} f^{IV}(z) r^4 - \dots . \tag{31}$$

So, if we take a junction P_0 on the axis and the five contiguous junctions P_1, P_1', P_2, P_3, P_3' (fig. 6), we have, dropping all terms of higher order than the fourth,

$$V_1 + V_1' - 2V_0 = h^2 f'' + \frac{h^4}{12} f^{IV}$$

$$V_2 - V_0 = -\frac{h^2}{4} f'' + \frac{h^4}{64} f^{IV}$$

$$V_3 - V_0 \quad hf' + \frac{h^2}{4} f'' \quad \frac{h^3}{12} f''' - \frac{13}{192} h^4 f^{IV}$$

$$V_4' - V_0 = -hf' + \frac{h^2}{4} f'' + \frac{h^3}{12} f''' - \frac{13}{192} h^4 f^{IV} .$$

(the values of f, f', etc., refer, of course, to point P_0).

In the case of a diagonal network, we may impose the condition that the error $v - V$ be zero to the fourth order approximation at all five points: in fact Kirchhoff's equation for point P_0 gives, with the conductances shown in fig. 6,

$$\left(C_0 - \frac{G}{4} + \frac{H}{2}\right) h^2 f'' + \left(\frac{C_0}{12} + \frac{G}{64} - \frac{13H}{96}\right) h^4 f^{IV} = 0 . \tag{32}$$

and it is satisfied for any function $f(z)$ if

$$G - 2H = 4C_0 , \tag{33}$$

$$3G - 26H = -16C_0 . \tag{34}$$

So we can choose at will a value for C_0, and determine G and H by means of (33) and (34), which give

$$G = \frac{34}{5} C_0 = 6.8 C_0 , \tag{35}$$

$$H = \frac{7}{5} C_0 = 1.4 C_0 . \tag{36}$$

In the case of a network without diagonals, that is with $H = 0$, we cannot

---

[4] See for instance V. E. Cosslett: *Electron Optics* (Oxford, 1950), p. 35.

satisfy both equations (33) and (34), and must be content with putting equal to zero only the second order part of the error: then (33) gives

$$G = 4C_0 , \tag{37}$$

and it remains an error of the *fourth* order.

Formulae (35), (36) and (37) have been used for starting the computations of table I.

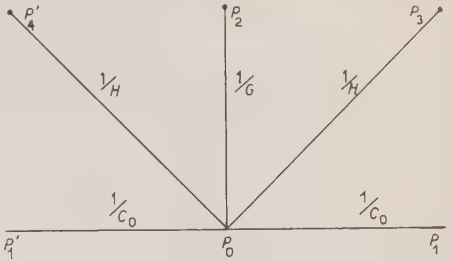

Fig. 6.

6. – Boundary meshes.

We consider now the problem of imposing the condition $V = V_c$ (V_c being a given constant) on a contour line c which, generally, will not pass through the junctions of the network.

Consider, for instance, the case of fig. 9, where three of the eight points connected to P_0 fall out of the boundary c. The network is so calculated that the potential at P_0 would take the right value (in our approximation) if P_1, P_2, P_3 were at the potentials [5]

$$\begin{cases} V_1 = V_0 + V_z h + V_{zz} h^2/2 \\ V_2 = V_0 + V_r h + V_{rr} h^2/2 \\ V_3 = V_0 + (V_z + V_r) h + (V_{zz} + V_{rr} + 2V_{zr}) h^2/2 . \end{cases} \tag{38}$$

Now, the current received by P_0 from P_1, P_2, P_3, in this hypothesis, would be

$$C(V_1 - V_0) + G(V_2 - V_0) + H(V_3 - V_0) .$$

In order that the same current be carried to P_0 from a point at potential V_c, this point must be connected to P_0 by a conductance S such that

$$S(V_c - V_0) = C(V_1 - V_0) + G(V_2 - V_0) + H(V_3 - V_0) . \tag{39}$$

We can realise this condition (without suppressing the connections existing in the network) in the following way. If S, calculated from (39), happens to be $> C + G + H$ (as will usually be the case) we put P_1, P_2, P_3 at potential V_c by means of a potentiometer, and add, between them and P_0,

---

[5] We work out the calculations for the case of cylindrical coordinates; the formulae for cartesian coordinates will be obtained simply by replacing the subscripts z, r with x, y and letting the coordinate r tend to infinity.

a supplementary resistor of conductance

$$S' = S - (C + G + H)\,, \tag{40}$$

as is shown in fig. 7. In the case $S < C + G + H$, we connect (fig. 8) P_1, P_2, P_3 (short circuited) to the point at potential V_c, through a resistor of conductance S'' given by

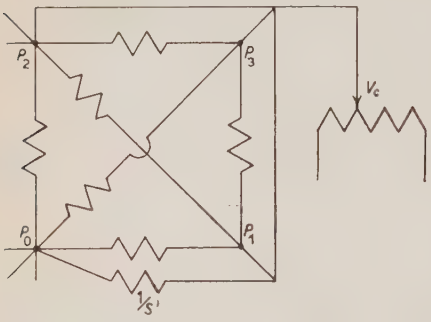

Fig. 7.

$$\frac{1}{S''} = \frac{1}{S} - \frac{1}{C + G + H}\,. \tag{41}$$

In this way, in both cases, the total conductance between P_0 and the point of the potentiometer at potential V_c will be S.

We now proceed to calculate S by means of (39). Using (38) and putting $V_c - V_0 = U$, this formula becomes

$$S = \frac{Ch}{U}\left(V_z + V_{zz}\frac{h}{2}\right) + \frac{Gh}{U}\left(V_r + V_{rr}\frac{h}{2}\right) + \tag{42}$$

$$+ \frac{Hh}{U}\left[V_z + V_r + (V_{zz} + V_{rr} + 2V_{zr})\frac{h}{2}\right].$$

The values of V_z, V_r, etc., in this formula will be so chosen, that for any point of the contour c, (of coordinates ξ, η with respect to P_0) the condition

$$V_z\xi + V_r\eta + \tag{43}$$
$$+ (V_{zz}\xi^2 + V_{rr}\eta^2 + V_{zr}\xi\eta)/2 = U$$

be satisfied as nearly as possible. Since the quantities at our disposal are five, but are related by equation (2), we can satisfy exactly this condition only at *four* points of c, which can be chosen at will in the vicinity of P_0.

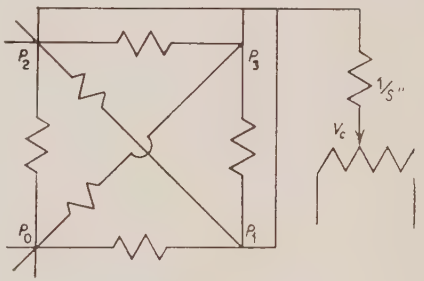

Fig. 8.

It seems quite natural to choose as two of these points Q_1 and Q_2 (see fig. 9), of coordinates $\xi = h_1$, $\eta = 0$ and $\xi = 0$, $\eta = h_2$: this gives the two equations

$$\begin{cases} V_z h_1 + V_{zz}h_1^2/2 = U\,, \\ V_r h_2 + V_{rr}h_2^2/2 = U\,. \end{cases} \tag{44}$$

Solving for V_z, V_r and replacing in (42), taking into account (2), we get

$$(45)\quad \begin{cases} S = Ch\left[\dfrac{1}{h_1} - (h-h_1)\dfrac{V_{rr}}{2U} + \dfrac{h-h_1}{2r}\left(\dfrac{V_{rr}}{2U}h_2 - \dfrac{1}{h_2}\right)\right] + \\ \quad + Gh\left[\dfrac{1}{h^2} + (h-h_2)\dfrac{V_{rr}}{2U}\right] + Hh\left[\dfrac{1}{h_1} + \dfrac{1}{h_2} + (h_1-h_2)\dfrac{V_{rr}}{2U} + h\dfrac{V_{zr}}{U}\right] + \\ \quad + h_2(h-h_1)\dfrac{V_{rr}}{4rU} - \dfrac{h-h_1}{2rh_2}\Bigg]. \end{cases}$$

Of course, if less, or more, than three junctions connected to P_0 fall outside the boundary, the formula will have less or more terms similar to those written

In the case of cartesian coordinates the formula reduces to

$$(46)\quad S = Ch\left[\frac{1}{h_1} - (h-h_1)\frac{V_{yy}}{2U}\right] + Gh\left[\frac{1}{h_2} + (h-h_2)\frac{V_{yy}}{2U}\right] + Hh\left[\frac{1}{h_1} + \frac{1}{h_2} + (h_1-h_2)\frac{V_{yy}}{2U} + h\frac{V_{xy}}{U}\right]$$

and since $C = G$, $H = C/4$

$$(47)\quad S = \frac{5}{4}Ch\left[\frac{1}{h_1} + \frac{1}{h_2} + (h_1-h_2)\frac{V_{yy}}{2U} + h\frac{V_{xy}}{5U}\right].$$

The cases of networks without diagonals can be obtained, of course, from (45) and (46) by putting $H = 0$.

We can now proceed to different kinds of approximations.

a) First approximation. – Neglecting altogether the second order terms in (45), this gives

$$(48)\quad S = C\frac{h}{h_1} + G\frac{h}{h_2} + H\left(\frac{h}{h_1} + \frac{h}{h_2}\right),$$

and for the cartesian coordinates, with diagonals

$$(49)\quad S = \frac{5}{4}C\left(\frac{h}{h_1} + \frac{h}{h_2}\right),$$

and without diagonals

$$(50)\quad S = C\left(\frac{h}{h_1} + \frac{h}{h_2}\right).$$

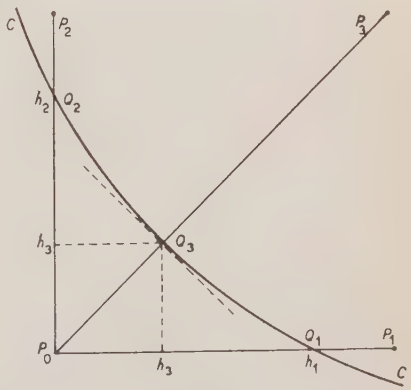

Fig. 9.

Last formula is that indicated by LIEBMANN, and employed also in the relaxation technique.

This approximation is equivalent to replacing the curve c with a straight line between Q_1 and Q_2: it will be sufficient in most cases, if c is not too sharply bent in the vicinity of P_0. But since the networks with diagonals allow using a larger value of h, in many cases h will be comparable with the radius of curvature of c, and a better approximation will be necessary.

b) Second approximation. – In order to determine V_{zr} and V_{rr} in (45), we need two more conditions, which can be chosen in several ways. One is to impose the condition $V = V_c$ to point Q_3 (where c crosses the bisectrix of the axes, fig. 9), of coordinates $\xi = \eta = h_3$, and to an infinitesimal element of the tangent to c at Q_3. Calling $\lambda = (\mathrm{d}\eta/\mathrm{d}\xi)_{Q_3}$ the slope of this tangent, we have, by differentiation of (43),

$$V_z + \lambda V_r + (V_{zz} + \lambda V_{rr})h_3 + V_{zr}(1 + \lambda)h_3 = 0 ,$$

and from the condition at Q_3:

$$V_z + V_r + (V_{zz} + V_{rr} + 2V_{zr})h_3/2 = U/h_3 .$$

Eliminating V_z, V_r and V_{zz} by means of (44) and (2), last formulae give the system of two equations in V_{rr}, V_{zr}:

$$\left[\left(\frac{h_1}{2} - h_3\right)\left(1 - \frac{h_2}{2r}\right) - \lambda\left(\frac{h_2}{2} - h_3\right)\right] V_{rr} + h_3(1 + \lambda)V_{zr} = \\ = U\left[-\frac{1}{h_1} - \frac{\lambda}{h_2} - \frac{h_1}{2rh_2} + \frac{h_3}{rh_2}\right] ,$$

$$\left[\frac{h_1 - h_2}{2} + (h_3 - h_1)\frac{h_2}{4r}\right] V_{rr} + h_3 V_{zr} = U\left[\frac{1}{h_3} - \frac{1}{h_1} - \frac{1}{h_2} + \frac{h_3 - h_1}{2rh_2}\right] .$$

Solving for V_{rr} and V_{zz}, and introducing the abbreviation

$$\Lambda = \frac{\dfrac{\lambda}{h_1} - \dfrac{1}{h_2} + \dfrac{1 + \lambda}{h_3} + \dfrac{(\lambda - 1)h_3 - \lambda h_1}{2rh_2}}{\lambda h_1 - h_2 + 2(1 - \lambda)h_3 + \dfrac{h_2}{2r}[(\lambda - 1)h_3 - \lambda h_1]} , \tag{51}$$

we obtain

$$\frac{V_{rr}}{U} = 2\Lambda , \tag{52}$$

$$\frac{V_{zr}}{U} = \frac{1}{h_3}\left(\frac{1}{h_3} - \frac{1}{h_1} - \frac{1}{h_2} + \frac{h_3 - h_1}{2rh_2}\right) - \frac{\Lambda}{h_3}\left[h_1 - h_2 + (h_3 - h_1)\frac{h_2}{2r}\right] . \tag{53}$$

These values must be substituted in (45) in order to obtain S and, therefore, by (40) and (41), the conductances S' or S'' to be put in parallel or in series with C, G, H. In this way, we have taken into account with a considerable accuracy the shape of the line c between Q_1 and Q_2.

If only two or three junctions are outside the boundary the formula is simplified in an obvious manner.

In the case of cartesian coordinates with diagonals, the final formula for S comes out, from (46),

$$S = \frac{5}{4} Ch \left\{ \left[\frac{1}{h_1} + \frac{1}{h_2} + A(h_1 - h_2) \right] \left(1 - \frac{h}{5h_3} \right) + \frac{h}{5h_3^2} \right\}, \tag{54}$$

(A being given by (51), but without the terms with $1/r$) and without diagonals

$$S = Ch \left\{ \frac{1}{h_1} + \frac{1}{h_2} + A(h_1 - h_2) \right\}. \tag{55}$$

Other cases of boundary meshes could be treated by the same method.

7. – Conclusion.

We believe that a resistor network, constructed as indicated, with the diagonal resistors, can give results much more accurate than one of the same number of resistors without diagonals, especially in regions where the high derivatives of V are appreciable, that is (in the case of electrostatic problems) where the field components are rapidly changing.

We think also that the ordinary network (without diagonals) for cylindrical coordinates, will give better results in the vicinity of the axis if calculated as indicated in section 4 rather than with de Packh's formula.

In both cases, the method indicated in section 6 enables to introduce the boundary condition with greater accuracy, especially in regions where the radius of curvature of the boundary is not very large in comparison with the mesh side.

A network with diagonals for cylindrical coordinates is now being constructed in this laboratory.

The Author is glad to aknowledge the assistance of Miss F. Magistrelli in performing the numerical calculations.

RIASSUNTO

In questo lavoro si studia la teoria di un tipo perfezionato di rete di resistenze per il calcolo numerico di una funzione armonica (in due dimensioni, o in tre con simmetria assiale) con dati valori al contorno. Il vantaggio dell'apparecchio qui studiato su quelli finora descritti è che esso tiene conto di termini di un ordine più elevato in h (h = lato delle maglie della rete) e permette quindi una precisione molto maggiore con lo stesso valore di h. Si dimostra inoltre che (anche per la rete del tipo usuale) il ragionamento basato sulla analogia con la vasca elettrolitica è fallace, e che il metodo corretto di calcolo conduce, nel caso della simmetria assiale, a valori delle resistenze che, in vicinanza dell'asse, differiscono sensibilmente da quelli adottati da Autori precedenti. Si indica infine un metodo per imporre la condizione al contorno sopra una linea curva non passante per i nodi della rete.

LETTERE ALLA REDAZIONE

(La responsabilità scientifica degli scritti inseriti in questa rubrica è completamente lasciata dalla Direzione del periodico ai singoli autori)

Ultrasonic Grating remaining after stopping the Supersonic Waves

A. Carrelli e F. Porreca

Istituto di Fisica dell'Università - Napoli

(ricevuto il 15 dicembre 1951)

During other optical researches on the solutions diffusing the light, the observations on a colloidal solution of starch in water (rice starch), $c = 0{,}1$ g/l, were showing a peculiar effect which we now describe. This solution was put under the action of standing supersonic waves produced by a quartz, $\lambda = 0{,}81$ mm; great care has been taken to obtain good conditions of standing supersonic waves; opposite to the quartz was disposed a brass blade which could be opportunely moved with micrometric movements.

We measured at first the distribution of the intensity of the fringes diffracted by the supersonic grating in pure water.

Table I shows experimental and theoretical values, which are in a satisfying agreement: we can think of having obtained stationary conditions. Putting instead of water the colloidal solution of starch in water, we could observe that when the circuit generating ultrasonics was interrupted, only the fringes of odd order disappeared, while those of even order remained clearly visible for a while (about 6 seconds), gradually reducing in intensity.

By means of a phosporoscope and using the photographic method, we measured the proceeding of the intensity of the first and second order, that remains when the ultrasonics stop, at the changing of time.

Table I.

Order of the fringes	Theoretical values	Experimental values
0	100	100
1	47.5	43.5 ± 5.0
2	15.5	17.7 ± 3.5
3	6.0	5.8 ± 2.0
4	1.5	1.4 ± 1.0

Reporting the time on the abscisses (the zero corresponds to the instant of opening of the circuit generator of supersonic waves) and reporting on the ordinates the intensity, we obtained the curves represented in fig. 1.

First we must observe that this effect is strictly connected with the presence of standing supersonic waves; as soon as the stationarity is destroyed, or only lessened by the displacing of the brass blade, the fringes are not preserved at the stopping of the ultrasonics.

It must be remarked that the measured variation of refractive index Δn of the considered solution is certainly inferior to 10^{-6}.

The distribution of the intensity of the fringes in the solution, when the ultrasonics are excited, is given by table II, which appears different from

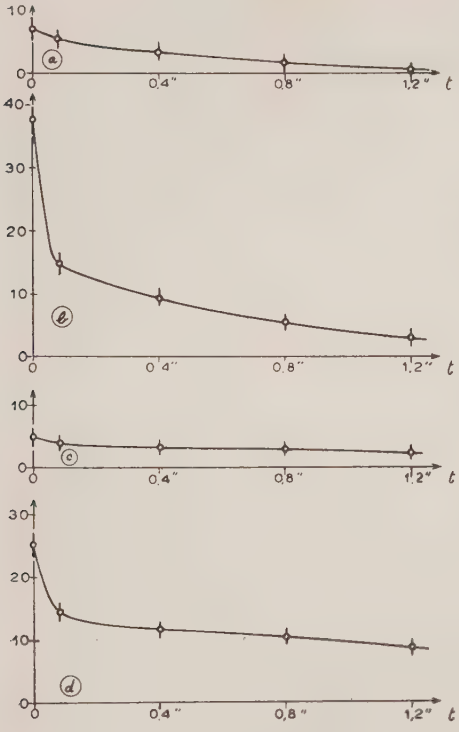

Fig. 1.

a) Order 2 Alcool and starch $c = 0{,}1$ g/l;
b) Order 1 Alcool and starch $c = 0.1$ g/l;
c) Order 2 Water and starch $c = 0{,}1$ g/l;
d) Order 1 Water and starch $c = 0{,}1$ g/l,

Table II.

Order of the fringes	Experimental values
0	100
1	52.0 ± 5
2	25.3 ± 3.5
3	$7.7 + 2$
4	4.8 ± 1

the values above related in tab. I. The same effects are present in solution of starch in alcool 95%, $c = 0{,}1$ g/l; but the intensity of the visible fringes when the ultrasonics stop, disappears more swiftly, as may be seen in fig. 1. Those effects do not appear in solutions of starch in benzol.

All solutions examined are absolutely invariable throughout the whole experience.

Further details will be published in a short time.

A Probable Example of Multiple Production of Mesons.

M. Demeur, C. Dilworth and M. Schönberg
Centre de Physique Nucléaire de l'Université Libre de Bruxelles

(ricevuto il 17 Dicembre 1951)

The star which we here describe was found in a group of plates exposed in a magnetic field of 22 000 gauss at the Pic du Midi (2 800 m). The emulsion was 600 micron thick, the Ilford G5 twice diluted [1] in order to compensate for the low field [2], and was processed by our standard methods [3]. This star presents several interesting features which, in our opinion, make it worthy a separate publication. A general outline will be given in this short letter and a more complete discussion will be published later.

The star (fig. 1) has six minimum ionisation branches of small angular divergence, no visible primary, and a single low energy proton track. There is a small angle pair 500 micron from the centre of the star, nearly parallel to, and two micron from, one of the branches.

The multiple scattering of the tracks was measured by the angular method [4], the movement of the stage being controlled throughout, the distortion of the emulsion was measured [5] and found to be negligible compared to the scattering of the tracks. The sign of the charge of five of the branches and of the two tracks of the pair could be determined with a reasonable probability [2], the sixth secondary had too short a track length. Grain counting on the six secondaries and the two tracks of the pair gave the same value within the errors of measurement. The total kinetic energy of the secondaries is $9 \cdot 10^9$ eV. The results are given in Table I.

The probability of the sign has been corrected for distortion, the correction in all cases being small. The angle ϑ is given with respect to the vertical during exposure.

It seems reasonable to assume that this star represents a multiple production, rather than plural, given the lack of an evaporation star. If we assume the sixth unknown charge to be negative, we can

[1] C. Waller: *Bristol Photographic Congress*, 1950.

[2] C. Dilworth, S. Goldsack, Y. Goldschmidt and F. Levy: *Phyl. Mag.*, **7**, 11 (1950).

[3] C. Dilworth, G. P. S. Occhialini and L. Vermaesen: *Bull. Cen. Phys. Nucl. Bruxelles*, no. 13a; C. Dilworth, G. P. S. Occhialini and A. Bonetti: *Bull. Cen. Phys. Nucl. Bruxelles*. no. 13b.

[4] Y. Goldschmidt: *Bull. Cen. Phys. Nucl. Bruxelles*. no. 14; *Nuovo Cimento*. **7**, 331 (1950).

[5] M. Cosyns and G. Vanderaeghe: *Bull. Cen. Phys. Nucl. Bruxelles*, no. 15.

have the conservation of charge required for multiple production. We therefore analysed the star on the basis of a nucleon-nucleon collision, though we cannot be certain that the primary was a neutron.

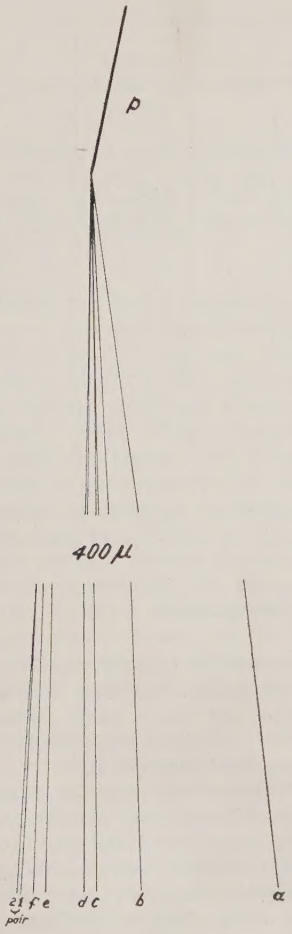

Fig. 1. – Scale, 5 mm = 10 μ
P is the low energy proton, *a*, *b*, *c*, *d*, *e*, *f* are the fast secondaries, 1 and 2 the two tracks of the pair.

At first sight our star looks rather like a low energy version of the star of SCHEIN (6) but the analysis shows that there are important differences. There is one evident fact which is difficult to fit into either of the current models of meson production (7,8,9). Given thenu mber of secondaries, their total energy is too low for the Fermi model and too high for the Heisenberg-Wataghin model. Also with such a multiplicity Fermi's model predicts that two thirds of the charged particles should be protons and antiprotons, whereas no negative proton has been detected in this star and all the particles could be eventually mesons.

On the other hand, if we assume that all the secondaries are mesons and take the energy of the primary to be $6 \cdot 10^{11}$eV as required by Fermi's theory for such a multiplicity, we find in the baricentric system all the charged particles emitted backwards. If we take the primary energy to be $1.5 \cdot 10^{10}$ eV as given by HEISENBERG for this multiplicity, we find that all the charged particles go forward in the barycentric system. Also on Heisenberg's theory the average angle would be about 23°, much larger than we have.

In order to have the same number of charged particles emitted forwards as backwards in the barycentric system, we must take for the energy of the primary $\sim 7 \cdot 10^{10}$ eV. If the slow proton is a recoil, it would then be emitted in the barycentric system with an energy of $6 \cdot 10^9$ eV, whereas the average energy of the mesons would be about 200 MeV. There should be an unobserved fast neutron with about $5 \cdot 10^9$ eV. According to this picture, only a small part of the energy of the nucleons in the bary-

(6) J. LORD, J. FAINBERG and M. SCHEIN: *Phys. Rev.*, **80**, 970 (1950).
(7) E. FERMI: *Prog. Theo. Phys.*, **5**, 570 (1950).
(8) W. HEISENBERG: *Zeits. f. Phys.*, **113**. 61 (1939); *Nature* **164**, 569 (1949); *Zeits. f. Phys.* **126**, 569 (1949).
(9) G. WATAGHIN: *Ann Acad. Brasil. Sc.* **8**, 129 (1943); *Phys. Rev*, **74**, 975 (1948).

centric system would be transferred to the meson field. This would seem unlikely either on the Heisenberg-Wataghin or the Fermi model.

The mesons are emitted in the barycentric system at rather large angles to the direction of the incoming particle. With a primary energy of the order of $7 \cdot 10^{10}$ eV no meson is emitted at an angle of less than 45° nor greater than 135°. This angular distribution is not quite what should be expected according to either of the two models. It is quite possible that the primary was not a neutron. If this is so the application of models of multiple production due to nucleon-nucleon collision may be misleading, especially if the primary had a weak interaction with nucleons, as is the case with photons. In order to know if this star represents a normal or an exceptional case of multiple production, it would be desirable to have more examples of this type of production.

Track	Direction in plane of plate θ	Dip φ	Angle of scattering °/100 μ 10^{-2}	Grain density /100 μ	Nature	Energy (for Meson) 10^9 eV	Sign	Probability
a	— 5° 2′	— 2° 30′	2,8	30 ± 1	$< P$	0,80 ± 1	—	75%
b	— 1° 15′	+ 1° 18′	3,1	30 ± 1	$< P$	0,70 ± 1	—	75%
c	+ 0° 18′	— 5° 0′	2,3	30 ± 1	?	1,0 ± 2	+	96%
d	+ 0° 25′	— 4° 0′	1,4	30 ± 1	?	1,7 ± 3	+	97%
e	+ 2° 6′	— 1° 12′	1,7	32 ± 1	?	1,4 ± 1	+	88%
f	+ 2° 18′	+ 14° 6′	3,2	33 ± 1	$< P$	0,7 ± 2	?	—
Pair						for electron		
1	+ 2° 21′	— 1° 42′	1,3	31 ± 1	*e*	2,0 ± 2	+	88%
2	+ 2° 9′	— 1° 54′	3,0	31 ± 1	*e*	0,9 ± 1	—	73%

Acknowledgements

We wish to thank Professors COSYNS and OCCHIALINI for their generous assistance and many useful discussions. We are grateful to Prof. GÉHÉNIAU for his interest in this work.

We acknoledge gratefully the assistance of Mr. WALLER of Ilford Ltd. and of the personnel of the Osbervatoire of the Pic du Midi, and our colleagues of Manchester University, who all contributed to the task of providing, transporting and exposing the plates.

LIBRI RICEVUTI E RECENSIONI

R. M. Bozorth – *Ferromagnetism.* Un vol. di xvii + 968 pp., con 825 figg., 91 tavole e 4 appendici. Van Nostrand, New York, 1951.

Un trattato sul ferromagnetismo, dove i numerosi e complessi aspetti scientifici e tecnici di questa importante branca della Fisica siano trattati abbastanza esaurientemente, quindi non a carattere monografico, desta sempre interesse: questo perchè pochissime sono le opere che, trattando esclusivamente del ferromagnetismo, soddisfano a questi requisiti.

Merita pertanto d'essere segnalato il bel volume che, preparato dal Bozorth, che è uno dei fisici più competenti di ferromagnetismo e lavora con la Bell Telephone Co., viene ora pubblicato sotto gli auspici di questo grande complesso industriale.

L'opera risulta divisa in quattro parti. La prima, in due capitoli, ha scopo introduttivo ed è utile per le definizioni fondamentali e per introdurre i non specialisti al linguaggio ormai generalmente fissato dalla consuetudine in questi studi. Scopo puramente informativo e generico ha del resto anche la quarta parte, pure molto breve, dove sono descritti nel loro principio di funzionamento i fondamentali metodi di misura delle grandezze più interessanti per il ferromagnetismo.

Ben diverso il carattere delle parti II e III, di gran lunga più interessanti. La seconda parte, in 373 pagine tratta delle proprietà magnetiche dei materiali, quindi del Fe, del Ni e del Co, e delle leghe di questi metalli tra loro e con altri elementi, quali il Si, il Mo, il Cr, il Cu, ecc.. Qualche pagina è pure dedicata alla leghe di Heusler. Un intero capitolo è infine dedicato ai magneti permanenti e alle varie leghe adatte alla loro preparazione, come pure alle speciali tecniche che per questo scopo sono state elaborate più recentemente (v., ad esempio, metallurgia delle polveri—magneti preparati con polveri di metalli o di ossidi magnetici, pressate, ecc.).

È questa una parte di notevole interesse, specialmente per i tecnici e i costruttori, perchè in essa si trovano ben classificati tutti i tipi di materiali ferromagnetici, con le caratteristiche più diverse: una grande quantità di utili diagrammi ne indica il comportamento e ne fornisce, insieme con le numerose tabelle, le principali costanti fisiche, magnetiche in particolare.

La terza parte (di oltre 400 pagine) è invece la più interessante per la fisica del ferromagnetismo. Dopo aver ricordato in essa le principali teorie sviluppate per la interpretazione del ferromagnetismo e per la rappresentazione della sua dipendenza dal campo e dalla temperatura, un intero capitolo è dedicato alla teoria dei domini e alla interpretazione con essa delle particolarità della curva di isteresi. Un altro capitolo si occupa delle proprietà magnetiche dei cristalli.

Più di cento pagine sono quindi dedicate alla descrizione dei vari fenomeni nei quali più evidenti risultano i fenomeni tra magnetizzazione, tensioni meccaniche e deformazioni. In particolare sono esaminati i fenomeni di magnetostrizione, sia dal punto di vista teorico come da quello dei risultati sperimentali: ben trattata la questione delle relazioni

tra il modulo di elasticità e lo stato di magnetizzazione.

Seguono due capitoli in cui sono studiate le relazioni tra temperatura e magnetizzazione nei ferromagnetici, con particolare riguardo ai fenomeni di carattere energetico che accompagnano il passaggio attraverso il punto di Curie. Un altro capitolo esamina i fenomeni della magnetoresistenza nei cristalli e nei materiali policristallini, in relazione anche con la temperatura.

Non molto esauriente appare invece il capitolo che si occupa dei cambiamenti di magnetizzazione col tempo, in quanto non vi sono considerati tutti i tipi di « after effects » che sono stati presi in esame anche nei recenti lavori di SNOEK. Vi è però considerata la risonanza ferromagnetica.

Troppo breve e frammentario appare infine il Capitolo 18 in cui, dopo aver preso in breve considerazione i vari tipi di energia magnetica che sono associati con la struttura a domini, viene indicata la possibilità di prevedere, in base al reciproco gioco di queste energie, da quali fattori possono essere influenzati la permeabilità iniziale e la forza coercitiva,

La vasta materia oggetto dell'opera, esposta in un inglese corretto e chiaro, è svolta in forma molto piana, con assai limitato uso di sviluppi matematici: le numerosissime figure, spesso costituenti schemi originali, sono disegnate con grande cura e chiarezza. Oltre 2400 lavori sono infine citati per una estensione degli argomenti trattati nel libro.

L'opera del BOZORTH, pubblicata 12 anni dopo il volume *Ferromagnetismus* di BECKER e DÖRING, appare pertanto interessante perchè aggiornata, e perchè contiene i dati tecnologici dei diversi materiali ferromagnetici, dati che altrimenti si dovrebbero rintracciare in libri come quello di MESSKIN e KUSSMANN (*Die ferromagnetischen Legierungen*) d'altronde vecchio di quasi venti anni.

Tuttavia, pur nella vastità degli argomenti trattati, il libro di BOZORTH delude forse un po' il fisico, che è portato piuttosto a considerare quest'opera come una enciclopedia sul ferromagnetismo.

Devesi però riconoscere che un maggiore approfondimento della trattazione delle singole questioni che interessano il ferromagnetismo avrebbe richiesto una mole assai maggiore di quella, già rilevante, dell'attuale volume di BOZORTH. D'altra parte la trattazione piuttosto sintetica di una materia vasta e difficile come il ferromagnetismo può presentare difficoltà anche maggiori: il modo come esse sono state, in generale, superate, attesta, se pur ve ne fosse bisogno, della competenza che il BOZORTH si è formata nello studio del ferromagnetismo.

A. DRIGO

Direttore responsabile: G. POLVANI Tipografia Compositori - Bologna

Questo fascicolo è stato licenziato dai torchi il 27-XII-1951